Master thesis : Integration of an Open Source Flight Controller into a Fixed Wing Remotely Piloted Aircraft

Auteur : Henrivaux, Benoît
Promoteur(s) : Dimitriadis, Grigorios
Faculté : Faculté des Sciences appliquées
Diplôme : Master en ingénieur civil en aérospatiale, à finalité spécialisée en "aerospace engineering"
Année académique : 2016-2017
URI/URL : http://hdl.handle.net/2268.2/3283

Integration of an Open Source Flight Controller into a Fixed Wing Remotely Piloted Aircraft

Graduation Studies conducted for obtaining the Master's degree
in Aerospace Engineering

Benoît Henrivaux

University of Liège - Faculty of Applied Sciences
University of Concepción

Academic Year 2016-2017

Contents

List of Figures

List of Tables

Abstract

This master thesis is about the integration of the open-source flight controller *APM 2.6* in an aircraft. It consists in the understanding of the functioning of the autopilot but also its installation and configuration.

At the beginning, the main characteristics of the aircraft are analysed. These ones include a strong stability enhanced by the position of the wing and the presence of a dihedral, a combustion engine and a landing gear with a tail dragger configuration. Furthermore, the radio *Taranis X9E* is entirely configured to accomplish the required tasks. It is a fully programmable radio and the main steps of its configuration are explained.

In this report, the installation of the autopilot and the other necessary components are detailed. Additionally, particular care is considered regarding issues about vibrations because of the combustion engine. *Mission Planner*, the software used as a ground control station, is also commented with different safety features and a presentation of the main flight modes of the flight controller is done.

The autopilot is based on a series of classical PID controllers. The philosophy of each controller is explained. The aim of the work is therefore to tune them correctly for the flight. A fully autonomous mission, including take-off and landing, is analysed to demonstrate that the system works well.

Acknowledgements

I would like first to thank Prof.Andrianne and Prof.Dimitriadis for the chance they offered me to go realising this work in Chile. This has been a fantastic experience from a personal and academic point of view. I am also thankful toward Prof.Dimitriadis for his advice during the writing of this thesis.

Special thanks are given to Prof.Tinapp from the laboratory of the University of Concepción for his follow-up during this work and to have put the needed material at my disposal. I am also grateful toward Mr.José for his help during the hours I spent repairing planes and during the flying sessions.

Finally, I want to express my profound gratitude to my family and, more particularly, to my parents for their patience and support along my studies.

Nomenclature

Mathematic symbols	Meaning
C_L	Lift coefficient
$e(t)$	Control error
E_K	Kinetic energy
E_P	Potential energy
E_T	Total energy
g	Gravity
K_d	Derivative gain
K_I	Integral gain
K_P	Proportional gain
Re	Reynold number
L	Characteristic length
P	Pressure
R_t	Turn radius
S	Wetted surface
$U(t)$	Controller output
V	Speed
V_{st}	Stall speed
W	Weight
$x(t)$	Real signal
$x_d(t)$	Desired signal
ν	Kinematic viscosity
ρ	Air density
Abbreviations	**Meaning**
APM	ArduPilotMega
BEC	Battery Elimination Circuit
Ch	Channel
FBWA	Fly-By-Wire-A
GCS	Ground Control Station
GPS	Ground Positioning System
HUD	Head Up Display
IMU	Inertial Measurement Unit
MP	Mission Planner
NN	Neural Network
PLA	Polilactic Acid
PID	Proportional Integral Derivative (controller)
PM	Power module
PWM	Pulse Width Modulation
RC	Radio Commanded
RPM	Revolutions Per Minute
RTL	Return To Launch
TECS	Total Energy Control System
UAV	Unmanned Aerial Vehicle

Table 1: List of abbreviations and symbols.

1 Introduction

In the recent decades, we have assisted to a rapid evolution of aircraft technology. In particular, the advent of unmanned aerial vehicles (UAV) has been spectacular. At the beginning, it was principally for military purposes. Over the years, the technology has matured more and more leading to prices that are more affordable but also to a greater accessibility. This has led to a spread of the use of UAVs in the world of professionals and the one of amateurs. These vehicles, also called drones, can be usually controlled manually or can accomplish missions autonomously. As a result, in order to plan the objectives and to monitor the flight, a ground control station (GCS) is often used.

Nowadays, these vehicles are used to fulfil different objectives. Amongst the most common missions, mapping, surveying or research are performed either from a military or a non military point of view. They are also capable to access difficult and/or dangerous areas such as the sides of cliffs or mountains. Additionally, they can give a quick overview over large areas at a small expense compared to classical aircraft or helicopters.

On the other hand, the evolution of UAVs is accompanied with the one of flight controllers. These are indeed necessary to monitor the attitude and the navigation of the vehicle if no human intervention is desired. Different autopilots exist from the most expensive commercial to the relatively cheap and open source options like those from the Ardupilot family.

In this perspective, this master thesis is about the installation and configuration of an autopilot in a remotely piloted aircraft in order to accomplish a fully autonomous flight. This first chapter, the introduction, presents the basics hidden behind the control theory of classical autopilots. Additionally, different orientations used to implement such systems are also described. Moreover, a first introduction to the autopilot used in this work, from the *ArduPilot* project, is carried out. Finally, the present chapter explains the objectives of the thesis as well as the conditions in which it was realised.

1.1 Autopilots

In the world of planes, autopilots are systems used to help with the navigation of the vehicle. Its objectives are either to assist the pilot by correcting only a part of the attitude of the aircraft or to take the complete control by flying, for example, a configured mission.

Flight controllers on their own are not enough to control a vehicle. Indeed, an autopilot system also needs different sensors in order to get information about the attitude, the position or other parameters of the plane. As explained in the following paragraphs, several types of approaches are possible.

1.2 Different control systems

Several techniques to control a plane are discussed in these paragraphs. Some of them are based on the vehicle dynamic and are therefore more difficult to put in place. This type of flight controller is, for example, simulated in [15].

Article [3] presents a survey of different autopilots. Some of the autopilots described in that article are also discussed hereunder but with additional details. Moreover, other information are also given regarding the different tuning possibilities of flight controllers.

PID control

The vast majority of controllers that are used for UAVs are based on PIDs controls. A PID law is represented mathematically as in Eq.1.

$$U(t) = K_p e(t) + K_I \int_0^t e(\tau)d\tau + K_d \frac{d}{dt}e(t) \tag{1}$$

where $U(t)$ is the controller output and $e(t)$ is the error. Therefore, it consists of three feedback controls that are related to the gains K_p, K_I and K_d. The control error is the difference between the desired signal, $x_d(t)$, and the signal obtained, $x(t)$, such as in Eq.2.

$$e(t) = x_d(t) - x(t) \tag{2}$$

The proportional term, related to the gain K_P, is proportional to the error and is used to diminish the error due to disturbances but too high gains can lead to instabilities. The integral gain K_I is used to remove any steady-state error. Any system with an integral term should reach the correct steady-state (it can take a long time...). Finally, the last term, based on the derivative of the error, increases the stability of the system by slowing down its dynamics. An example of a block diagram of a PID controller is given in Fig.1. However, there are also other types of configurations but the different terms (and gains) keep playing a similar role.

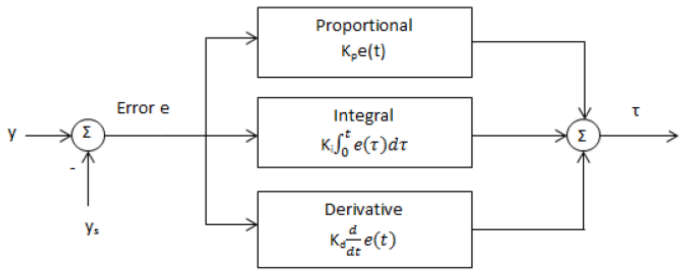

Figure 1: Example of a block diagram of a PID controller [19].

The objective of the PID design is therefore to find the right combination of the three gains in order to have the desired behaviour of the system. For that, the tuning has to be such that the error converges towards zero in an acceptable time lapse.

Commercial autopilots such as the Piccolo, the Kestrel, the Xbow Stargate, etc are all based on the traditional PIDs as described just above. These PIDs controllers are usually easy to integrate onto a small UAV platform but has limitations when optimisation is required. Another problem is the robustness: indeed PIDs are tuned for a specific flight condition but aircraft parameters can evolve during a flight (e.g. fuel consumption, release of payloads) or between flights (e.g. different loads, weather conditions, etc). Moreover, some issues may arise when tuning the parameters.

In order to tune the gains of classical PIDs, several possibilities exist based on different techniques. Manual tuning is possible but it can be rather lengthy because it is mainly based on a trial and error approach. Other techniques are also explained in [34]. It is also possible to have a more automatic manner than the manual approach. For instance, the master thesis in [17] is about the realisation of an auto-tuner.

Fuzzy Logic Control

As discussed in [8], this control logic is based on many logic values, which can include different operating conditions for example. The fuzzy control is also analysed in [4]. Based on the design of many logic values that are nearly human language, fuzzy rules are used to make decisions. These rules come from human experience. Using the decisions from the fuzzy logic, PIDs gain are somehow actualised such that

$$K_P = K_{P0} + \Delta K_P$$
$$K_I = K_{I0} + \Delta K_I$$
$$K_D = K_{D0} + \Delta K_D$$

The architecture of a fuzzy adaptive controller is given in Fig.2. As indicated in this scheme, the traditional PID controller receives the updated gains from the fuzzy control.

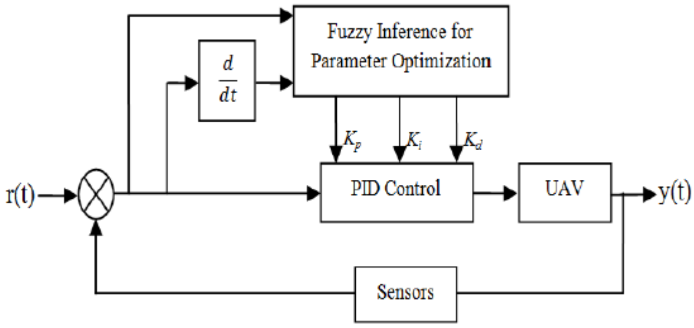

Figure 2: Architecture of adaptive fuzzy PID controller [8]. *r(t)* is the desired behaviour while *y(t)* is the attitude of the UAV.

In this example, the fuzzy control takes as inputs the error between the desired attitude of the UAV, *r(t)*, and the real attitude, *y(t)*, observed by the sensors. The second input of the fuzzy logic is the rate of this error. The fuzzy rules for this controller are given in Fig.3.

e \ $\dot{e}$ (u)	**NB**	**NS**	**Z**	**PS**	**PB**
NB	NB	NB	NB	NS	Z
NS	NB	NB	NS	Z	PS
Z	NB	NS	Z	PS	PB
PS	NS	Z	PS	PB	PB
PB	Z	PS	PB	PB	PB

Figure 3: Example of fuzzy rules for the fuzzy controller [8]. Legend: (NB) negative big, (NS) negative small, (Z) zero, (PS) positive small and (PB) positive big.

As a result, compared to classical PID control, the system has a better performance when dealing with external disturbances such as wind and UAV parametric uncertainties. Consequently, the system compensates well uncertainties as well as non linearities. Therefore, its robustness is enhanced.

Adaptive neural network

This technique is described in articles such as [7], [10], [13] and [35]. The advantage of this kind of systems is mainly based on two unique features: on the one hand, it is able to process a large quantity of information in real time. On the other hand, it is able to learn: to adapt itself to variations in its environment.

The principle of a neural network system is illustrated in Fig.4. This consists of several inputs and outputs composed of processing elements that are simple and similar. These processing elements have a number of weights, which are in fact kind of internal parameters that can be modified to change the behaviour of the system. The objective is therefore to accomplish what is called "the training of the network": to choose the different weights in order to have the desired outputs.

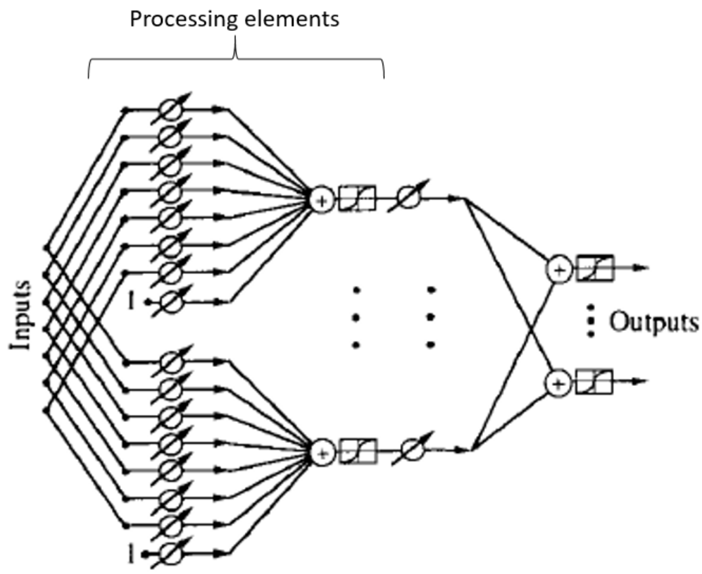

Figure 4: Principle of a neural network [1].

Eventually, combining the adaptive neural network with the fuzzy logic can give stronger and more versatile models. This leads to "Adaptive Neuro-Fuzzy Inference System" as studied in [9]. Indeed, it is advantageous because the control problem is solved with a fuzzy logic and the control parameters are optimized using the self learning process of the neural network. It uses control augmentation commands in order to learn to remove errors based on the recognition of pattern in the behaviour of the error.

LQG and H_∞ flight controllers

This last category presented here is model based. It relies on a linear model, which is an approximation of the highly non linear dynamics of UAVs. Different references such as [5] uses a Linear Quadratic Gaussian method with a Kalman filter in order to have better performances. It is a problem of pole placement and is composed of a time varying Kalman filter and a time-varying linear quadratic regulator. The Kalman filter estimates the states of the system from measurements that can be noisy. It is a recursive estimator because it is based on the current information given by the sensors but also the states from the previous time step. The linear quadratic regulator is an optimisation method whose aim is to minimise a desired objective function by changing the dynamic behaviour of the system according to some particular requirements.

On the other hand, techniques such as described in the book [12] dealing with the H_∞ loop shaping, has also resulted in a better robustness. A typical block diagram representation of this technique is presented in Fig.5. This contains two main parts: the controller and the plant. There is the control input u, which is the output of the controller and represents the actuators of the plant. The second input is a collection of exogenous inputs, which are disturbances $d(t)$. Concerning the outputs, there is the measured signals, $y(t)$, which serves as inputs for the controller. Based on them, the controller is going to change the control inputs such that the plant has the right performances $z(t)$. The problem is therefore to build the controller for the plant in order to minimize the infinity norm of the transfer function between the disturbances, $d(t)$, and the performance output, $z(t)$.

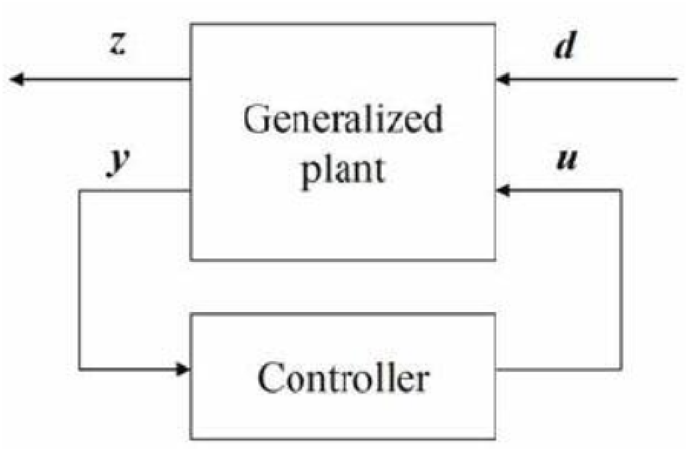

Figure 5: Block diagram representation of H_∞ control systems [18].

1.3 The ArduPilot project

The flight controller used to realise this thesis is the *APM 2.6* from the ArduPilot project [20]. It is an autopilot that has a series of PIDs controllers in order to manage the attitude of the aircraft as well as to track its trajectory. The aim is therefore to tune the different gains in order to accomplish a good navigation. Furthermore, this autopilot whose code is open source also includes failsafe that can deal with unexpected situations such as the loss of a sensor.

This flight controller is part of the ArduPilot family, which is shown in Fig.6. The evolution of these autopilots has seen drastic changes and improvements such as the introduction of an inertial measurement unit (IMU) instead of the thermopiles for the board of the family (APM 1) and the introduction of a new 32 bit platform (PixHawk) instead of the previous models that were only 8 bit. In addition to that, it is an autopilot based on the Arduino system, which is a prototyping platform used to create interactive electronics objects. In order to function, the autopilot needs additional sensors to have information about the attitude and the position of the aircraft.

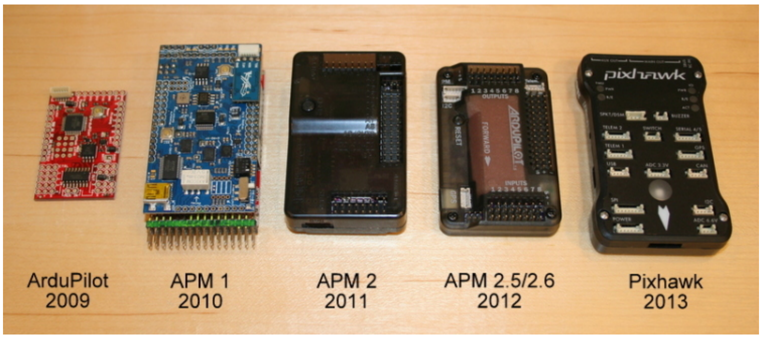

Figure 6: Evolution of the different flight controllers [24].

Moreover, these controllers can be used not only for planes but also for multi-copters, boats and cars.

1.4 Objectives of the thesis

This master thesis aims in the understanding of an autopilot and its components in order to make a completely autonomous flight. The autopilot that is used throughout this work is the *APM 2.6* whose source code is "open". This means that it is possible to use and modify the code for free (unless it is done with a business perspective). Starting from a plane that is initially remotely piloted, the final objective of this work is therefore to realise a completely autonomous flight.

Additionally to this main goal, other aspects have been learned. These include the characterisation, the functioning and the maintenance of the plane. Moreover, learning to fly manually was also necessary. Firstly, a flight simulator was used. Then, the learning was also realised in real conditions using a first plane, which is smaller than the one in which the autopilot is installed (and also easier to repair). This first plane called *Plane X1* is represented in Fig.7. Indeed, to have a good feeling of how a plane behaves in practice, it is difficult to only rely on the simulator as there are always things that are unplanned in reality. Furthermore, an important step to pilot the aircraft was the complete configuration of the radio transmitter.

Figure 7: Photo of the *Plane X1*.

The *Plane G5*, the aircraft in which the autopilot is placed, is displayed in Fig.8. It has a wing span of about two meters and a weight of $5.6\ kg$ when the flight controller is installed. Before this work, the plane was used as a pedagogic tool with different cameras installed in the vehicle. Therefore, it was already a modified version of the original plane whose instruction manual is [41], but modifications were also made in the work. More details are given in Section 2, which presents the aircraft as well as its operation. Additionally, the present thesis also aims to keep the spirit of the past work and to keep free the different places where the cameras were installed.

Figure 8: Photo of the *Plane G5*.

Along these objectives, the author has also realised several repairs due to accidents caused by a variety of reasons on both planes. Additional details are given in the report about the repairs of *Plane G5*. In other words, the guidelines of this project is to install and configure a flight controller in a plane, which will be used by other students for a variety of purposes.

In this thesis, the plane is first introduced as well as its operating way. Particular attention is paid regarding the operation of the engine and its main aerodynamic properties. After that, a section is also about the configuration of the radio controller because the *Taranis X9E* differs from the vast majority of RC controllers by the fact that it is fully programmable. Then, an important chapter describes the autopilot as well as the sensors needed to ensure a safe and reliable flight. Additionally, its integration in the plane is also explained. The rest of the report aims to give an overview of the autopilot configuration. Moreover, results from a real flight test are also discussed.

2 Presentation of the aircraft

The aircraft that is used to perform the present work is briefly presented in this section. A photo of the plane is displayed in Fig.8. It is a tail dragger aircraft powered by a combustion engine. It presents a two-meter wing span while its fuselage is more than one meter and a half long. In the RC world, its dimensions are already quite large. Firstly, its origins as well as the modifications that were made are discussed. Then, the main features of the plane are described.

2.1 Origins and modifications

Originally, the plane was bought by the aerospace laboratory of the University of Concepción. It came as an Almost Ready To Fly plane meaning that the only thing that needed to be done before flying was to assemble the different parts and install an engine.

After that, as the objectives of the aircraft were purely pedagogical, a first series of transformations was realised. These include a modification of the canopy, the installation of a payload bay with a trap door and the change of the landing gear configuration to a tail-dragger. Meanwhile, a control bay to install the receptors and the batteries was created above the payload bay. The main advantage of the payload bay is that it is easily accessible because it is a drawer. In other words, it is not necessary to remove the wing to gain access to any payload. Thanks to these changes, a set of three cameras were placed at different locations around the aircraft. One camera was placed in the cockpit, another under one of the wings and the last camera, which is retractable, in the payload bay. Therefore, the plane had an objective of filming different areas. Throughout this work, the location of the different components will be such that the re-installation of these cameras is still possible while using the autopilot.

In this work, the plane also experienced several transformations. The first one is that the payload bay was emptied and therefore the retractable camera removed. Initially, it was to place the autopilot there but, as discussed further in the report, it eventually fits better in another place. Then, the plane crashed twice: the first time because the flight instructor failed to land in windy conditions (Fig.9 shows the plane after the first accident) and the second time due to a human error in the mode selection of the autopilot while taking off for its maiden flight (without any gain adjustment). Consequently, a series of repairs were made around the plane. The material used to make them was the one available within the laboratory and the objective was to repair the structure and reinforce it while keeping as much as possible the initial design. It consists mainly of balsa, which is a wood that is extremely light and easy to work. Other pieces of wood are also used for their rigidity and their better resistance. Most of the parts are assembled using a cyanoacryllic glue, which is very strong with a good adherence to wood and dries rapidly. Another type of glue, a mixture of Epoxy and a resin is also considered to assemble the most important parts because it is much stronger but requires more time to dry and is more difficult to apply adequately.

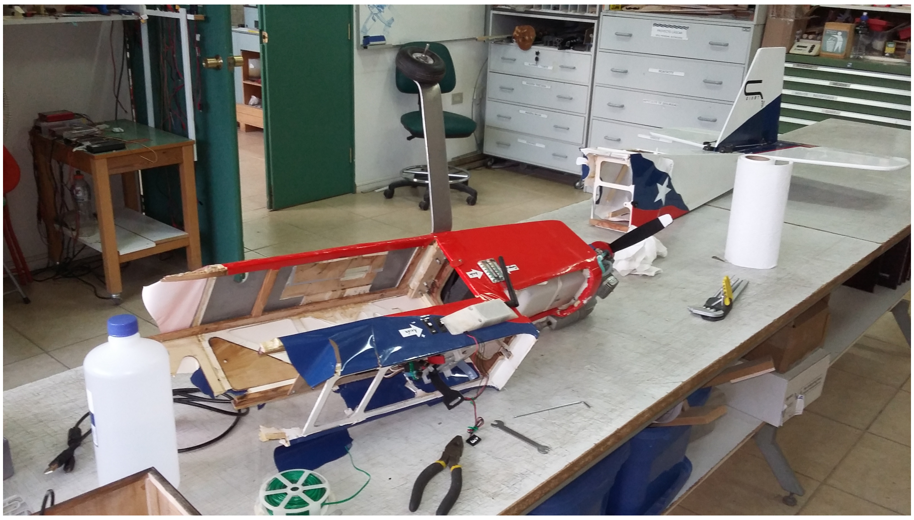

Figure 9: Photo of the plane after a crash.

The main changes caused by these repairs are, on the one hand, that the camera from the cockpit was removed because its support had been broken and, on the other hand, there are some slight modifications to the structure in order to reinforce or replace the broken parts. Nevertheless, these repairs have not influenced the positioning of the autopilot within the plane. Moreover, it is still possible to re-install the different cameras at their locations.

2.2 Main features

The following paragraphs aim to present the key characteristics of the aircraft. The objective is also to explain their impact on the flying properties. Additionally, some manipulations of the planes are described.

2.2.1 The propulsive system

The first system described in this report is the engine, which is a thermal engine. This is different from the vast majority of the RC aircraft because the trend is to power them electrically. Indeed, the use of fuel induces additional risks linked to the configuration of the engine because there are more parameters to account for, such as combustion (explained here-after). Furthermore, it is not that handy compared to electric aircraft because of the need to reload the fuel and to clean the aircraft due to the oil present in the fuel.

For the purpose of this work, the engine used is a MAX 55 AX glow engine (which was already installed on the plane). This is a two-stroke engine. It is mounted at the front of the aircraft with a propeller 12×6. The mounting of the engine is not optimised from an aerodynamic point of view, but is such that it allows cooling by natural convection of the airflow around the engine. Consequently, weight and complexity are saved because it avoids the addition of a cooling system. The propulsive system of the plane is represented in Fig.10.

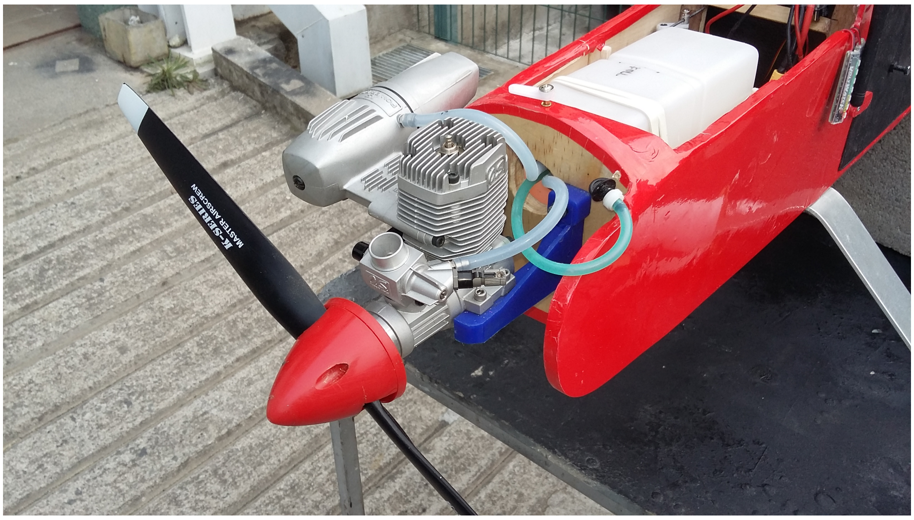

Figure 10: Photo of the engine and the propeller.

The remaining of this paragraph provides an overview on the operation of the two-stroke motor and how to operate it safely. The principle of the two-stroke engines is illustrated in Fig.11. As it can be seen, the engine is going to perform the four steps of any motor using only one piston (and therefore two strokes). One cycle of combustion works as following.

- Combustion stroke: The spark plug ignites the compressed fuel/air mixture, which creates an explosion that pushes the piston downwards. As the exhaust port is uncovered, the exhaust gases leave the cylinder. When the piston reaches the bottom, the pressurised mixture present in the crankcase enters the cylinder and pushes the remaining burned gases out.

- Compression stroke: The momentum of the crankshaft drives the piston upwards. This motion compresses the mixture in the cylinder against the plug. In addition, a vacuum is created in the crankcase, which opens a valve and sucks air and oil from the carburetor. Once the piston reaches the top, the spark plug ignites the mixture and a new cycle starts.

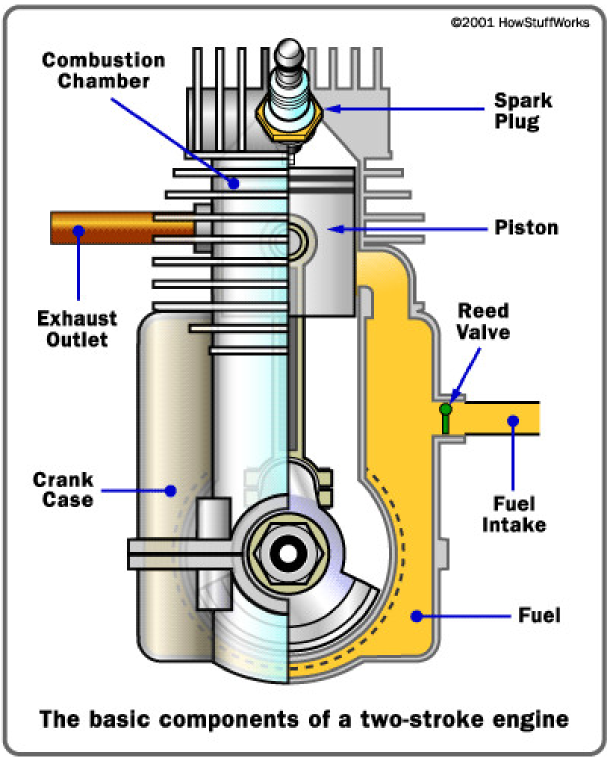

Figure 11: Illustration of a two-stroke engine [23].

The spark plug is different from the everyday applications of engines such as in cars or in other vehicles. It uses a glow plug: this has to be heated up in order to start the engine by an external device called a plug igniter such as the one shown in Fig.12. However, once the engine is running, the heat produced by the combustion is sufficient to keep the spark plug sufficiently warm from one cycle to the other.

Figure 12: Photo of the plug igniter and its charger.

Furthermore, it is critical to use the adequate air to fuel mixture. An inadequate fuel mixture would have adverse consequences for the motor performances. Indeed, if too much fuel enters the engine, it is going to consume a lot of fuel from the tank without burning it and, consequently, the consumption will be high and the flying time shorten. On the other hand, if the mixture is too poor in fuel, the engine might be unable to follow an acceleration and extinguish, which can cause a crash.

In order to control the mixture, two ways are provided. The first one is the mixture control valve. This valve, mainly based on factory setting, monitors the fuel flow when the engine is not operating at maximum throttle. In other words, it guarantees the operation of the engine when the throttle is closed and opened. The other valve is the needle valve and needs to be adjusted. It consists mainly in establishing the basic mixture to produce maximum power at full throttle. The optimum position of the needle valve can be explained using Fig.13. Initially, the motor is started using a rich mixture. As the valve is progressively closed, the mixture is now poorer and the increase in RPM leads to a distinct sound. The optimum is reached when this sound starts to change meaning that the RPM is going to reduce. In practice, it is better to keep a mixture that is a little richer than the optimum in order to guarantee the engine will not stop working; in particular, in the case of sudden and large accelerations.

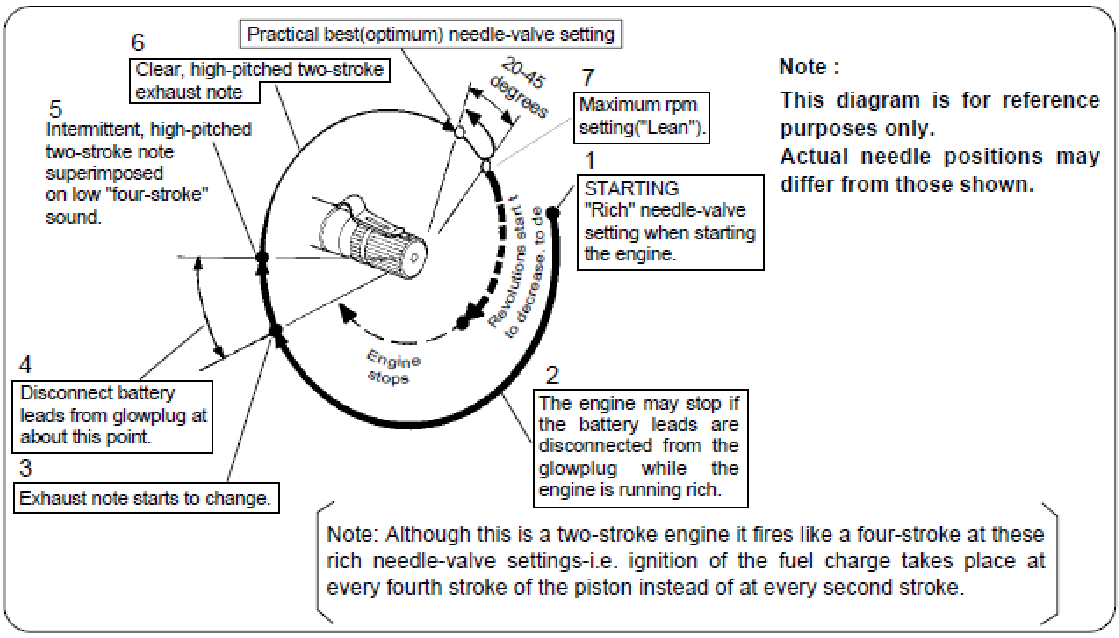

Figure 13: Needle-valve adjustment diagram [38].

Furthermore, the quantity of air entering the engine also impacts the functioning because it is going to cause the motor to accelerate or decelerate. Indeed, it modifies the combustion as it controls the charge entering the cylinder. It is controlled using the throttle (commanded by the pilot) depending on the desired velocity. Consequently, it impacts the force produced by the motor and the resulting thrust. In appendix A, the measurements of the static thrust for different positions of the throttle are provided.

Compared to four-stroke engines, two-stroke engines are less complex and also lighter because they do not have valves. They are also advantageous because they present a higher power-to-weight ratio than their counterparts. However, they often have a shorter life time due to the contact and it is necessary to use a fuel that contains a lubricant. This leads to a combustion that might be incomplete and higher pollution. Indeed, this is visible when operating the aircraft as oil is present over the structure after the flight.

2.2.2 The wing configuration

The wing configuration is also an important feature to consider in an aircraft because this is the part that will generate most of the lift required to fly. This aircraft has a straight wing with no sweep. In addition, the wing is located on top of the fuselage and presents a dihedral, which influences the flying properties of the vehicle.

Indeed, having a high-positioned wing leads to an aircraft that is more stable. As represented in Fig.14, the airflow distribution is affected by the fuselage. In a top wing configuration, it leads to a high angle of attack on the rolling side and a small angle on the other side. As a result, the lift on the low wing is increased while the one of the high wing is decreased and a restoring moment is produced.

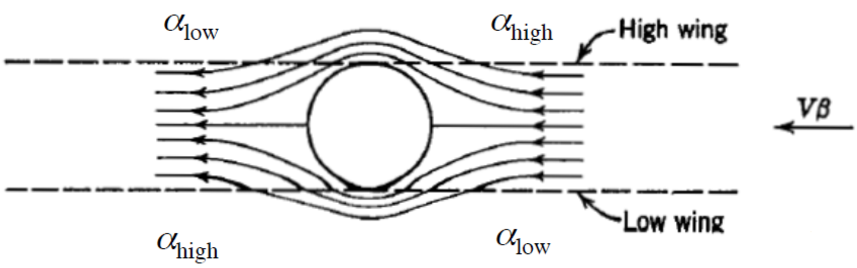

Figure 14: Airflow around the fuselage for a high wing configuration [36].

This lateral stability is even enhanced by the presence of a dihedral. Indeed, in sideslip, the dihedral implies that the trailing wing has low drag while the leading wing has high drag. In consequence, a restoring moment in yaw is created. In addition, a similar conclusion is also reached in roll because dihedral causes a lift asymmetry with the high wing getting low lift while the low wing has high lift. As a result, a restoring moment in roll is also created.

Consequently, the plane has a trend to be stable in flight and complex manoeuvres are not advised. This is not an acrobatic aircraft and it travels smoothly. However, it also means that the plane needs time (and space) to do some manoeuvres like turning because its turn radius will be relatively large.

Furthermore, from the airfoil profile, it is also possible to have an idea of the stall velocity of the aircraft in cruise, which is an important parameter to consider. Fig.15 is a comparison between two airfoils: the one that was drawn from the plane and the N-10 airfoil that closely matches the real airfoil. The latter is used to compute the property.

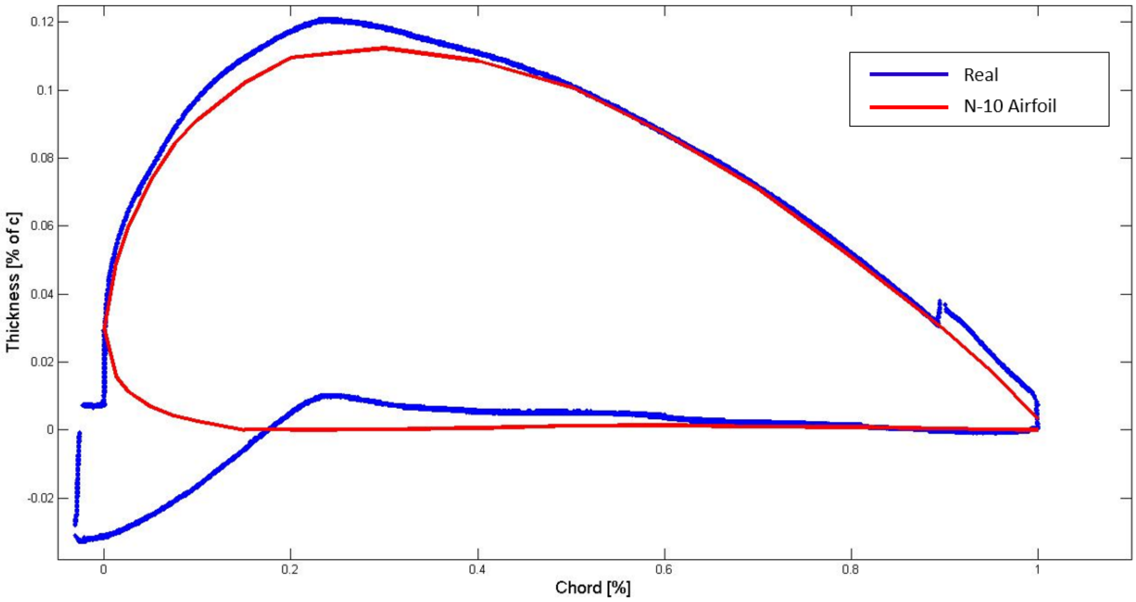

Figure 15: Comparison between the airfoil profile of the plane and the one used for the analysis.

Both airfoils are nearly the same but there are some differences. In fact, the real airfoil is the perimeter of the centre part of the wing because it is the only section of the wing that can be drawn. However, this airfoil also contains the different parts that are used to fix the wing to the aircraft. Indeed, the front of the wing is blocked into a special cavity of a section of the fuselage while the rear of the wing is screwed in the fuselage. That way, the wing is maintained in place. This means that there is an extension to the form of the ribs to have the form that will enter the cavity while they are reinforced at the back to make sure that the wood will resist to the screws.

Using the N-10 airfoil, it is possible to estimate the aerodynamic properties such as the lift coefficient that is of interest in order to compute the stall velocity. In order to do that, *Xfoil* is used. These properties also depend on the Reynolds number. Therefore, it is computed in Eq.3 considering a cruise velocity of $16\ m/s$, a wing chord of $0.38\ m$ and a kinematic viscosity of $1.5 \times 10^{-6}\ m^2s^{-1}$.

$$Re = \frac{UL}{\nu} = \frac{16 \times 0.38}{1.5 \times 10^{-6}} \approx 4053333 \tag{3}$$

Using this value of the Reynolds number and a Mach number of 0.048, which corresponds to the previous velocity, it is possible to compute the lift coefficient for different angles of attack. The result is shown in Fig.16.

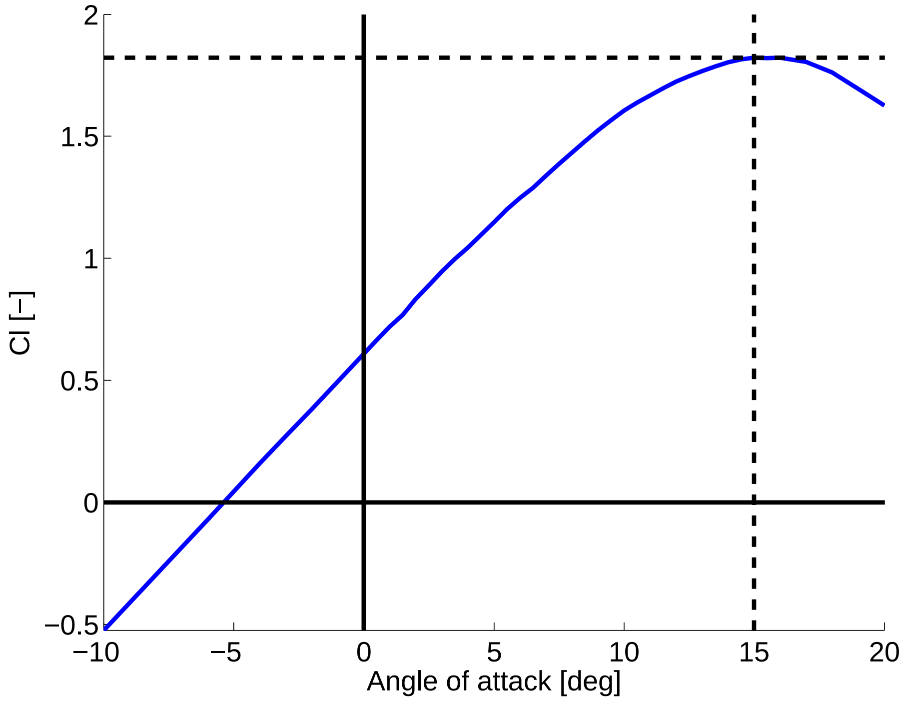

Figure 16: Lift coefficient (Cl) with respect to the angle of attack.

From this figure, it is possible to determine the maximum lift coefficient, which is 1.82. To compute the stall speed, the 3D maximum lift coefficient is required. It is approximated by using Eq.4, from [33], where k_s is taken to be 0.88 because the wing is not tapered.

$$CL_{max} = k_s \frac{Cl_{max,root} + Cl_{max,tip}}{2} = 1.6 \tag{4}$$

Then, the stall velocity is given using Eq.5 and considering a mass of $5.6\ kg$, a wetted surface of $0.795\ m^2$ and an air density of $1.225\ kg/m^3$.

$$V_{st} = \sqrt{\frac{2 \times W}{\rho \times S \times CL_{max}}} \tag{5}$$

Using such a technique, a stall velocity of $8.39\ m/s$ is obtained. However, this has to be taken with care because some estimates were made in the computations such as the exact mass because it varies with the fuel consumption. When the plane was weighted, the fuel tank was nearly empty. Any increase in that parameter will tend to make the stall velocity higher. Other features such as a camera under one part of the wing can also affect the lift produced and, consequently, reduces the maximum lift coefficient. Therefore, it is better to consider a higher velocity of the stall velocity such as $9\ m/s$. It will be discussed further but in order to give a sufficient safety margin with respect to the stall velocity while flying autonomously, a minimum airspeed of $11\ m/s$ is imposed to the autopilot.

2.2.3 The landing gear configuration

Another feature that will influence the beginning and the end of each flight is the disposition of the landing gear. The present plane is a tail-dragger meaning that it has a main landing gear, close to the centre of gravity, and a small wheel below the tail.

Generally speaking, two main types of landing gear exist: the tricycle (or nose-wheel) and the tail-dragger configurations. The large majority of planes use the nose-wheel configuration because it is usually much easier to handle in take-off and landing, in particular on a paved runway. On the other hand, the second configuration offers a reduction in drag compared to the first one. Additionally, it is said to be better when landing on grass or on rough surfaces because a nose-wheel can be fragile.

Furthermore, it is important to notice that the small wheel (under the tail) is fixed and cannot rotate. This means that the plane is nearly impossible to control on the ground at low velocities because the rudder is not sufficient to change the direction. Active control is only provided when the velocity is sufficient to raise the tail from the ground. Additionally, as the plane takes off in a straight line, it is important to make sure that no obstacle (e.g. small stones or holes) is present in the trajectory. Otherwise, the plane could brutally change its direction with potentially dangerous consequences for its integrity.

Consequently, in the RC world, there is not a large difference between the two configurations of landing gear and the one that is used here is the tail-dragger one. Actually, this leads to additional parameters compared to the tricycle landing gear while adjusting the parameters of the autopilot. This will be discussed in sections 6.3 and 6.4 about automatic take-off and landing.

2.2.4 Others features

Regarding the structure of the different parts of the plane, it is mainly a truss structure covered with a MonoKote. The truss structure made of wood gives the properties of rigidity, resistance as well as the shapes of the different parts. On the other hand, the MonoKote, which is a type of thin thermo-retractable layer of plastic, is the skin used to guarantee the aerodynamic but also a level of protection against moisture or the oil contained in the fuel.

Below the wing, there are two different spaces to fit different items. The bottom one, which is accessed like a drawer, serves as a payload bay. Additionally, it has a trap door. In this project, this part of the plane was kept empty but a retractable camera can be installed there (like it was done before). The second space is much smaller and is a volume of a height about $5\ cm$ located between the payload bay and the wing. In this work, it is called the control bay. This control bay and the payload bay are shown in Fig.17.

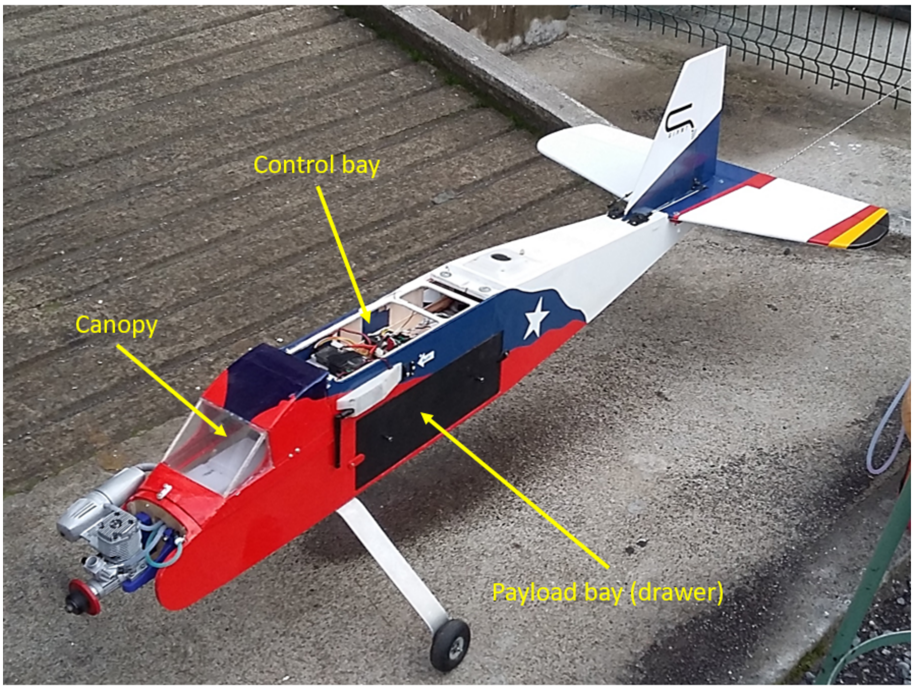

Figure 17: Photo of the plane during a motor test.

Another characteristic of the front part of the fuselage is the canopy, which can be easily removed to access a volume where the fuel tank is. However, behind the tank, there is also a free space. It will be used in order to install the battery of the autopilot.

All in all, this aircraft stands out from the ordinary by its dimensions and propulsion system. From its wing configuration, it is a very stable airframe that is advantageous to record videos but that is not suitable for acrobatics or races. Additionally, it was used to place cameras and, during this work, a guideline for the integration of the flight controller and its components is to keep places for the re-installation of the different cameras in the plane.

3 Radio Controller Taranis X9E

The radio controller used throughout the realisation of this project is the *Taranis X9E* that is owned by the University of Concepción. This radio differs from the vast majority of the control radios in the RC world because it is fully programmable. As a result, the first task is to configure all the different menus and options in order to assign the movements of the different control surfaces of the plane (and also the other necessary actions). The radio itself is presented in Fig.18. The original battery was replaced because it was having voltage issues when there was a change in the ambient temperature, probably due to a problem with the battery internal resistance.

Figure 18: Photo of the radio *Taranis X9E*.

3.1 Pulse Width Modulation (PWM)

Firstly, the type of signals used for the transmission of the information between the different elements is presented. The instructions sent over the different channels of the radio are of the form of PWM signals. A typical signal is shown in Fig.19. This is actually a common way to transmit a proportional control signal to a servomotor. The signal is a square wave that oscillates according to a frequency and a duty cycle. The frequency is how often the pulses are repeated while the period, the inverse of the frequency, characterises the time required for a cycle. On the other hand, the width of the pulse is given by the duty cycle.

In the figure below, a PWM signal with a duty cycle of 0% has no pulse while if it is at 100%, the signal is always at its maximum. If the duty cycle is of 25%, the pulse will last during one-quarter of the period.

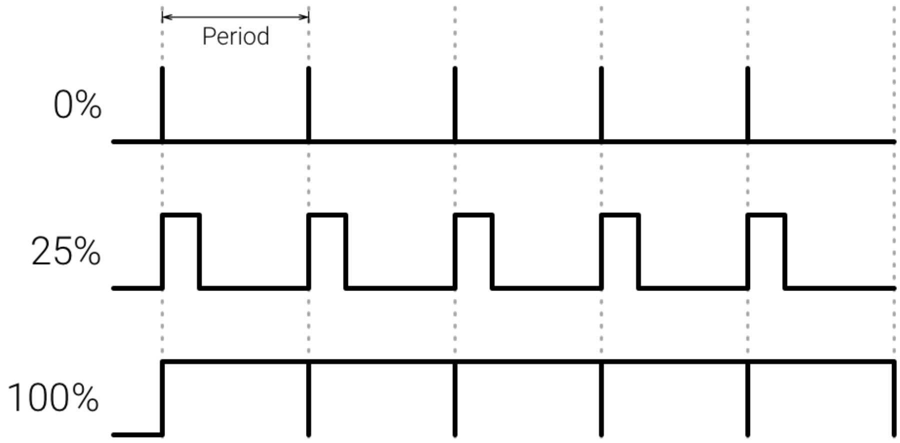

Figure 19: Examples of PWM signals [28].

A typical receiver has a frequency of about $49\ Hz$ while the frequency of the output of the autopilot is ten times higher. Consequently, the duty cycle is used to modulate the signal according to the instructions. In the rest of this report, the term PWM refers to this type of signal and is measured in μs, which corresponds to the time that the signal passes at its maximum value.

3.2 Configuring the radio

Different sets of options have to be configured to obtain a system that does the job correctly. The baseline is to define what are the different inputs that are given to the radio, then to tell the radio what to do with the human inputs and finally select the outputs. When creating a new model in the radio[1], the main four standard functions regarding the basic control surfaces can be assigned through a graphic interface. These were modified afterwards to consider additional features as explained hereunder.

The inputs

In the menu *Inputs*, the different inputs that the pilot can deal with are written. In addition, a button is also associated to that input. This obviously includes the main controls: the elevators, the throttle, the rudder and the ailerons. These are controlled using the sticks. Their assignment is free but four configurations dominate the RC world. In this work, the configuration known as *Mode 1* is used to pilot the vehicle. The movements are controlled such as represented in Fig.20 where the right stick is used for the throttle and the roll while the left stick deals with the pitch and the yaw. The choice is simply based on the habits of the flight instructor as well as those of the University of Concepción.

[1]As the radio can be programmed in order to be used for different planes, a model gathers all the different parameters for a given aircraft.

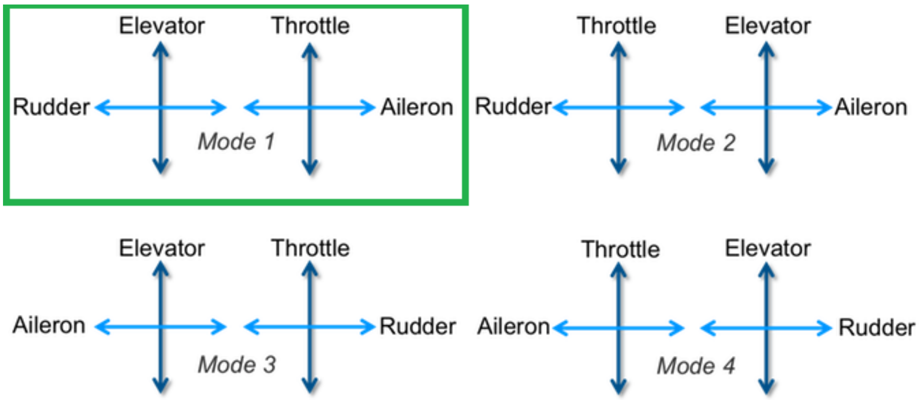

Figure 20: Configuration of the main modes for the assignment of the commands to the radio transmitter. In this work, *Mode 1* is used.

Two other specific commands are going to be set: one six-position switch is used for the flying modes and another switch is used to activate or deactivate the geofence feature as it will be explained later in the report. A geofence is a border that should not be breached by the plane. If it is breached, the aircraft automatically goes to a specific point. The other switches do not require to be set in this menu because no special function is given to them. An action will be assigned if they are in a particular position but they will not influence the behaviour of the aircraft directly because their signal is not sent through a channel to the receptor.

In the meanwhile, as can be seen in Fig.21, the ailerons and the elevators have two lines because a dual-rate was implemented. It is used if you want to pilot more acrobatically or more gently. Indeed, in the first case, the total deflection of both control surfaces is available while, in the second case, only 60% of the deflection is possible.

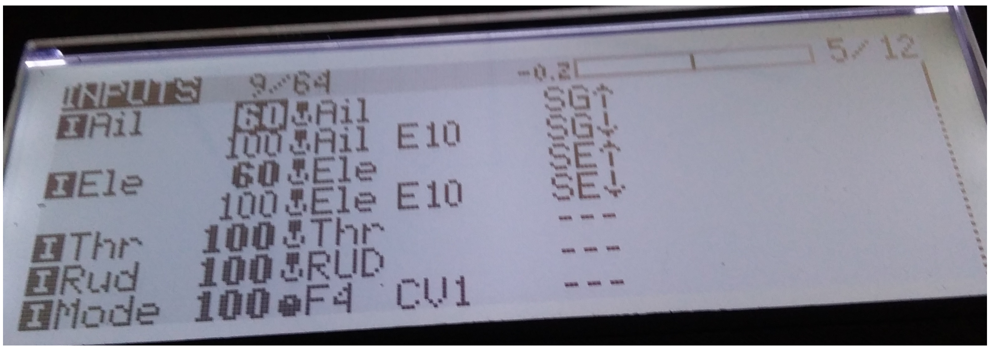

Figure 21: Menu of the inputs of the radio.

Additionally, as seen in Fig.21, it is possible to modify the different switch or stick actions. By default, the value given is proportional to the displacement of the stick. For instance, if you move the stick at mid-course, the mid-value will be given. This is illustrated in Fig.22 with the blue and the green curves. However, it is possible to modify this behaviour. In the figure of the inputs, this was done by adding exponential to the ailerons and the elevator. This has the consequence that the region around the neutral position is less sensitive to the movements of the stick as shown with the red curve of Fig.22. However, although it is called "exponential", an exponential function is not used. Indeed, it is Eq.6 that is considered where k is the so-called exponential parameter chosen by the user, x the percentage of the stick movement and y the percentage of the surface deflection.

$$y(x) = \frac{1}{256}\left(\frac{k \times x^3}{1024^2} + x(256 - k) + 128\right) \tag{6}$$

Moreover, this curve is also constrained to pass by a specific set of points entered by the user. It is recommended to, at least, enforce the extremities $(-100, -100)$ and $(100, 100)$ as well as the neutral point $(0, 0)$. In such a way, when the stick is at the maximum (resp. minimum) value, the surface deflection is also at its maximum (resp. minimum). The neutral position is also important because it corresponds to the position that the stick has if the pilot is doing nothing. The addition of the exponential parameter to a curve might ease the piloting of the vehicle and this choice depends on the pilot's preferences.

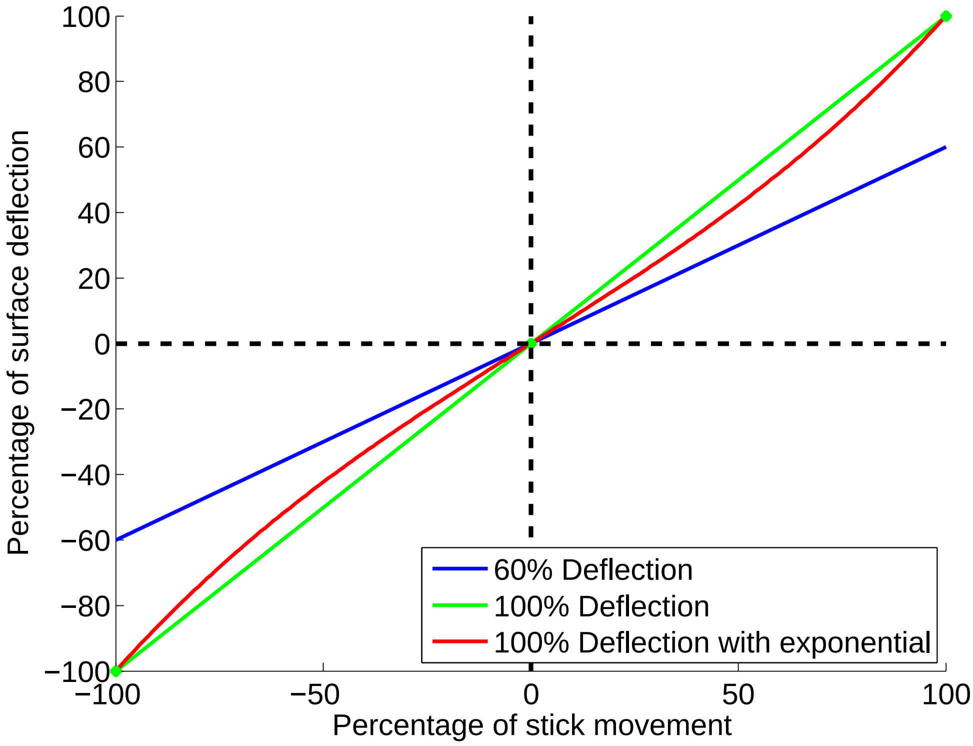

Figure 22: Different possible curves used to modify the behaviour of the control surfaces.

Furthermore, the behaviour of the six-position switch is modified by a special curve. The reason for this actually depends on the operation of the autopilot. Indeed, six flight modes will be accessible from the radio through this six-position switch. However, the flight controller uses different ranges of PWM signals to determine the mode that is currently activated by the *Taranis*. Consequently, the PWM emitted by each position of the switch needs to be more or less at the middle of an interval of the flight controller. Indeed, at the beginning, the six positions of the switch corresponds to PWM taken at equally distant intervals between the minimum and maximum PWM emitted but this does not work with the autopilot. This is indicated in Table 2.

Mode number	Autopilot range [µs]	Switch (initial) [µs]	Switch (objective) [µs]	Percentage [%]
1	0-1200	1000	1000	-95
2	1231-1360	1200	1300	-40
3	1361-1490	1400	1410	-18
4	1491-1620	1600	1530	6
5	1621-1749	1800	1700	40
6	1750 +	2000	2000	95

Table 2: Table presenting the different PWM required to be outputted by the radio controller to correctly represent the selected mode of the autopilot.

By comparing the second and the third columns of the table, some flight modes of the autopilot will never be used (mode 2 and mode 5) if nothing was changed. Other values are close to the limitations of the range imposed by the flight controller and it is always better to be towards the middle of an interval. It is a philosophy to have additional safety because it could cope with small mistakes of the values.

The PWM sent by the *Taranis* is modified in order to obtain the PWM indicated in the fourth column of Table 2. To achieve this, a curve with six points is edited (in the page *Curves*). The x-axis represents the different points and are equally spaced. The y-axis is the percentage of PWM that is going to be sent for a given position of the switch. -100% is a PWM of 1000 µs, which is the minimum signal sent to the channel while 100% is the maximum signal, which corresponds to a PWM of 2000 µs. The 0% is the neutral position, which is 1500 µs. The percentages corresponding to the objective values are therefore computed in between. These are the values that are entered in the radio to build the curve, represented in Fig.23.

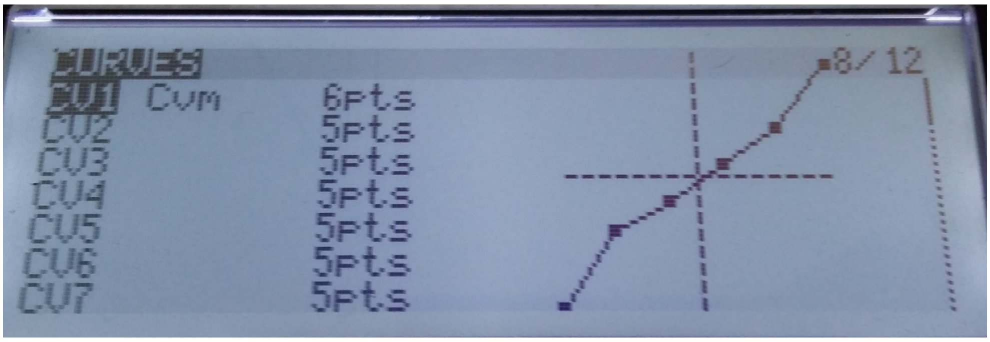

Figure 23: Curve used to modify the PWM of the channel in order to have the flight mode corresponding to the switch position.

By using this curve to modify the PWM outputted on the transmission channel, the appropriate flight mode of the autopilot is therefore correctly selected according to the switch position.

The mixer

This menu is where the radio will know what to do with the given inputs. The plane, as described below, has a classical wing and tail configuration. As a result, most of the inputs are simply passed through to the outputs. However, if differential ailerons were used, for instance, it is the place where this could be implemented.

In this menu, it is also decided which channel will be used to control a given input. As seen in Fig.24, six channels are necessary to transmit all the necessary information from the receiver of the radio controller to the flight controller in order to control the plane. For example, the first line means that 100% of the input named ail (defined in the menu *Inputs*) is passed to channel 1. Although the last two channels were purely the choice of the author, the first four appear to be a standard considered by a lot of people (and by the University of Concepción).

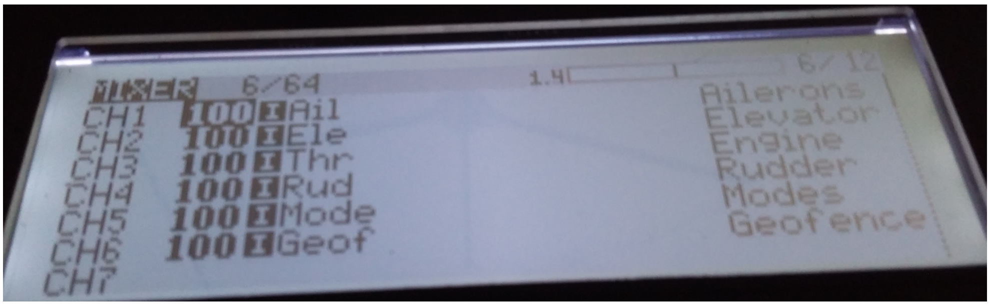

Figure 24: Menu of the mixers of the radio.

The output

This menu shows how the information has been interpreted and what is actually sent to the servomotors[2]. In this set of options, it is also possible to sub-trim, on the ground, the model. It is also possible to visualise the trim applied in flight there. Trimming an aircraft is used to correct slight defects in the airframe in order to keep a correct neutral position i.e. to fly level without inputs from the pilot. A better technique is obviously to modify the mechanical arm of the servo in order to avoid to use trims.

In this menu, it is also possible to reverse the way the control channels work. This should be checked before a flight in order to ensure that the control surfaces move in the right direction for a given input [3].

Special functions

This menu is used to design special functions to have some specific actions and is illustrated in Fig.25. It is the place where actions that are not passed directly through the receiver are implemented. Nevertheless, these might influence the commands of the stick. For instance, there is a security switch that, when activated, it is impossible to accelerate because the channel corresponding to the throttle is over-written. Although it has a limited use here because the plane has a combustion engine, with an electric aircraft, it is important in order to guarantee that once the battery is connected, the propeller does not start rotating because the throttle stick was not at its minimum position.

[2]Actually, as a flight controller is used, the receiver sends its information to the autopilot and its outputs are sent to the servomotors. These might or not differ from the commands given by the radio depending on the flight mode selected. Additional details are given in the section regarding the flight modes.

[3]This is part of the check-lists that have to be performed before any flight to ensure that the plane as well as the autopilot work correctly and are ready to fly. Those used for the flight tests are given in the appendix C.

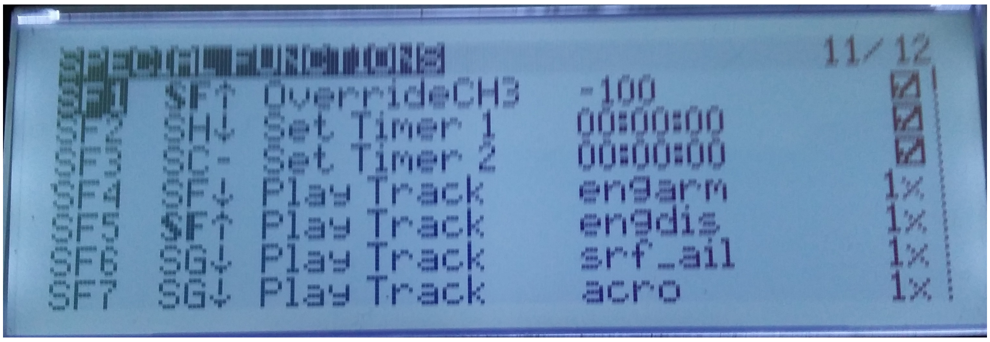

Figure 25: Menu of the special functions of the radio.

Additionally, other functions impacting only the radio can also be implemented in order to ease the work of the pilot. For example, it is possible to attribute a function of reset of the chronometer to a switch when it passes in a given position. This is particularly useful to monitor the flight time. This chronometer starts only when a first acceleration is given with the throttle and is reset with the corresponding switch. Another chronometer can also be used: this one modifies the rate of the time according to how much throttle is used.

Moreover, it is possible to play sound tracks when switches are changed. This helps to make sure that the right switch is in the right position. For instance, it is used to tell the flying mode when the flight mode is changed. Different sounds are played when changing from acrobatic to sport or vice versa. Eventually, a beep-sound is played every $5\ s$ when the geofence is activated to warn the pilot that it is activated because it might be impossible to land when it is switched on as it will be explained afterwards.

3.3 Binding the receptor

In the plane, it is necessary to install a receptor (also called receiver), as shown in Fig.26. This device has two antennas that receive the information from the radio. In turn, it will then send to the corresponding servomotors the right electric signal if no flight controller is used. If an autopilot is installed, instead of transmitting the information to the servomotors, the signals will be given to the flight controller, which is the device that will control the servomotors.

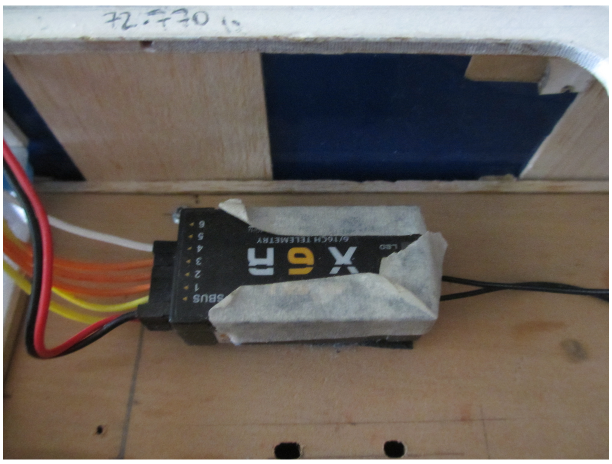
Figure 26: Photo of the receptor installed in the plane and bound to the *Taranis X9E*.

To have a communication between the radio and the receptor, they have to be bound together. This aims to establish a recognition link between them and to avoid that, if several pilots are flying in the same area at the same time, interferences occur between the different radios and receptors.

This is relatively simple: it is necessary to go in the binding option of the radio and, while this option is blinking (meaning that the process is engaged), powering on the receptor by pushing the failsafe switch. The failsafe switch is pushed until the red blinking light of the receptor becomes solid green.

Actually, the light of the receptor helps to see the state of the connection:

- if it is off, it is likely that there is a wiring or power issue.
- if it is red (and blinking), it looks for the RC radio to be connected.
- if it is solid green, there is a communication with the RC radio.

It is easily tested by connecting a servomotor to one of the outputs of the receptor.

In this section, the configuration of the radio as well as the philosophy hidden behind the radio has been depicted. This radio is the first element to this work because it would have been impossible to make any test or any flight without it.

4 The autopilot

The autopilot is the central device of this work. It is actually the tool that is used to accomplish the autonomous flight. It collects the data from several sensors in order to determine what is the current attitude of the aircraft and, then, sends the correct outputs to the different parts of the plane to fulfil the given mission.

At the beginning of the work, a problem occurred with the autopilot caused by a deficient regulator of voltage of $3.3\ V$. This component was rather challenging to replace by a new one because the soldering tools of the laboratory are not adequate to solder surface mounted devices (smd). Indeed the component has five little legs and is very small: about $1\ mm$ x $2\ mm$. In order to remove the old component, hot air was used, but the new one was soldered using the traditional tools of the laboratory and the technique explained in the appendix B.1. After the repair, it was checked that the correct voltage was being delivered to all the outputs of the flight controller board.

4.1 APM vs. Pixhawk

During the course of this work, the autopilot used is the *APM 2.6*; it is a widely used autopilot (which is now replaced by the *Pixhawk*) whose source code is open source. The user manual as well as the code can be obtained from the website ArduPilot [20].

The main difference between the *APM 2.6* used along this thesis and the new version of the autopilot, the *Pixhawk*, is the memory. Indeed, the last firmware version that is available for planes on the *APM 2.6* thoroughly uses the memory of the board. It means that a piece of the information given in the website, regarding the *Pixhawk*, had to be adapted or could not be used. Moreover, some minor changes in some algorithms are not available and it is impossible to use a sensor of distances. However, the work was carried out without any serious problems due to this lack of space in memory.

4.2 The firmware

Throughout its evolution, the ardupilot family has passed through a series of updates with constant improvements of the autopilot. However, as explained just above, an *APM 2.6* is used to realise this work and the last firmware developed cannot fit this board due to a problem of memory. The firmware that is used in this project is the *ArduPlane 3.4*, which is the last one that can be flashed using the *APM 2.6*. However, already for that firmware, memory issues started to arise and not all the functions of that release are available.

4.3 The hardware

A photo of the *APM 2.6* is presented in Fig.27, which shows the enclosure of the flight controller. A number of ports are present around the autopilot in order to connect different devices. Indeed, the autopilot on its own is unable to operate properly. As a result, other instruments have to be added to the system. The complete electronic circuit, which includes the autopilot, is discussed in detail in the following paragraphs.

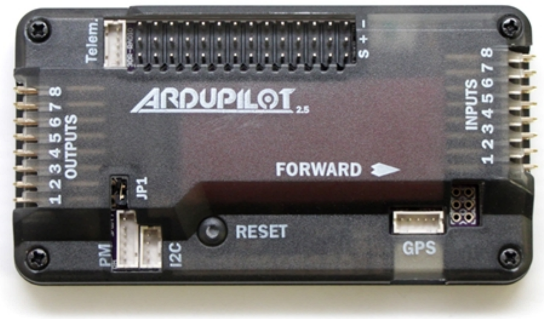

Figure 27: Photo of the flight controller *APM 2.6*.

From Fig.27, it is already possible to briefly explain what are the main interactions with the system. First of all, the autopilot requires an external source of power, to be supplied by a battery placed in the plane. Then, in the right side of the figure, the input pins collect the information passed by a receiver. This corresponds to the commands given by the radio *Taranis X9E*. In other words, these are used, for example, to control the plane manually as if there was no autopilot. On the other side, the output pins are connected to the different servos of the plane and are used to actuate the control surfaces as well as the engine. Moreover, a telemetry port is present in order, for instance, to monitor the behaviour of the aircraft in real time with a ground control station such as a computer. Finally, a series of other pins is also available to connect other external devices.

The autopilot also includes different on-board sensors. The main elements of the board are shown in Fig.28. They include an inertial measurement unit (IMU) which consists of a three-directional accelerometer and a three-directional gyroscope. The IMU is used to determine the attitude of the plane during flight. It needs to be calibrated according to the instructions before being used. Finally, a barometer is also present and is used to determine the altitude of the vehicle.

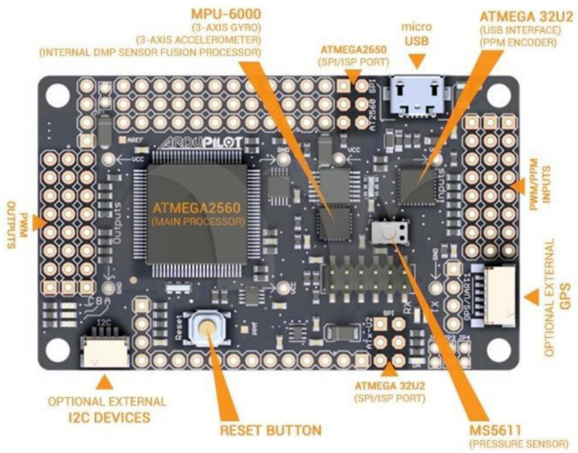

Figure 28: Main elements of the board of the *APM 2.6* [37].

4.4 Powering the flight controller

It is critical to understand how the different components or input/output pins can be powered. There are actually two power circuits that can be dependent or not. As can be seen in Fig.29, it is possible to add a jumper to the board. If the jumper is used, the board will be completely powered with the power module port or the USB cable while if the jumper is absent, the output rail is disconnected from the main power circuit. As a result, the output pins need to be powered separately. In this work, the latter configuration is adopted because the servomotors that will be connected to the output pins and that will actuate the control surfaces can drive too much current from the board and, eventually, damage it. The other option might be useful if the APM board is used as a measurement device with additional sensors connected to the outputs.

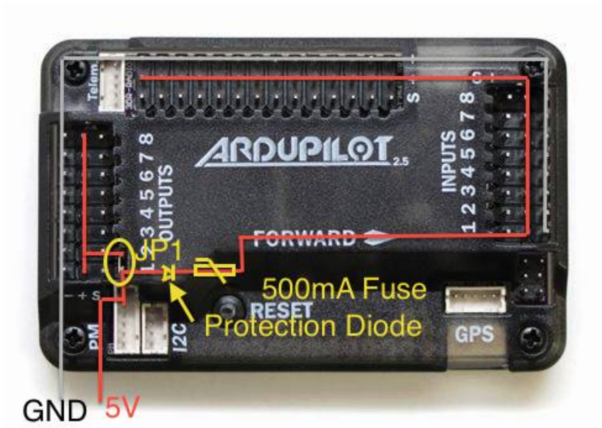

Figure 29: Power distribution lines in the autopilot [20]. This is a photo of the *APM 2.5* but the energy distribution is exactly the same as for the *APM 2.6*.

In addition, the board can be powered in two different ways. The first one is using the USB port to power the board from the computer. However, this does not provide sufficient current to play with servomotors, but is useful to access the memory and to download it. The other method is obviously to take the energy from a battery as it will be explained in the following paragraphs that present the different external required components.

Both the servomotors and the flight controller work with a voltage of $5\ V$ but need different currents. Indeed, the autopilot functions with a current of $0.5\ A$ while the servomotors might require a much higher current, which might go up to $5\ A$. The $0.5\ A$ in the autopilot explains the need of a $500\ mA$ fuse: it is to protect the board against currents that are too high.

4.5 External sensors

In order to ensure adequate operation of the autopilot and to fly autonomously, the flight controller should be integrated within an electronic circuit, which consists of different elements. These are required either to give energy to the flight controller or to give information about the attitude of the aircraft. The following paragraphs describe the circuit represented in Fig.30, which is the diagram representing the heart of the system. In addition, they aim to briefly discuss the working principles of some of the different components.

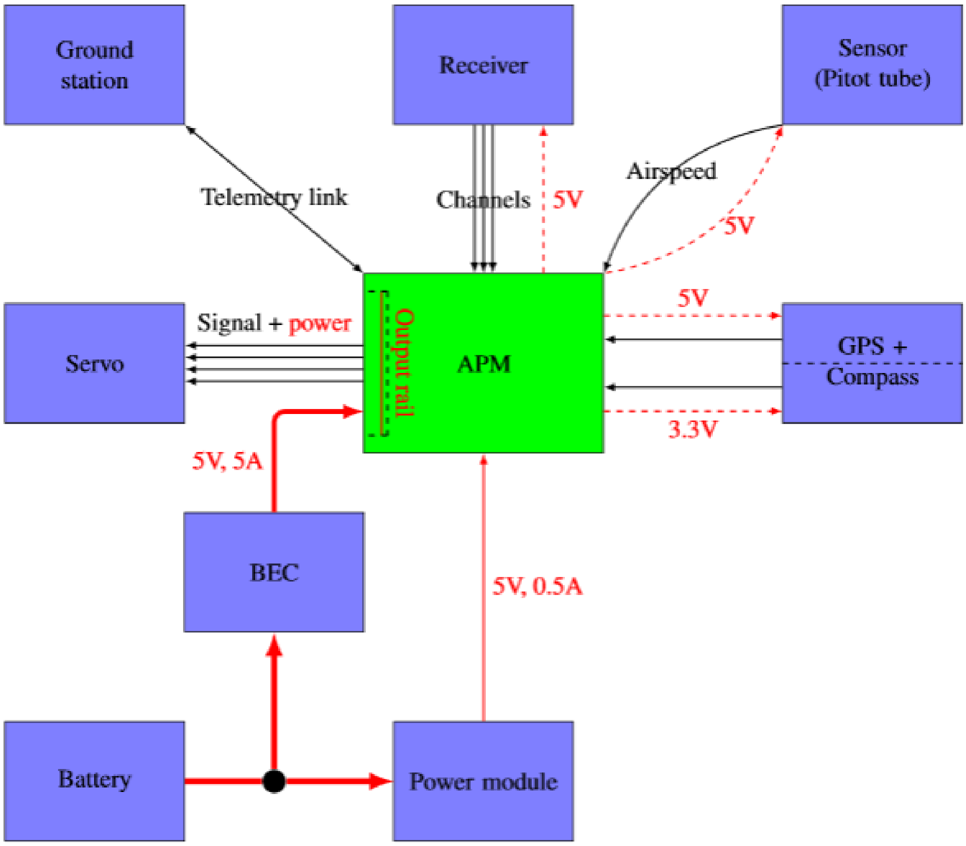

Figure 30: Scheme of the different components that are used with the autopilot.

4.5.1 Energy supply

The complete system is powered using a battery. However, the APM board can only work with a given voltage and current which are $5\ V$ and $0.5\ A$. As a result, in order to power the hardware safely, a power module is used. The role of this component is therefore to give to the autopilot the correct amount of electric current and voltage. In other situations, where the engine is electrically powered, the power module can also deliver the required energy.

The outputs need to be powered by another source as discussed above. Therefore, a battery elimination circuit (BEC) is used to transform the current produced by the battery in one that can be used to power the servomotors. They require a voltage of $5\ V$ and a current up to $5\ A$ because of the geometry of the aircraft, which is not that small for a RC plane.

Furthermore, the servomotors of the control surfaces are linked to the output rail of the autopilot. Basically, a servomotor is connected using three wires: the black one is the ground, the red is the positive, used as a reference, and the last wire, orange or white, is the signal indicating the position that the servomotor should have.

Other instruments are also used. From an electrical point of view, they are all powered by the $5\ V$ voltage that the hardware delivers at their port with the exception of the compass that uses $3.3\ V$, but there is a voltage regulator that does the conversion on-board the autopilot. These components are presented below in separate paragraphs for the sake of clarity.

4.5.2 Pitot tube

This instrument is used to measure the velocity of a fluid that flows around it. A schematic representation of a Pitot tube is given in Fig.31. The measurement consists in the difference between the static and total pressure. The static pressure is measured by the pressure tap parallel to the flow (point B), which should not be directly affected by the velocity and measures only the atmospheric pressure. On the other hand, the other tube (point A) measures the total pressure, which is the ambient pressure and the one caused by the velocity.

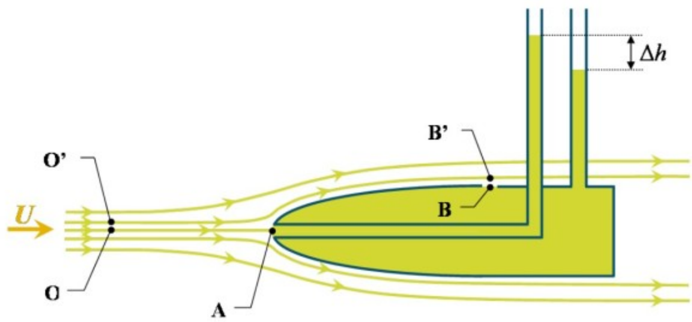

Figure 31: Schematic representation of a Pitot tube [25].

In order to obtain the velocity of the flow, Bernoulli's equation is used. The total pressure can be written as the sum of the static and dynamic pressures in Eq.7.

$$P_t = P_s + \frac{1}{2}\rho v^2 \tag{7}$$

The air density ρ is calibrated when the board is powered according to Eq.8.

$$\rho = \frac{P}{R \times T} \tag{8}$$

where R is the gas constant for air. The pressure is based on the barometric measurement while the temperature is the minimum between the barometer temperature and $25°C$ (converted in Kelvins). After, a correction is applied according to the altitude at which the plane is flying. The temperature is not actualised because it could lead to some issues as the electronics is warmed up. In addition, the Sun can also impact the measurement.

Solving Eq.7 for velocity leads to

$$v = \sqrt{\frac{2(P_t - P_s)}{\rho}} \tag{9}$$

In order to use this instrument, the information needs to be converted electrically through a pressure transducer. The latter is placed close to the Pitot tube installed in the wing of the plane. The conversion is accomplished through the deformation of a physical diaphragm, which introduces strain to the gages. In turn, this strain generates a modification of an electrical resistance that is proportional to the pressure. The system measures a pressure between -2 and $+2\ kPa$ with a typical error of $2.5\ \%$ [39].

As a remark, the difference of pressure between the two holes of the Pitot tube is not very high because the velocity is low in the current application. Therefore, it might be difficult to obtain accurate measurements as the error of the instrument might be relatively large compared to the values it measures. This will be observed in the analyses of the results: when the plane is at rest, a speed is indicated but when it is flying, the Pitot Tube is in its good range of operation and works accurately.

In addition to that, the measurements have to be taken away from any boundary layers, engine wake or any other source of perturbations of the flow. This means that particular attention is needed when installing the Pitot Tube in the aircraft as explained in section 4.6.

4.5.3 GPS

The GPS or General Positioning System is the instrument used to determine the position of the aircraft. It is based on a constellation of satellites, which orbits the Earth at a distance of $20,000\ km$. In order to have a relatively accurate measurement of the position of the plane, the receiver module must see several satellites. It operates based on two pieces of information. It is necessary to know the position of the satellites, but also the distance between each satellite and the receiver. This principle is illustrated in Fig.32.

Satellite position is obtained from the almanac, which consists of generic satellite constellation data. From this time table, the receiver is able to determine which satellite is in view and can be used. The almanac is permanently broadcasted by all the satellites. Moreover, the receiver also receives the information of the ephemeris, which concerns the orbit of the observed satellite.

The ranging between the receiver and the satellite is calculated by measuring the time required by a radio signal to travel from the satellite to the receiver. The distance is the product of the velocity, which is the speed of light, and of that time.

Theoretically, to apply the process of triangulation, three satellites should be enough. However, the error would be significant because the receiver does not have an accurate enough crystal to measure the time. Consequently, when all the measurements are correct, the four spheres in Fig.32 should intersect in a single point, which is the position of the receiver.

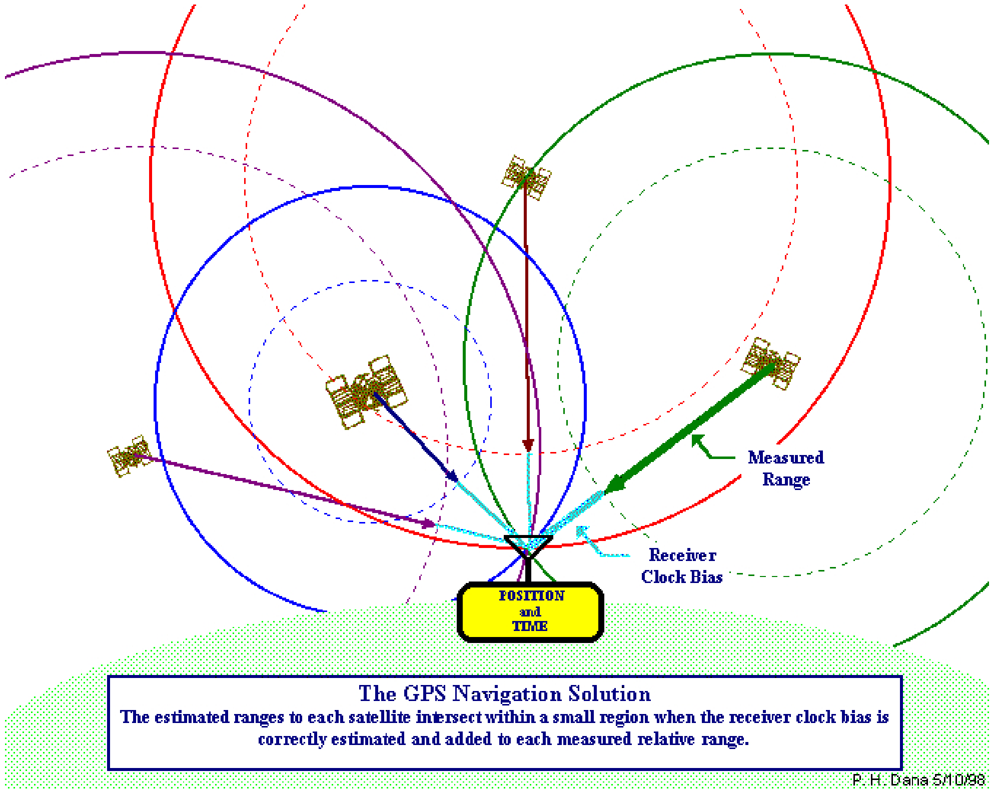

Figure 32: Principle of GPS localisation [26].

Nevertheless, the use of additional satellites is often required to improve the measurement because different sources of errors can alter the expected result. These sources include the following

- Satellite clock
- Receiver clock
- GPS jamming
- Atmospheric errors
- Multipath error

The two first have the most significant effect. Multipath errors are mainly present close to buildings or mountains where the waves could be reflected. However, the club of aeromodelism used to test fly the aircraft is situated in farmland and this phenomenon is negligible. The same is true regarding the atmospheric errors, which might be caused by bad weather such as clouds or rain. However, it is impossible to fly the present aircraft when there is too much wind or when it rains. GPS jamming is caused by interferences with other devices, which are often prohibited by law.

Considering these errors, in practice, more than six satellites are needed to obtain a correct estimate of the position. During the flights, this was never an issue because more than nine satellites were always available (between nine and fifteen satellites).

4.5.4 Compass

The compass is an instrument used to supply the plane heading to the autopilot based on the Earth magnetic field. Concerning planes, this instrument is not a requirement in flight because the velocity is sufficient to give an accurate direction with the information from the GPS. The only moment where the compass is important is to keep the heading during the first phase of an automatic take-off because the plane has initially no velocity and therefore the GPS is inaccurate. As a comparison, the same is often observed with a GPS in a car; while it has not started to move, the indicated heading is often wrong.

Other types of vehicles like copters or quad-planes which may operate at low speeds or even be stationary need to have a compass on board during the flight in order to tell the autopilot what is the current heading.

Additionally, the compass is an element influenced by all the magnetic sources in its environment. These include the difference between the real magnetic declination of the Earth and the North pole, which differs from place to place. The magnetic declination can be acquired automatically using the GPS position or simply given to the autopilot manually.

The compass is also influenced by all the metallic parts of the plane and a magnetic offset is computed based on a calibration manipulation. This consists in turning the plane along all the directions in order to teach the plane what the heading should be. Another solution, only available for planes, is an automatic procedure along during the offset is learned automatically by means of a first flight.

Furthermore, it is important to keep the compass away from magnetic sources present in the UAV: the battery, the engine, the wires, etc. It is the reason why this component is placed away from all the others: this is explained in further details in the section corresponding to the installation of the flight controller and its components in the UAV.

4.5.5 Telemetry radio

It is possible to communicate with a ground station (a computer) during the flight. This is particularly useful to adjust the parameters of the autopilot in order to teach it the way the aircraft reacts. Moreover, it gives also the possibility to monitor flight data and the progress of the mission directly.

In order to establish the communication between the aircraft and the computer, a telecommunication link based on two antennas is established. One of the radio used in the present project is shown in Fig.33. Two models of the radio are available with a different frequency depending on the laws of the region in which the plane is flown.

Figure 33: Photo of an antenna used to establish the communication link between the ground station and the plane.

In order to ensure communication between the correct antennas, the same identification number should be used for both of them. This can be easily changed using *Mission Planner*, the software used to configure the flight controller, which allows the user to update the firmware of the antennas and also to change the ID numbers. Additionally, these antennas have two LEDs (Light Emitting Diodes) indicating their status.

- Off: No power.
- Green blinking: Looking for another antenna.
- Green solid: Telecommunication link established.
- Orange blinking: Transmitting information.
- Orange solid: In firmware updating mode.

Furthermore, the antenna can be rotated if necessary. Different configurations were tested but no major difference was observed. The range of communication is indicated to be around $500\ m$, but it was observed that the antennas still work for a greater distance (tested up to about $900\ m$). However, the space between the antennas should be cleared of any obstacle to reach that distance.

4.5.6 Receiver

This last component has already been discussed in section 3 because it is the device that is used to communicate with the radio controller. Each channel is connected to the corresponding channel of the inputs of the autopilot. By default, the autopilot uses the same channel numbering scheme as the one selected for the radio controller. Table 3 details the channel numbering of the input rail.

Channel (autopilot)	Function	Channel (receiver)
1	Ailerons	1
2	Elevators	2
3	Throttle	3
4	Rudder	4
5	Flight modes	5
6	Geofence	6
7	Not used	/
8	Energy supply of the receiver	SBUS

Table 3: Table presenting the connections between the autopilot input channels and those of the receiver.

As seen in the table above, the receiver is powered by the autopilot connecting the power source as well as the ground between the two components (last line of the table). Indeed, all the channels share the same ground and energy reference. Therefore, giving energy to one will power all the rest. On the receiver side, the SBUS connection is used: this is normally used to transfer information from several channels with a single cable. However, for the sake of clarity in this project, it was preferred to use common (basic) connections and to employ the SBUS to connect the energy source. The reason was also that, at the very beginning, there was only four channels used: those for the control surfaces and the throttle. The two others were added afterwards. In the future, if additional functions are needed to be transferred to the autopilot, some modifications in the wiring between the two components should be made and the use of this SBUS plug could be a solution.

4.6 Integration of the electric circuit in the plane

The different components discussed above have to be installed in the aircraft. However, their positions cannot be arbitrary because some of them have specific requirements. Moreover, the philosophy while placing them in the aircraft is to still be able to install the cameras. As a result, the different sites where cameras were fixed before the present project remain free. These sites include the drawer (payload bay), the cockpit and the camera of the wing (only the latter is physically present during the work).

4.6.1 The flight controller

The flight controller is placed in the control bay: the area above the drawer just below the wing, shown in Fig.34. In such a way, it has the advantage to be placed close to the centre of gravity of the plane, which should be located $100\ mm$ behind the leading edge of the wing. The centre of gravity is discussed in section 4.7.

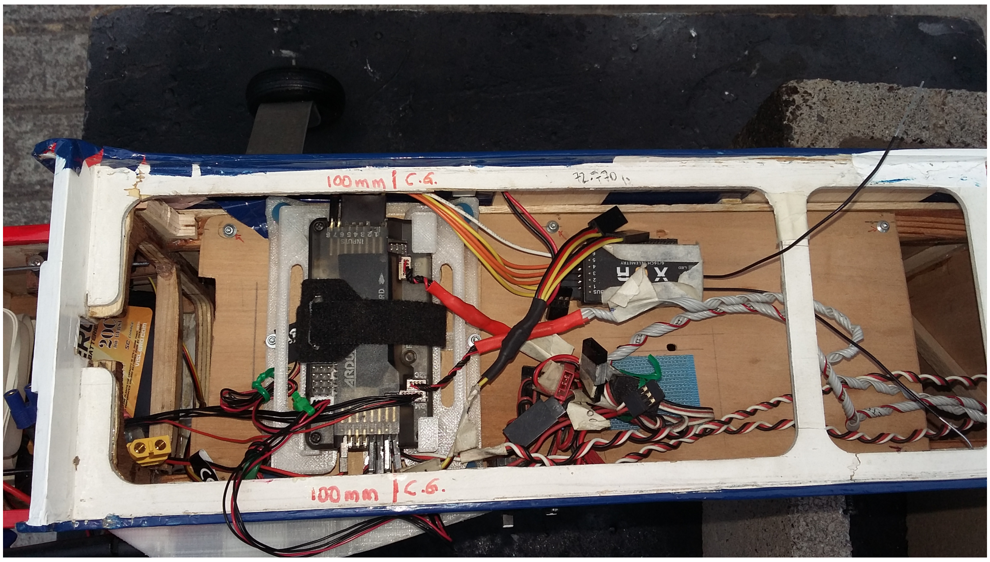

Figure 34: Photo of the control bay with the autopilot and the receiver installed. The complete wiring of the flight controller is also present.

The autopilot was not placed in the default orientation but was rotated in yaw by $90°$ (to the right). This orientation allows easier access to the USB plug, which lies to the left of the board. Indeed, between two flights, using this orientation, it is possible to access the memory by removing the canopy only and not the entire wing. This is much more practical. It is therefore essential to configure the autopilot using the correct (non-default) orientation.

The plane uses a combustion engine, which tends to produce a lot of parasitic vibrations. Consequently, a suitable support was designed and built using the 3D printing machine of the laboratory[4], aiming to attenuate the level of vibrations of the autopilot. Indeed if the accelerometer observes excessively high vibrations, the information received by the autopilot about the attitude of the plane might be uncorrected or biased. Consequently, it is necessary to keep the vibration level within given limits that are indicated in the documentation of the flight controller.

Although the design of the damping support is inspired by other common designs that can be found on internet and in the manual of the flight controller, it presents additional features. As can be seen in Fig.35, the system is based on two platforms linked by a type of rubber used to attenuate vibrations. The CAD drawings for the two platforms are given at the end of these paragraphs on page 38 for the bottom support and on page 39 for the top support. The four rubber shock absorbers have an inclination of $45°$ to impact as much as possible all the directions of space because they tend to have the best resistance in their axial direction. As a result, if they were placed vertically, this direction would be strongly impacted while the two others would have nearly no attenuation. Holes were designed in the platform in order to save weight (which is a design objective for any aircraft).

The bottom platform is also glued on a thin wooden platform, which contains holes. The latter gives more rigidity to the assembly and is used to avoid to fix anything directly in the plane. The philosophy was to be able to remove everything from the plane easily. Four small screws are used to fix the wooden frame inside the aircraft.

[4]More information about the 3D printing machine and process is presented in the Appendix B.2.

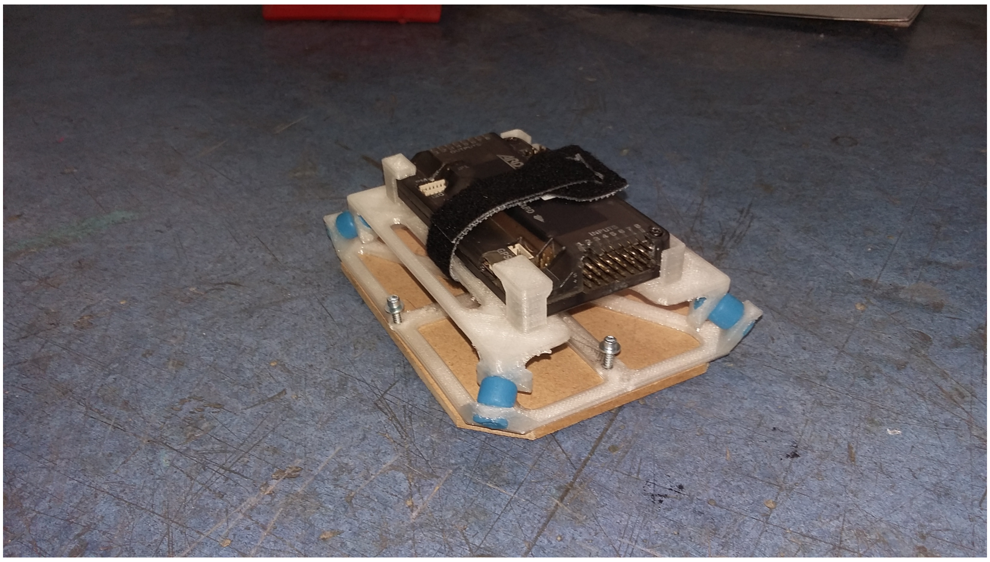

Figure 35: Photo of the flight controller attached to its anti-vibration support.

For the same reason, the APM is not glued on its support. It would have been easy to glue it on four anti-vibration foams to the upper platform. However, easy removal of the APM is desired[5] and it is attached to its support using a *Velcro* patch. Additionally, some specific angle guides were printed to ensure the correct placement of the flight controller.

Fig.36 presents the vibration level during an automatic mission in level flight. As it can be seen, the level of vibrations is within the limits in green given from the autopilot documentation. When between these limits, the vibration level is said to be good (more than acceptable). Consequently, the vibration damping support designed in this work seems to be sufficient.

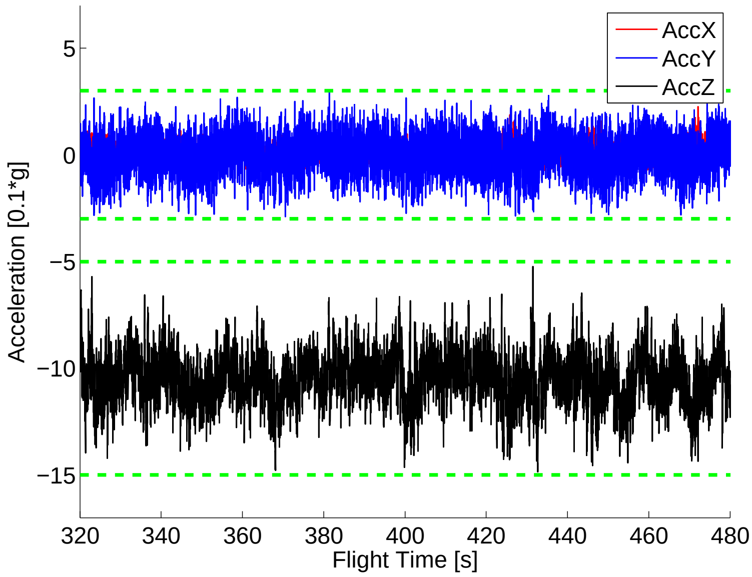

Figure 36: Vibration level of the accelerometer of the flight controller in cruise during a mission.

[5]It is even more important here to be able to remove the autopilot because there is not sufficient space to connect the wiring. As a result, the cables are attached before installing the board.

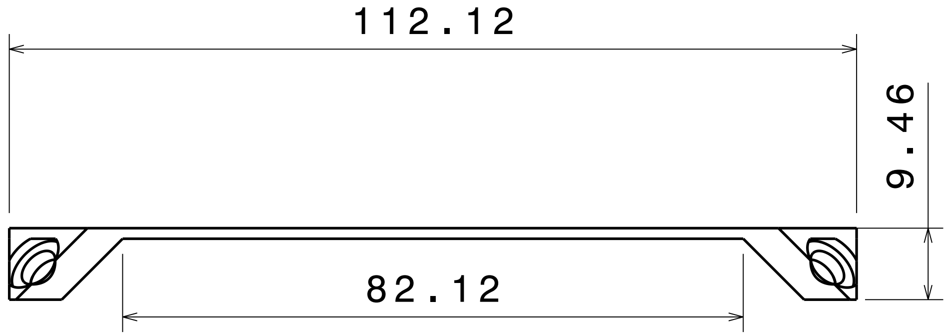

Front view
Scale: 1:1

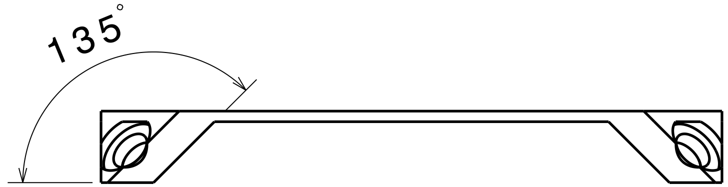

Left view
Scale: 1:1

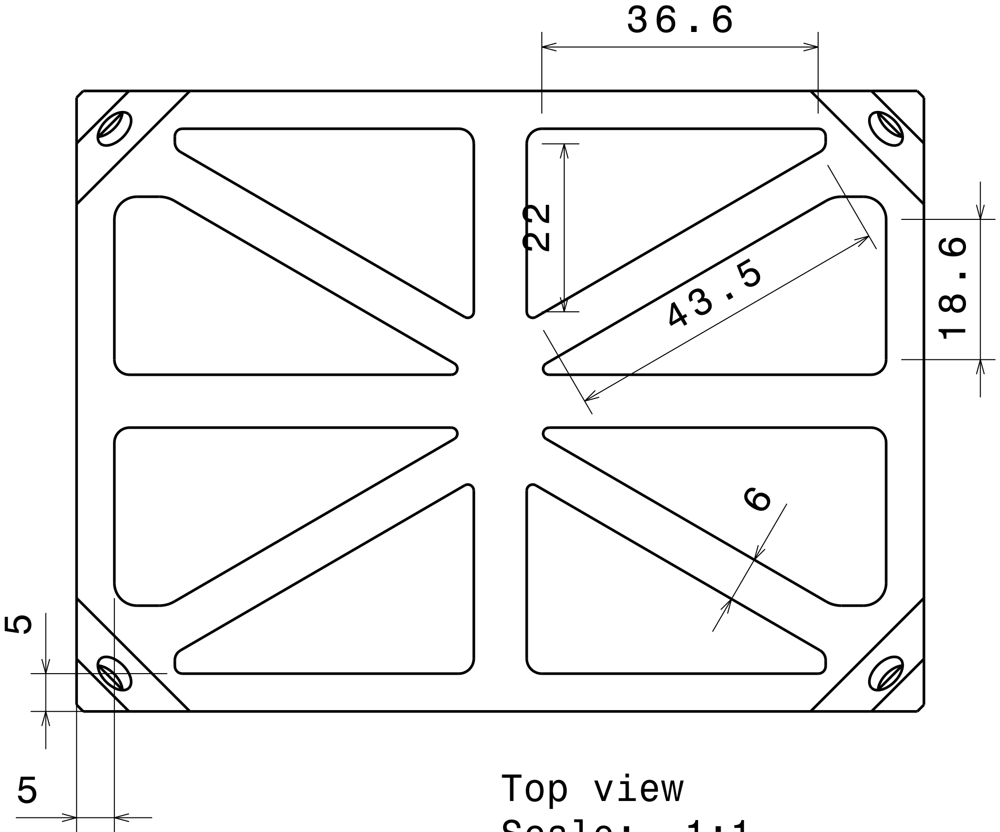

Top view
Scale: 1:1

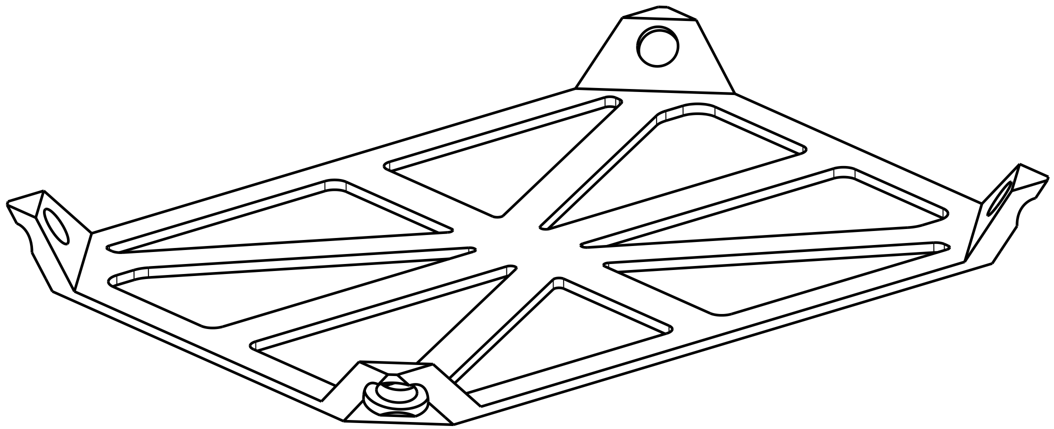

Isometric view
Scale: 1:1

Bottom support of the autopilot

Drawn by: B.HENRIVAUX

Date: May 2017

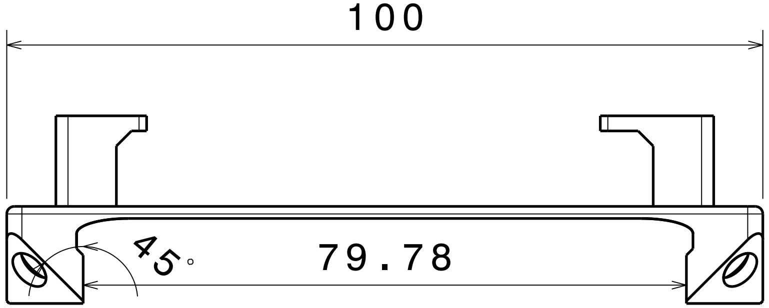

Front view
Scale: 1:1

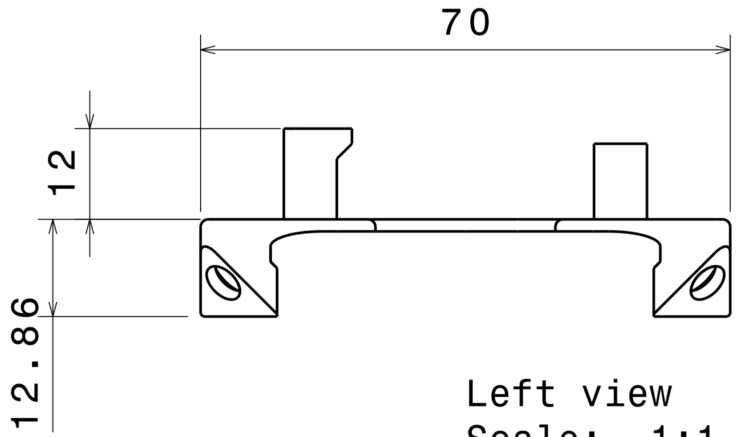

Left view
Scale: 1:1

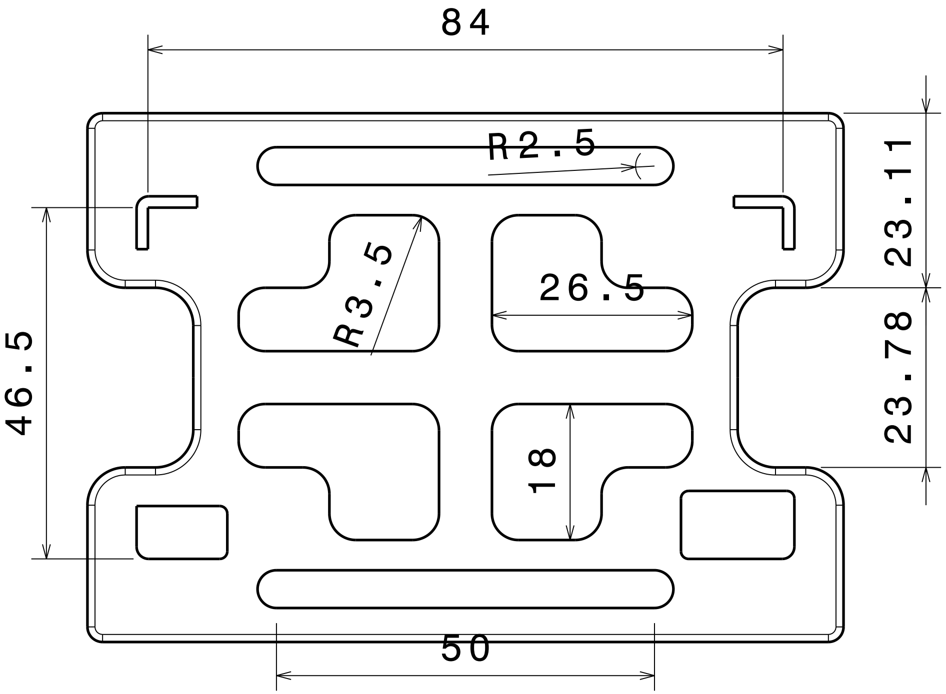

Top view
Scale: 1:1

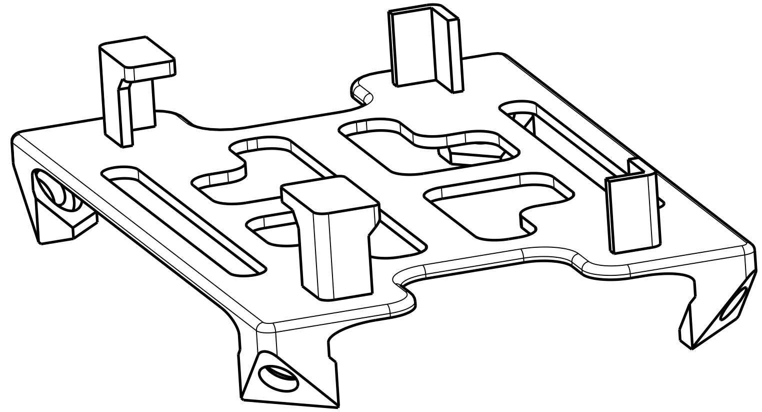

Isometric view
Scale: 1:1

Upper support of the autopilot

Drawn by B.HENRIVAUX

Date: May 2017

4.6.2 The other components

The installation of the rest of the components is discussed in this section.

The receiver of the radio controller *Taranis*

The receiver of the radio controller is placed close to the flight controller in the control bay, as shown in Fig.34. It is attached to the plane using a *Velcro* patch. The antennas should be placed with an orientation of 90° to each other.

However, it was noticed during the flight tests that the signal between the *Taranis* and the aircraft was sometimes weak (without causing any catastrophic issue - a range test was performed beforehand). This phenomenon might be caused by the fact that the antennas are inside the plane, which could attenuate the signal. Additionally, on-board electronic components may also have affected the signal. In the future, replacing the original antennas of the receiver by much longer ones that can be fixed outside the vehicle may improve the situation.

As a personal opinion, it would have been better to include the receiver on the damping mount of the autopilot. That way, the wiring between the two components would not participate to the transmission of the vibrations.

The battery

This component is placed behind the fuel tank as shown in Fig.37 because there is sufficient space and it is not too far from the centre of gravity. Additionally, for the flight, sponges are placed on top of the battery to make sure that it remains in place. Indeed, this rather heavy component could cause a serious accident if it was disconnected and moved freely inside the fuselage.

Figure 37: Photo of the battery and the fuel tank.

The antenna

The antenna used for the communication between the computer and the aircraft is placed on the side of the fuselage. It is fixed to the plane by means of a 3D printed support that was designed for this purpose. The photo in Fig.38 presents the mount on the aircraft. The design has two main characteristics. On the one hand, slopes were added to the front and to the rear of the support in order to delay flow separation as much as possible (the plan with the main dimensions is given in the following page). On the other hand, slopes are actually empty in the aim of saving weight.

Figure 38: Photo of the antenna mounted on the side of the fuselage.

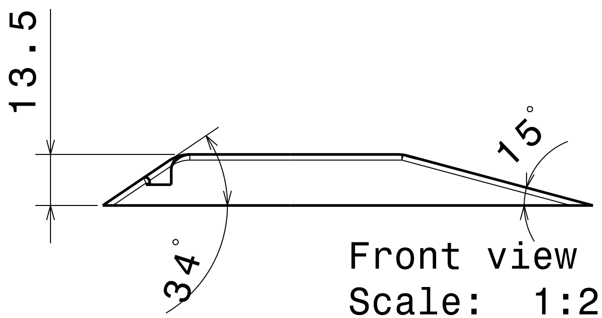

Front view
Scale: 1:2

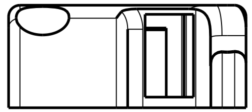

Left view
Scale: 1:1

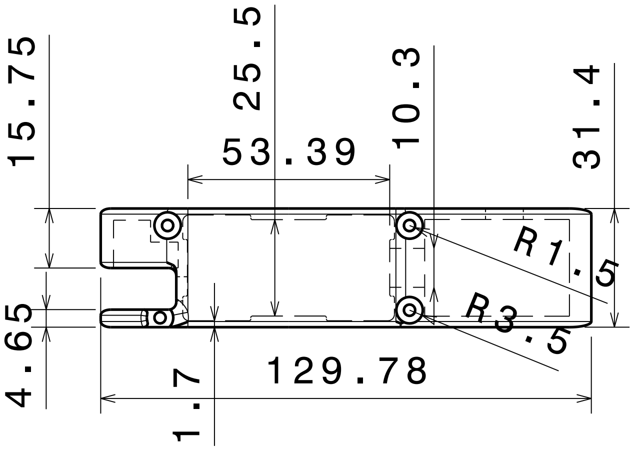

Top view
Scale: 1:2

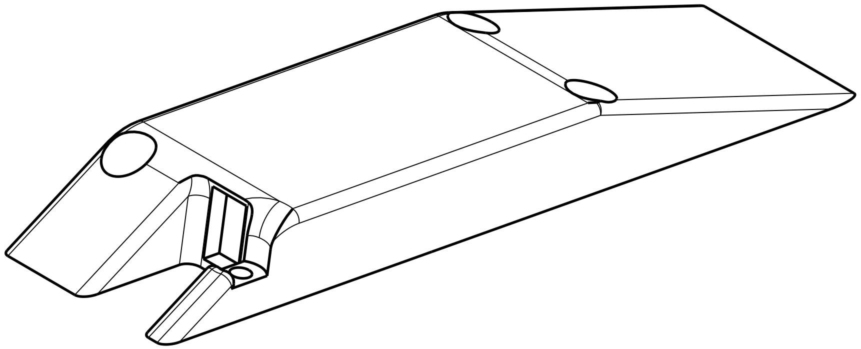

Isometric view
Scale: 1:1

Antenna support

Drawn by: B.HENRIVAUX

Date: May 2017

The GPS and the compass

A single component contains the GPS and the compass; consequently, they are together. Two important factors have to be taken into account. The first one is that this module needs a clear view of the sky for the GPS to work correctly. As a result, it should be placed above the fuselage. The second factor concerns electromagnetic interference. Indeed, the compass is sensitive to the magnetic variations and distortions in the vehicle. Consequently, the module is placed behind the rest of the components, far from any electrical sources or metallic parts. It is positioned behind the wing on a lid used to access the rear of the fuselage and is displayed in Fig.39.

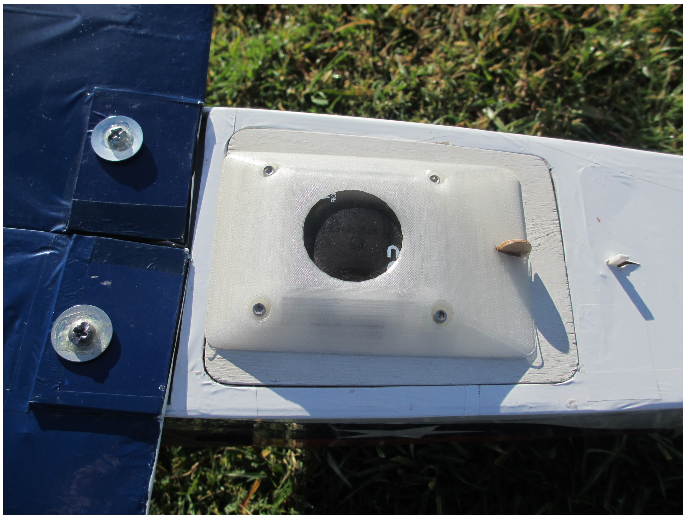

Figure 39: Photo of the mount and the module with the GPS and the compass on the plane.

The mount is presented on the next page with its main dimensions. On each side, there is a slope used to try to delay the flow separation. The one at the back of the mount is longer as the effect is more important than at the front. The slopes of the slides are also used to hide the wiring.

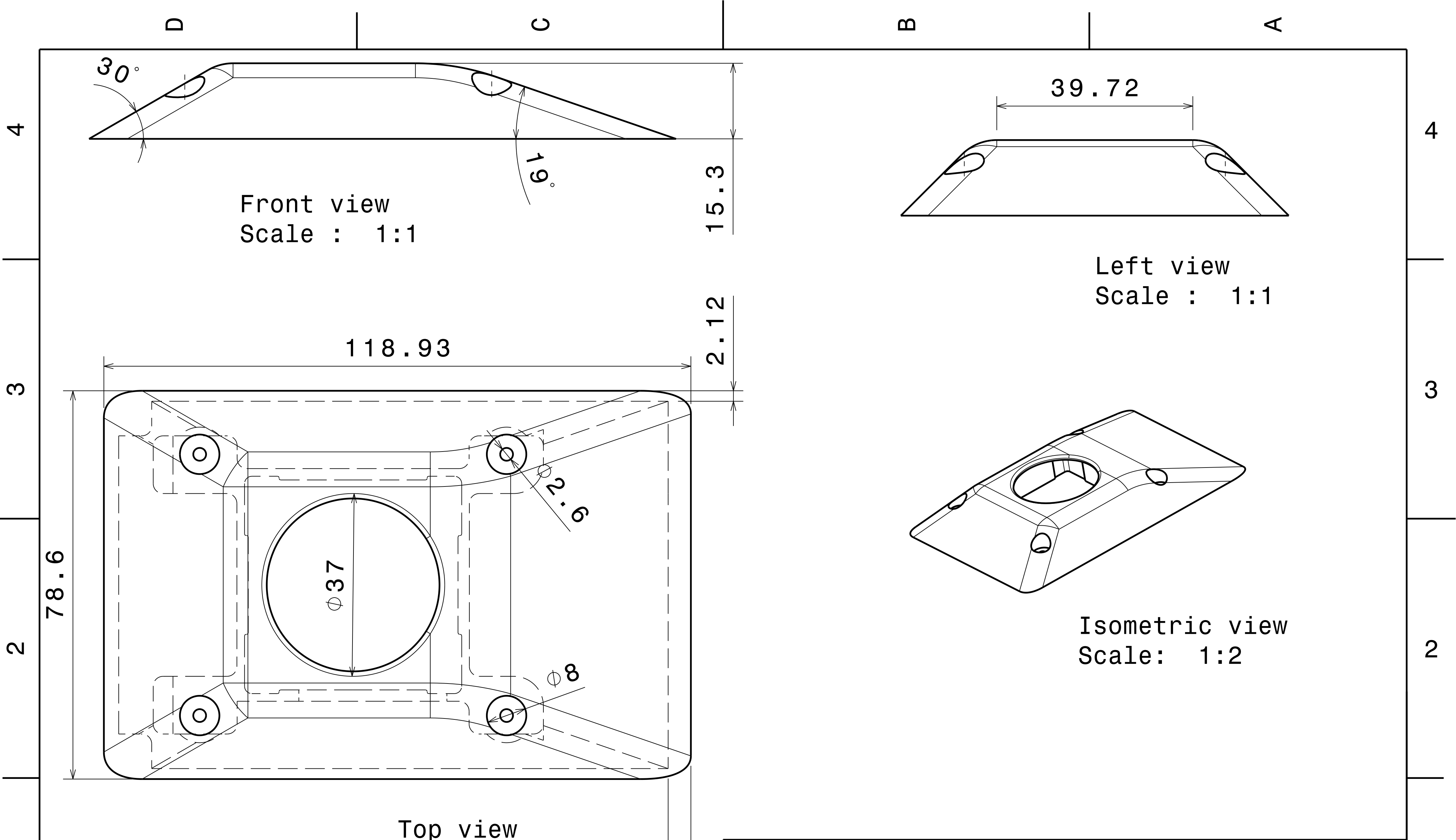

GPS support

Drawn by B.HENRIVAUX	Date: May 2017

The Pitot tube

The Pitot tube used to measure the airspeed of the aircraft is placed in the leading edge of the wing as displayed in Fig.40. It has to be placed sufficiently far away from the fuselage in order to avoid being influenced by the propeller wake. As a rule of thumb, a distance larger than twice the diameter of the propeller is needed (for RC aircraft) [40]. In this project, it is fixed at the leading edge, on a rib located at about 2.5 times the diameter of the propeller.

Furthermore, the Pitot should not be in the boundary layer region around the wing. The Tube documentation recommends that the static holes need to be at least $1\ cm$ away from the structure.

Finally, the Pitot needs to be oriented in the direction of the airflow. This was more challenging because, on the ground, the plane presents a pitch angle due to the configuration of the landing gear.

Figure 40: Photo of the Pitot tube installed in the wing.

After installation, the Pitot Tube was calibrated and its readings were validated by comparing the velocity given by the Pitot to the ground velocity calculated from the GPS. An example of such observation is described in section 6.2.2 where the plane flies a circular path. On average, the ground velocity from the GPS and the airspeed indicated by the Pitot should be equal. Another verification was carried out in order to ensure that the sensor is outside the wake produced by the propeller. Indeed, when the aircraft is at rest on the ground, the Pitot tube should indicate the same value whether the engine is on or not.

Global view

A summary of the positions of the different components used to make the autonomous flight is presented in Fig.41.

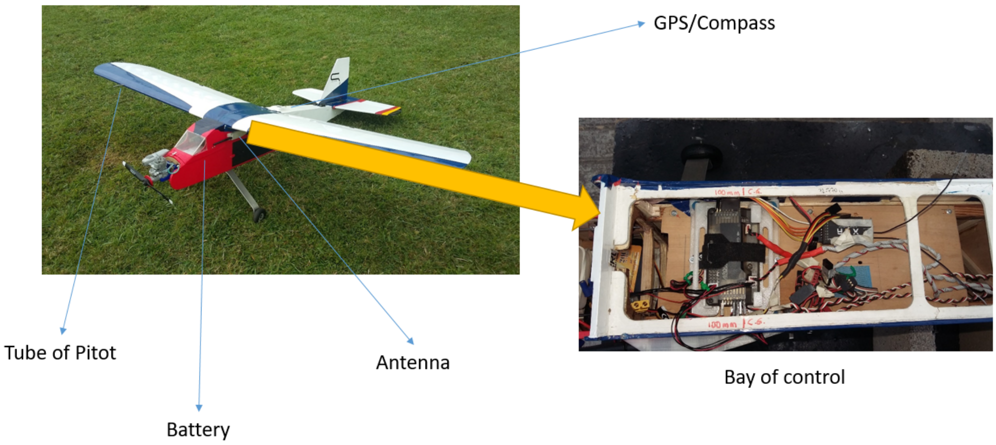

Figure 41: Summary of the positions of the different elements in the plane.

4.7 Centre of gravity

Another important feature to consider is the fact that when modifications are carried out in the vehicle, its weight and the position of its centre of gravity are also modified. However, the centre of gravity cannot be placed arbitrarily because it influences the stability of the aircraft. Indeed, the centre of gravity of the vehicle is the point around which the moments balance. According to the initial documentation of the aircraft given in [41], it should be located $100\ mm$ behind the leading edge of the wing. However, as explained before, the various components are placed according to other requirements based on their operation. This means that a ballast is necessary to keep the centre of gravity at the recommended position. In order to determine the mass and the position of this ballast, the device shown in Fig.42 is used. Basically, the wing of the aircraft is placed on two wooden plates, which are free to rotate around a point. The aim is that, by modifying the mass and its distribution in the vehicle, the aircraft has a zero pitch angle when the centre of gravity is as indicated in the plane manual. In addition, it is better to place the added mass as far as possible from the centre of gravity to maximise the moment arm and to minimize the weight.

Figure 42: Device used to adjust the position of the centre of gravity.

Eventually, a weight of $0.8\ kg$ is added to the front of the plane to bring back the centre of gravity to its correct position. This ballast is placed below the fuel tank at the front of the aircraft. This is visible in Fig.43. Moreover, some sponges are also added to ensure that nothing will move when flying. The masses are prevented to move upward by the fuel tank.

Figure 43: Ballast in the plane. The front of the aircraft is to the top of the photo.

This mass of $0.8\ kg$ might appear to be very high but there was already a mass re-distribution before the present work in the plane resulting from the first series of modifications that were made. Mainly, when the drawer was built and when the different cameras were used, the servomotors of the elevator and the rudder that were close to the centre of gravity were displaced much further. Actually, they are near the tail. Moreover, these components together weight nearly $0.2\ kg$ and have a very long moment arm. As a result, they have a huge influence on the centre of gravity.

Fig.44 shows the total weight repartition of the plane. The addition of the flight controller and its components represent about 7% of the total mass or about $360\ g$. It is also visible that the ballast is a non negligible weight in the vehicle as it corresponds to 14% of the mass.

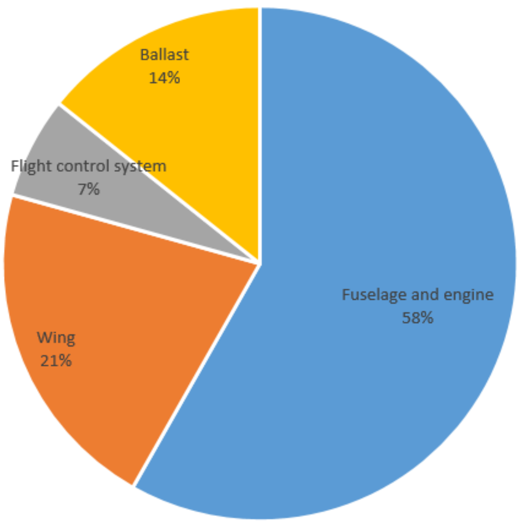

Figure 44: Weight repartition of the aircraft.

The part corresponding to the autopilot can also be analysed, as presented in Fig.45. Clearly, the battery is the heaviest component. A smaller battery could be used to reduce the weight because a flight of about 20 minutes uses approximately 6% of the battery autonomy. Amongst, these components, only the GPS and its support increase the ballast weight because they are placed behind the wing while the others are close to the centre of gravity.

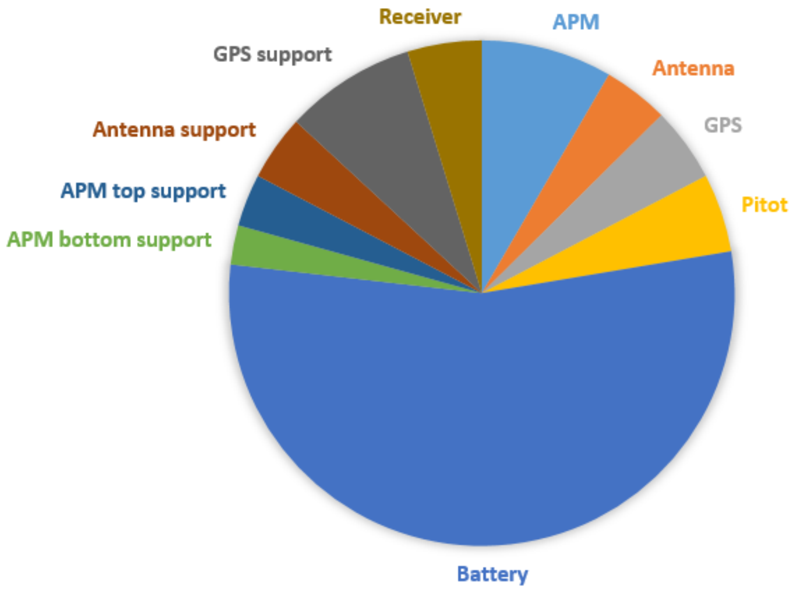

Figure 45: Weight repartition of the different components of the flight control system.

5 Flight preparation

The following chapter presents the necessary steps to prepare a flight. It includes information about *Mission Planner*, the software that is used to configure and communicate with the autopilot. It also presents the different flight modes that were used during this work. Additionally, safety features are discussed.

5.1 Presentation of Mission Planner

Mission Planner (MP) represents the interface that is used in this thesis to access the information of the flight controller, whether to download the autopilot memory on the computer or to monitor the plane in flight (as a ground control station). Four main menus are available in MP and are described here-under.

5.1.1 Flight data

The first tab concerns the flight data. It is used to monitor the behaviour of the aircraft in flight by plotting its instantaneous position on the map as well as the time-variation of various characteristics[6] such as the demanded attitude in roll and in pitch, the realised roll and pitch, the speed, the altitude, etc.

An example of this menu is given in Fig.46. There is a Head Up Display (HUD) indicating the behaviour of the plane and other information. To the right of the figure there is the map with the path that the plane is following. At the top of the screen, there is the possibility to visualise in real-time different flight parameters. The bottom left corner presents different actions that can be accomplished using the computer.

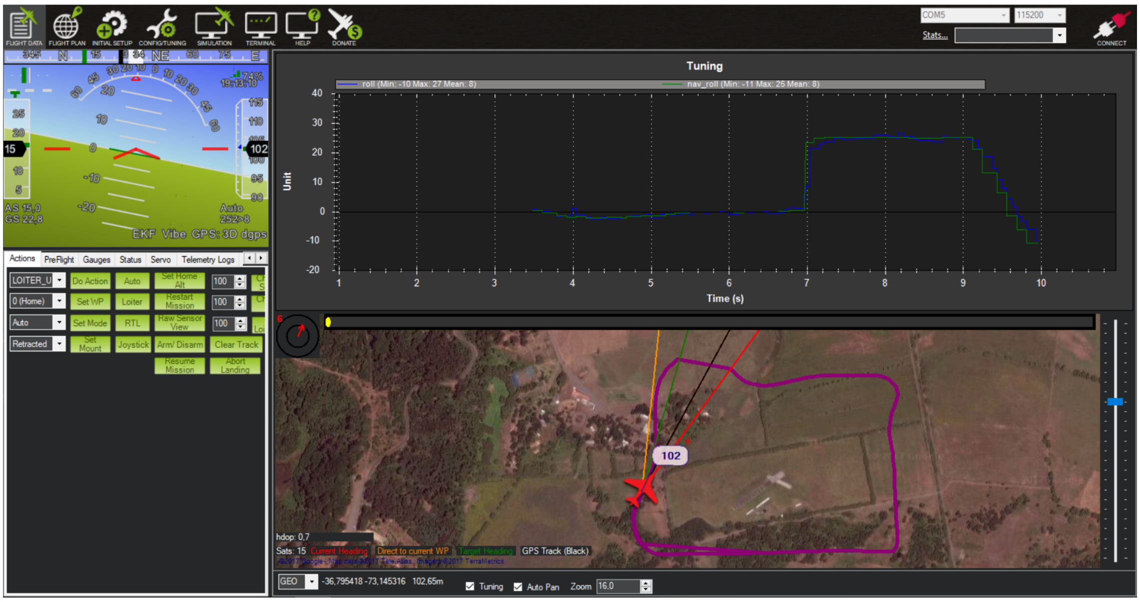

Figure 46: Example of the flight data window.

[6]There may be a time shift between the information in the Ground Control Station (GCS) and the one presented in MP because of the necessary time to transmit the information to the computer.

Regarding the actions that are possible using the GCS, it is mainly possible to change the flight mode, the speed, the altitude and the path of the plane. In addition to that, there is the button to arm/disarm the aircraft. This is important and will be discussed in the following part of this chapter. Other actions are also available but they are either specific to other planes (e.g. flaps) or were not important to accomplish this project.

A zoom on the HUD is given in Fig.47. The different elements of the figures are identified in Table 4.

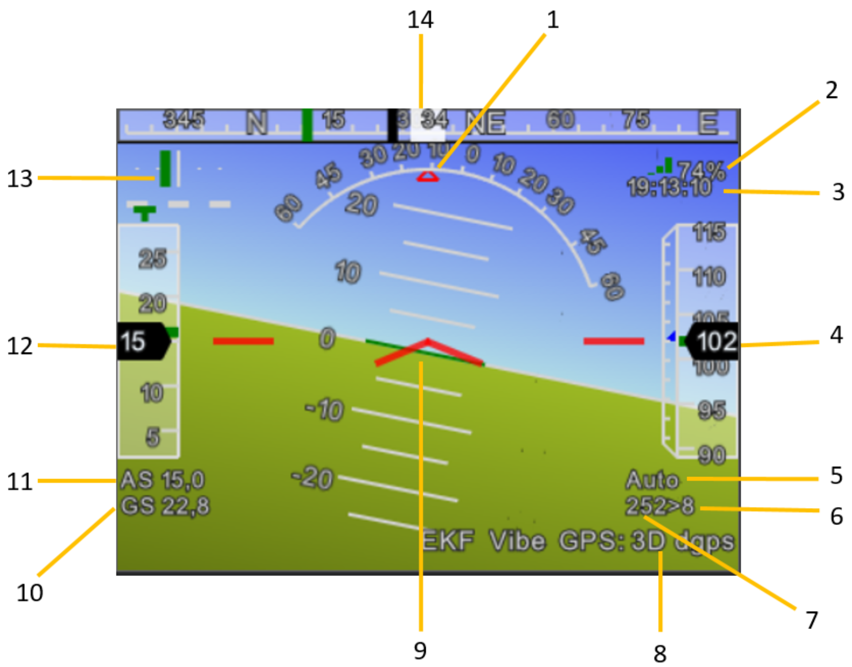

Figure 47: Zoom on the HUD of the previous figure.

Number	Explanation
1	Bank angle
2	Telemetry transmission
3	GPS time
4	Altitude
5	Flight mode
6	Numbering of the next waypoint in the mission
7	Distance to the next waypoint
8	GPS
9	Pitch angle
10	Ground speed
11	Air speed
12	Air speed (or ground speed if there is no Pitot tube)
13	Cross track error
14	Orientation

Table 4: Table presenting the different elements of the screen with the HUD.

As a remark, it is important to note that when the plane is turning, it is the horizon that rotates and not the red lines. Furthermore, it is also possible to add information about the battery voltage of the aircraft. However, in this project, this is not critical because a combustion engine is used. As a result, the battery is not used that much: only to power the servomotors and the flight controller. It was observed that a flight of about 20 minutes uses more or less 6% of the battery. Measuring and displaying fuel consumption data would also have been very valuable but implementing such a system was not part of this work.

All flight data is stored in the memory of the flight controller. Although the plane can fly for about 20 to 25 minutes depending on the wind, only the last ten minutes of flight are recorded in memory. Actually, the recording time depends on which flight parameters are desired in memory. However, to obtain a full overview of the flight and of the system, it was necessary to record most of the flight data. This means that the recording time was rather limited. In future work, mainly if using cameras is an objective, it can be decided to store only part of the data. In addition, the use of a *PixHawk*, the current version of the autopilot includes a SD card, which can store a greater amount of data.

Lastly, the map is used to monitor the path of the aircraft. As it can be seen in Fig.48, the trajectory flown by the plane is represented in purple while the meaning of the other colours are indicated in Table 5.

Figure 48: Zoom on the map of Fig.46.

Colour	Explanation
Purple	Path flown
Red	Current heading
Orange	Direct line to the current waypoint
Green	Target heading
Black	GPS track

Table 5: Meaning of the different colours present in the map.

The current heading is what is given by the compass and takes into account a possible side-slip. The GPS track concerns the motion of the plane seen by the GPS system and is therefore the direction in which the aircraft is moving. In flight, the motion is mainly based on the GPS track while the compass heading serves mainly for take-off when the plane has not acquired any velocity yet. The target heading is the direction that the plane would like to take and it also includes correction for cross-track errors. The latter are lateral deviations from the desired path.

Other information is also displayed, such as the altitude or the number of satellites currently seen by the GPS. It is also possible to represent on this map the current mission. The mission is discussed in the following paragraph.

5.1.2 Flight plan

This menu is concerned by the plan of the mission. An example of a mission is given in Fig.49. The following explanations are only about the commands that were used in this work. Other commands exist but they were irrelevant to the present work. To the right of the figure, the mission instructions are listed while, on the left, the representation of the mission path is displayed.

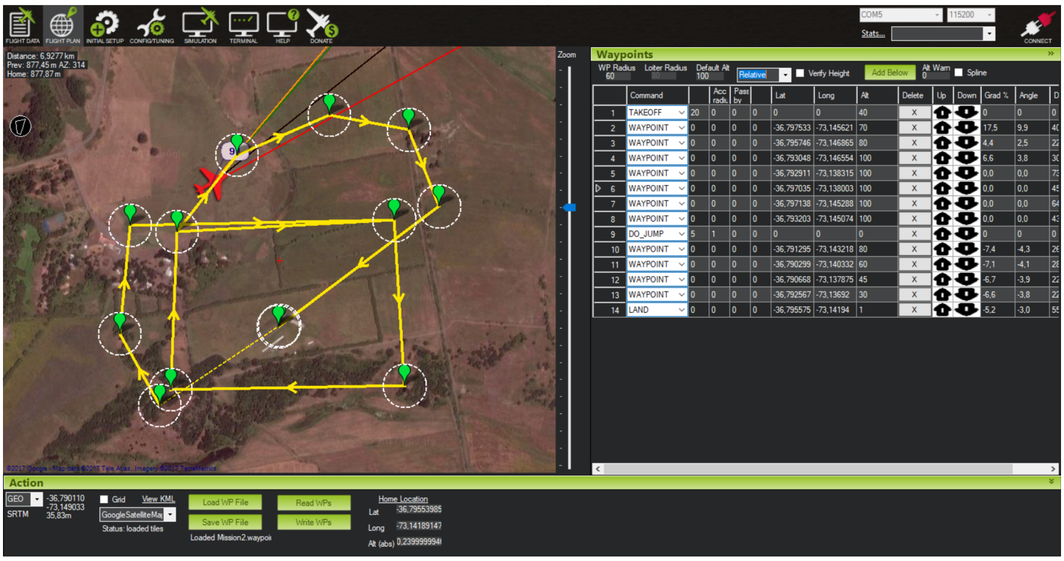

Figure 49: Example of mission planning.

Basically, planning a mission consists in placing the different waypoints through which the plane needs to pass. However, other commands also exist such as instructions for take-off and landing. Moreover, it is also possible to repeat the mission by jumping to a specific mission command.

Concerning the waypoints, it is necessary to give an altitude as well as a radius. Indeed, the plane considers that it has reached the waypoint target when it touches its radius. Consequently, it does not necessarily pass exactly through the waypoint.[7] Regarding the altitude, this mission is flown at a height of $100\ m$ because it is below the maximum height allowed by the law (about $125\ m$) but is sufficiently high to fly above any obstacle and to carry out manoeuvres with a safety margin. In addition to that, there are three ways to demand the altitude depending on the way it is measured:

- Absolute: with respect to the sea level
- Relative: with respect to the home position
- Terrain: with respect to the terrain

The aeromodelism club used for the test flights is located on flat land close to the sea. Therefore, the three different choices are equivalent. However, for additional safety, it is better to select the relative altitude and, if there are hills, the terrain altitude should be chosen in order to ensure that the plane will avoid them. Nevertheless, it is necessary to remark that, in terrain, trees, pylons or other high obstacles are not taken into account (only the relief).

The setting of the home position is particularly important because it defines the position that the aircraft will try to reach automatically if a problem arises. It could even attempt a landing there if it is configured. Moreover, in a mission that is not terminated by a landing command, the plane will also go to the home position and loiter over it while waiting for another order. Therefore, it is necessary to make sure that this position is at the right location. This position can be set in two ways: it is automatically set up when the plane is armed at the position of arming but it can also be defined explicitly in the mission planning screen.

5.1.3 Initial set-up

This is the menu where the different sensors and other components discussed in section 4 are configured. Some of them require a calibration step while for others, this is not necessary. The calibration procedure of the different elements is carried out according to the different instructions from the different windows. A calibration is required for:

- The accelerometer
- The compass
- The radio
- The Pitot tube

The accelerometer can be calibrated with the flight controller removed from the plane. The procedure consists in placing the autopilot in different orientations (on the top, on the bottom, with a rotation of $90°$ in roll, etc) in order to make sure that the autopilot knows the indication of the accelerometer for the different spatial directions.

[7] Justifications regarding the different selected parameters are given further in the report.

There are different ways to calibrate the compass: the aim is to teach the autopilot what are the offsets of the compass due to the magnetic interferences present in the plane. As a result, the autopilot needs to be installed (and a new calibration is needed if a modification is applied to the plane). On the one hand, the compass can be calibrated manually by rotating the plane in different positions while an offset is computed in MP. On the other hand, it can be calibrated using a more automatic procedure by flying a first flight. The second method is much easier to put in place due to the dimensions of the plane and has yielded good results.

About the radio, the aim is to tell the flight controller what are the minimum and maximum of PWM that can be sent on each channel. Therefore, it consists in moving each channel signal to its extremities (minimum and maximum) and also to indicate the neutral position. In addition to that, it is important to ensure that each control surface moves in the right direction.

Finally, the Pitot tube requires a calibration step too. In order to do this, it needs to be in a calm environment (without any wind). The aim is to set the pressures corresponding to a zero speed. However, the Pitot tube does not work well for all airspeeds. Indeed, when it is at rest in a place without wind, it should indicate $0\ m/s$ but it indicates oscillations around $2\ m/s$ to $3\ m/s$. This is because the Pitot tube needs to work in its operational range to give accurate results (above $5\ m/s$). The accuracy of the measurement is verified by comparing the air speed with the ground speed velocities on a calm day while the plane flying in cruise. These should be nearly equal. An alternative is to use the Loiter mode because, in that mode, both velocities should be nearly equal on average. Indeed, the plane circles around a point; thus it sees the wind from all the directions. An example is given in the results and discussion section.

5.1.4 ConfigTuning

This is the place where all the parameters can be accessed and modified. Several windows exist in order to give different ways of monitoring the autopilot. There is a window with only the main parameters used for the navigation qualities. Other windows consist of the full list of parameters (with, sometimes, a word of explanation about the parameters).

5.2 Flight modes

In this part, the flight modes used during the thesis are explained. However, other possibilities also exist but will not be detailed in the present document.

Manual

The first mode is the manual one. It means that the pilot controls the aircraft as if there was no flight controller. It uses the radio controller (*the Taranis*) to modify the behaviour of the plane. This is a mode for which the autopilot simply copies the information from the inputs to the outputs. However, there are exceptions to this behaviour:

- If a geofence is planned and the plane goes beyond the limit.
- If a failsafe feature triggers (e.g. loss of communication with the RC radio).
- If a V-Tail is implemented (specific mixer)
- If elevons are used (specific mixer)

In the present work, only the first two possibilities could occur because the plane has a classical tail configuration and has normal ailerons. The manual flight mode is mainly used in the beginning to ensure that all sensors function properly (maiden flight). It is also in this flight mode that the trim of the aircraft is accomplished. After that, manual mode is used from time to time during the tuning process of the parameters e.g. to take-off and to land.

Fly-By-Wire A (FBWA)

The second mode presented is crucial in the tuning procedure and is called FBWA: it is a flight assisted mode. It works in the following way. When the pilot does not input anything, the flight controller will tend to level the aircraft automatically. However, the pilot also has the possibility to modify manually the trajectory of the aircraft. Nevertheless, he does not have the same freedom as when using the Manual flight mode. Indeed, he has limitations in the way of flying e.g. the plane has a maximum angle of roll, of pitch, etc.

For instance, if the pilot wants to turn, he applies a deflection of the ailerons (which is limited by the maximum bank angle) but the plane will try to maintain the pitch level automatically. This does not mean that the aircraft will keep its altitude because the latter also depends on the airspeed that is mainly influenced by the accelerator.

Additionally, although there is a partial control of the elevator and of the ailerons by the autopilot, the throttle and the rudder are still fully controlled by the pilot. It means that the speed is not adjusted automatically, although it is constrained by the minimum and maximum throttle parameters.

Furthermore, the rudder can also move automatically if rudder mixing is configured (with the aim of doing coordinated turns). As a result, when turning with the ailerons, the flight controller will also deflect a bit the rudder in the same direction depending on the rudder mixing parameter.

Autotune

This flight mode is similar to the previous one (FBWA) in the way the plane is controlled but Autotune also offers the possibility to tune "automatically" the control systems in roll and in pitch. This will be discussed in more detail in the section about tuning procedures.

It means that this flight mode is only necessary to tune the plane. Once tuning is completed, Autotune becomes useless unless modifications are made to the structure and/or the components.

Automatic (AUTO)

This mode is used to fly autonomously. When the plane flies in this mode, it follows a series of instructions such as waypoints, etc[8]. The mission is saved onto the memory of the APM board.

If the pilot switches to another mode while being in AUTO, and then, switches back to the AUTO mode, the aircraft will resume the mission from where it was unless the mission was reset by the GCS.

[8] See the mission planning section 5.1.2 for more details.

Return to launch (RTL)

This mode is more a safety mode rather than a flying mode. Indeed, if a problem arises, the plane will enter RTL and come back automatically to the home position. At the end of a mission in AUTO that does not have a landing, the plane will also enter RTL. Once it reaches this home position, it loiters there until it receives a new instruction (or run out of fuel).

Loiter

In Loiter, the plane will continuously circle around the position where it started the manoeuvre while maintaining its altitude constant. The radius of the loiter circle is defined by a specific parameter but can also be influenced by the maximum roll angle as well as the navigation tuning parameter. The latter influences how aggressively the plane tends to turn.

Circle

This mode is similar to Loiter but does not keep the position. It is more a failsafe mode (that was never used in this work) when a failsafe event occurs e.g. the loss of a signal like the one of the GPS or the radio transmitter. Indeed, the plane should enter the Circle mode for $20\ s$ before switching to RTL.

5.3 Safety features

In this part of the report, different aspects that are used to help prevent an accident are explained.

5.3.1 Arm/Disarm

Before flying, the plane needs to be armed. The disarmed state guarantees that the motor is not going to turn when the pilot is not ready and prevents flying (and take-off) while the autopilot is not fully ready to fly.

In order to arm the aircraft, two solutions are possible: either to use the GCS, which can send a specific arming command or deflecting the rudder to the left for a few seconds. Although the second solution might appear more handy, the first one has the advantage to give clues about potential problems if the flight controller refuses to arm.

When the aircraft is disarmed, it is impossible to use the throttle stick and the plane cannot accelerate. The controller either inputs the minimum value of the throttle on the corresponding output channel or no value at all. For this plane, these two options give similar results because it is necessary to let the throttle free (i.e. to arm the aircraft) to start the combustion engine. Otherwise, the second solution might appear to be safer but is not always possible depending on the electronic speed controller (in the case of electric propulsion).

Arming also influences the memory because the autopilot starts saving data in its memory from the moment it is armed. When it reaches the maximum capacity of the memory, it overwrites the beginning.

Finally, as explained above, the home position is fixed at the location where the plane is armed if it is not directly set in the autopilot. Additionally, the reference of the altitude from the barometer is also set when the plane is armed.

5.3.2 Stall prevention

The stall prevention technique is a method to ensure that stall is not going to occur. This could cause a crash. Stall can occur at any airspeed but is particularly likely at low velocities and when turning. Indeed, when the plane is turning, part of the lift of the wing is lost in order to accomplish the turn. Consequently, the aircraft should fly with a higher velocity or should have a sufficient security margin from the stall speed.

If roll is controlled, the flight controller will consider the demanded roll angle and figure out if there is a safe margin above the stall speed in order to accomplish the demanded turn. Otherwise, the roll angle will be limited to the safe limit. However, a roll of $25°$ is always possible to ensure that the plane is still manoeuvrable if the airspeed is poorly estimated (e.g. without the use of an airspeed sensor).

If the throttle is also controlled by the autopilot, the flight controller raises the minimum airspeed to the level that can be reached in a safe way for the corresponding bank angle. As a result, the plane will tend to speed up or to pitch down to have sufficient velocity to achieve the desired turn.

An additional feature also occurs when flying in FBWA. As the pilot has control of the throttle, it might be difficult for him to judge if there is enough power (in particularly if he is flying along long straight lines). Consequently, the autopilot tends to lower the nose depending on the position of the throttle stick. The so-called $Stab\_Pitch\_Down$ parameter is set to the default value of $2°$. When the throttle is at its minimum, there is full pitch down while when it is at its trimmed position or higher, no down pitch is added. In between, a linear proportion is used. The amount of pitch needed depends on the airframe of the vehicle and, particularly, the drag it produces.

5.3.3 Geofencing

It consists in putting a fence in the mission planning screen. Once the plane breaches this boundary, the plane automatically (even if the flight mode is manual) goes to the return position, which can be a prescribed point or a waypoint.

Limitations in altitude whether minimum or maximum can also be set. All in all, Geofencing confines the plane within a cube over a specific geographic region. It is sometimes a requirement of aero-clubs or of certain competitions. Additionally, it is an additional safety feature to avoid losing the plane from the flying zone.

As a remark, when Geofencing is activated, it might be impossible to land (due to a minimum altitude). As a result, an alarm on the radio reminds the pilot that this feature is activated every $5\ s$ under the form a "beep". During an automatic mission including take-off and/or landing, the geofence can be[9] automatically set up after take-off and turned off before landing. Although this technique has not been extensively used to realise this work, it was successfully tested and could be interesting. It could also be used for flight training.

[9]if this option is activated

6 Parameter tuning and flight analysis

This chapter details the main guidelines for the procedure to tune the aircraft. The complete procedure is given in the autopilot documentation but some explanations about the main controllers are provided here-after. In addition, the complete list of the exact parameters that were used at the end of the procedure is given in the appendix.

After the tuning procedure, an example of flight is analysed: a complete mission including take-off and landing is described. This aims to demonstrate that the system works well.

6.1 Flight tuning

Different control systems are implemented in the source code of the autopilot, they are often in the form of PIDs controllers. The aim is therefore to find the right proportional, integral and differential gains.

6.1.1 Pitch and roll

The first controllers to be discussed are the ones relating to the pitch and the roll. These two controllers are the most important because they guarantee that the realised pitch or roll is the same as the one demanded. It is therefore necessary to give the right PID gains to obtain the expected behaviour.

In this work, there was initially a bit of trial and error in the assisted mode in order to ensure that the plane has acceptable handling qualities (and that the pilot is at ease with the aircraft). By default, the gains are very low: this causes the plane to react slowly but, at least, ensures that it does not go out of control immediately. Then, an automatic adjustment of the gains was accomplished. This consists in flying with the flight mode Autotune and giving inputs with the stick at more than 80% of its maximum rate in one direction and, then, in the other. A progressive improvement was monitored on the screen: the procedure had to be repeated 20 times according to the documentation. Once the roll behaviour had shown satisfying results, the same procedure was used to tune the pitch.

A fully manual gain tuning procedure is also available but is much slower. Moreover, the automatic procedure gives adequate results. Fig.50 shows the results during a flight for the roll. As it can be seen, the demanded and realized roll angle curves superimpose indicating that the roll control system is well tuned. The mission is a rectangle, which is the reason why the plane tends to turn to the same side. Indeed, when it turns it keeps an angle of $25°$ for a certain time. Negative values are also observed because the plane flies a couple of oscillations after a turn before tracking the path perfectly.

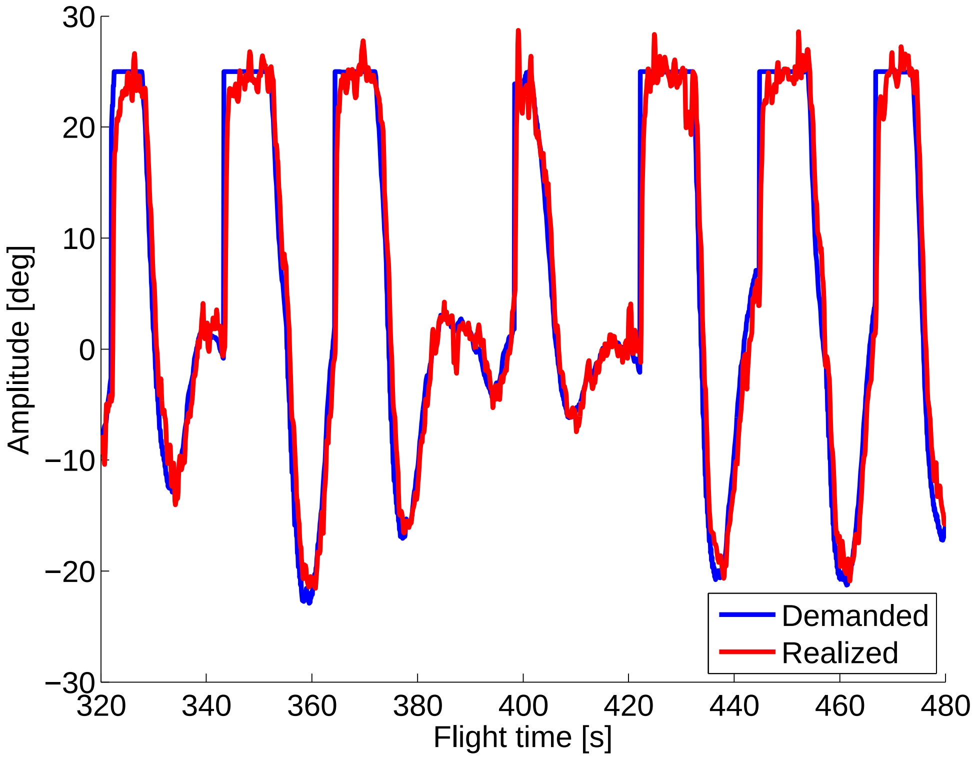

Figure 50: Demanded roll vs achieved roll.

Fig.51 plots the results of the pitch tuning procedure. The agreement between the demanded and realized signals appear to be not as good as those obtained for the roll. However, the general trend is well represented and there is no clearly visible steady state error between the two curves. Although some manual adjustments were tried, they did not lead to major improvements. Additionally, when flying, no particular problem was observed: as explained in more details below, the altitude is kept fairly constant during the mission and a good behaviour of the pitch is observed during take-off and landing.

The main difference between Fig.50 and Fig.51 is the scale of the y-axis. Indeed, the amplitude of the roll varies between $\pm 25°$ while the amplitude of the pitch is between $\pm 4°$. Therefore, errors of about $1°$ are much more visible when the amplitude is low, which is the case in the pitch plot.

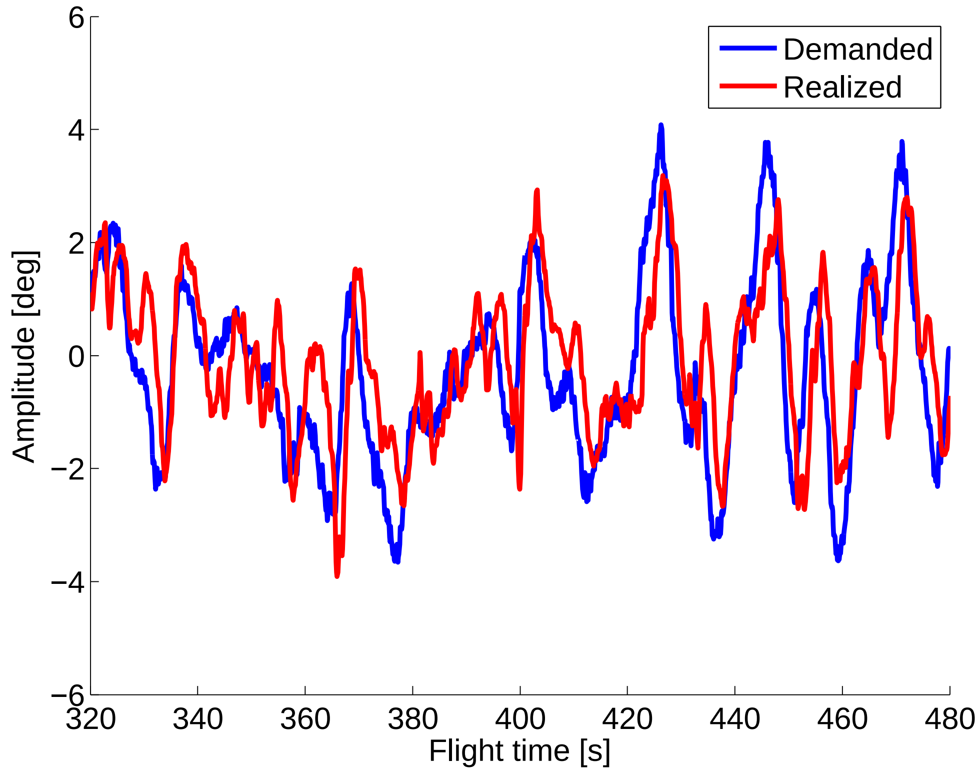

Figure 51: Demanded pitch vs achieved pitch.

6.1.2 The yaw controller

Yaw control is tuned manually. Additionally, it is much less important than the roll and pitch tuning because its effect on the trajectory of the aircraft is smaller. Nevertheless, yaw tuning can help improve performance.

This controller is mainly based on a combination of two ideas: a yaw damper and a side-slip controller. The latter is only effective if there is enough fuselage side area because it relies on measurements of the lateral acceleration. In this project, the plane needs both the yaw damper and the side-slip controller, but this is not the case for a flying wing or a glider for examples. The tuning of the yaw controller is carried out according to the documentation.

6.1.3 The navigation tuning

This controller is used to teach the plane how to follow its trajectory. As a result, it influences how the aircraft turns: aggressively or gently. Navigation tuning is based on an algorithm that is a modified version of the one explained in the article [2].

Basically, it consists in adjusting a PD controller by selecting the right $L1$ distance as illustrated in Fig.52 for a linear (or curved) path to follow. Before the first waypoint of the mission, the reference is basically the next waypoint. Afterwards, it depends on whether the plane is far from the mission trajectory or not. If it is far from where it should be, the $L1$ reference point will be taken nearly perpendicular to the aircraft. On the other hand, if the vehicle is already in proximity of the target trajectory, the angle between the $L1$ line and the mission path will be much smaller and the reference point will be ahead of the plane. As a result, the plane follows a non linear logic.

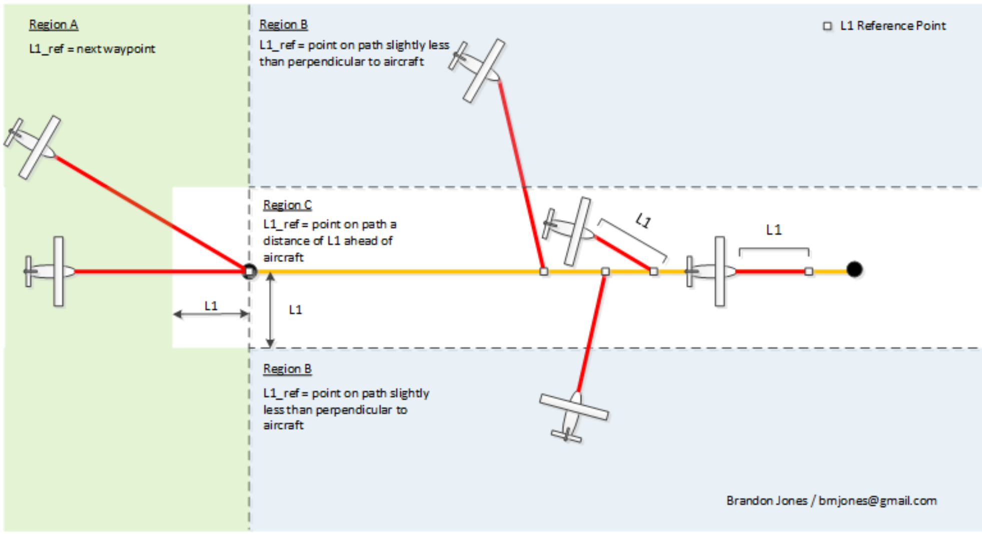

Figure 52: Illustration of the principle of the algorithm for the navigation along a trajectory [22].

A similar idea is followed when the plane is making a circle (e.g. in Loiter mode). As shown in Fig.53, when the plane is far from the target radius, the $L1$ distance points directly to the centre of the circle that should be followed. However, when the plane is close to the right radius, the reference point is further ahead.

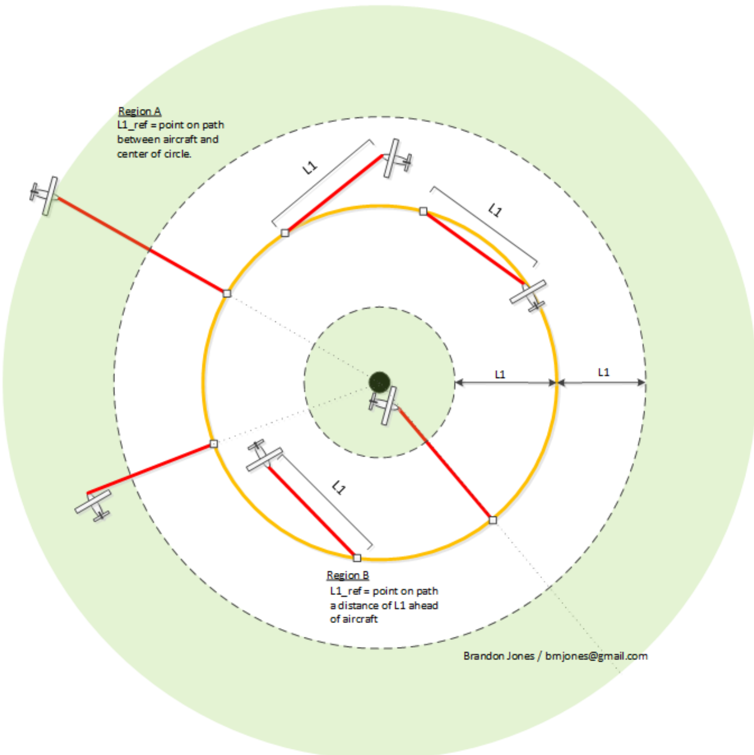

Figure 53: Illustration of the principle of the algorithm for the navigation along a circular trajectory [22].

The tuning procedure consists in flying a rectangular mission in AUTO mode. The aim is to adjust one parameter that influences the $L1$ distance of the algorithm. The main effect visible on the map is the presence or the absence of oscillations when the plane turns. Indeed, if a shorter distance is selected, the plane will exit region C more rapidly and will, therefore, have a more aggressive behaviour: this will lead to bigger oscillations along the trajectory. Conversely, it is possible to suppress most of the oscillations with a larger distance because it leads to turns that are less aggressive as the plane finds it easier to remain in the white region of Fig.52. Consequently, the reference point is ahead of the aircraft instead of being perpendicular to the mission path.

6.1.4 Total Energy Control System (TECS)

TECS is the last controller that is required to guarantee adequate flight performance of the aircraft. It aims to ensure that the total energy of the plane is correct depending on the desired mission parameters such as altitude and velocity. The total energy, E_T is the sum of the potential and kinetic energies

$$E_T = E_P + E_K \tag{10}$$

the potential energy, E_P, is influenced by the altitude of the aircraft while the kinetic term, E_K, depends on its velocity.

As a result, the algorithm has to fulfil two objectives. On the one hand, to guarantee that the sum is correct and, on the other hand, to ensure the proportions of potential and kinetic energies. Consequently, the TECS acts as a height and speed controller.

For instance, the drag continuously affects the total energy of the plane because it causes a loss of it. The effect of the present controller is to monitor the required total energy based on the mission altitude and velocity, obtained from the barometer and the airspeed sensor. Therefore, it adjusts the throttle to keep the energy at the desired value.

Even if the sum of the potential and kinetic energies is right, the two terms taken individually could be wrong. Indeed, if the plane is flying too fast and too low, it is possible to have the right total energy but the two terms of the sum of Eq.10 are wrong. The controller tries to re-establish the balance between the two types of energies by adjusting the nose of the plane. Indeed, if the demanded pitch is increased (nose up), it will lead to a gain of altitude and it will also reduce the velocity of the aircraft. The opposite is also true if the aircraft is flying too slowly and too high.

In this work, an even weight is placed on speed and height errors, but in other cases e.g. if no airspeed sensor is used, the weight could be different such that the pitch is used to control the height without the throttle.

The adjustment of the parameters consists in measurements of different manoeuvres. It consists mainly in measuring different velocities and adjusting the throttle accordingly. In addition, some climb rates have to be measured and indicated to the autopilot in order to be able to climb with the maximum speed and to descend without overpowering the aircraft.

6.2 Flight examples

6.2.1 An autonomous mission

This section presents an example of an autonomous mission. The mission consists in a rectangle as shown in Fig.54. Here, only the flight in cruise is discussed, the take-off and the landing are detailed afterwards.

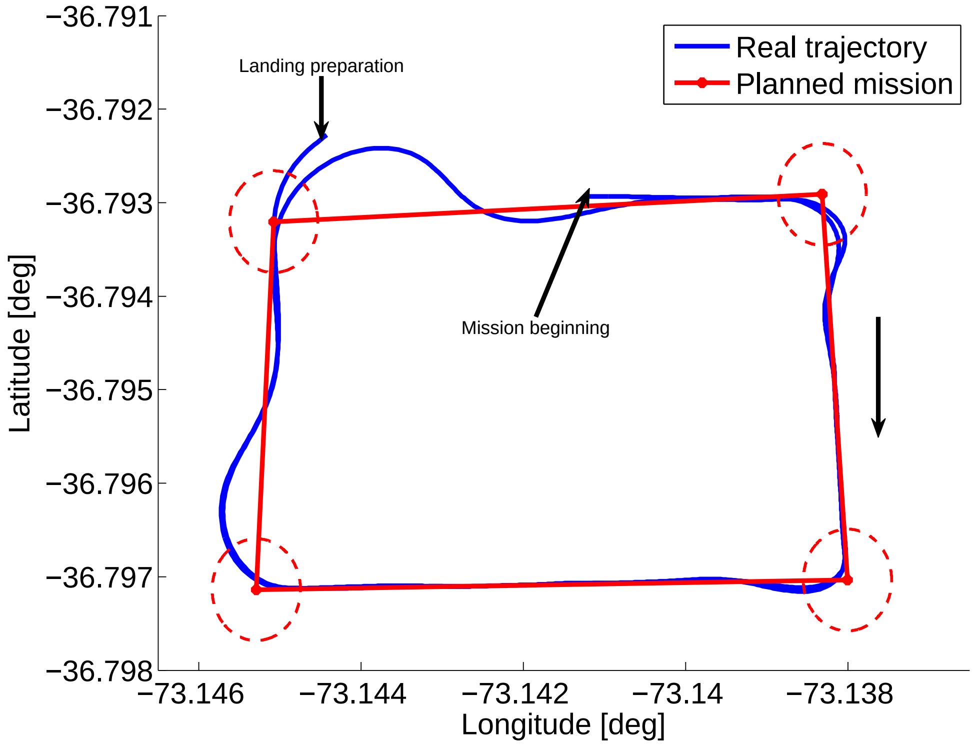

Figure 54: Comparison between the planned path and the one flown by the plane.

The planned and real trajectories are most of the time superimposed except after a turn where oscillations may be noticed. The plane is starting its mission from the top right corner and follows the rectangle in a clockwise fashion. Moreover, it repeats the mission once, thus two rectangles are actually drawn even though the aircraft has followed nearly the same path twice. In addition, the line that leaves the top left corner is actually the beginning of the preparation for the landing at the end of the mission. This will be discussed, like the take-off, in later paragraphs.

The dashed lines represent the radius of the waypoints. This influences if the plane turns before or after the waypoint. Indeed, the vehicle considers that it has reached the point that it needs to pass through when it touches the radius of the waypoint. However, in practice, this does not mean that it starts turning at the exact location of the intersection between the radius and its trajectory. This results from the fact that a time is necessary to obtain the information from the satellite. Additionally, a small time is also needed before a noticeable turn is occurring when the ailerons are deflected. Consequently, if the radius is small, the plane will tend to pass through the centre before actually turning whereas, if the radius is rather large, it will turn before reaching the exact position of the waypoint.

In this project, the choice of the radius is based on the fact that it is better to start turning a little before the waypoint because it results in neater turns, a fact that was confirmed after several flight tests. A radius of $60\ m$ has shown good results. Indeed considering a plane flying at more or less $16\ m/s$ and that the GPS has a lag of about $0.6\ s$, the aircraft already travels $25.6\ m$ before having the information that it has reached the waypoint. Then, the plane needs time to change attitude (it is not an acrobatic aircraft as explained in section 2); therefore $1 - 2\ s$ or more is actually needed. For a similar reason, the turn radius is rather large because the maximum bank angle is relatively small $(25$ degrees): the turn radius can be determined according to Eq.11.

$$R_t = \frac{V^2}{g \times \tan \phi} \approx 55\ m \tag{11}$$

Considering two seconds for the change of attitude and the time that it has a noticeable impact on the trajectory results in a waypoint radius of $25.6 + 2 \times 16 \approx 57\ m$, which was rounded up to $60\ m$. Therefore, the indicated value corresponds to a turn that is initiated just before the planed waypoint. A bigger turn radius would lead to a turn that is initiated earlier.

Furthermore, in Fig.54, it is also visible that after a turn, there are oscillations: these are influenced by the radius of the waypoint but, more particularly, by the navigation controller whose logic was explained in section 6.1.3. Indeed, the bigger the distance $L1$, the smaller the oscillations but also the less aggressive the turn. As a result, the aim is to select the parameter such that it turns sufficiently fast but without producing too many oscillations in the path following the turn. In the present result, the amount of oscillations was judged acceptable because the mission path is well tracked before reaching the next waypoint.

It is also clear that although all the turns are planned to be $90°$, the amplitudes of the subsequent oscillations are not always the same. This is an effect of the wind and it can be understood by observing Fig.55. Indeed, it is clear that the ground speed differs from the airspeed. While the first one is an indication given by the GPS, the second is a measurement of the Pitot tube. The difference between the two curves is caused by the wind the plane sees. Indeed, the plane flies with a constant airspeed velocity but, in the presence of a tailwind, it has a ground speed that is higher than the airspeed (and vice versa).

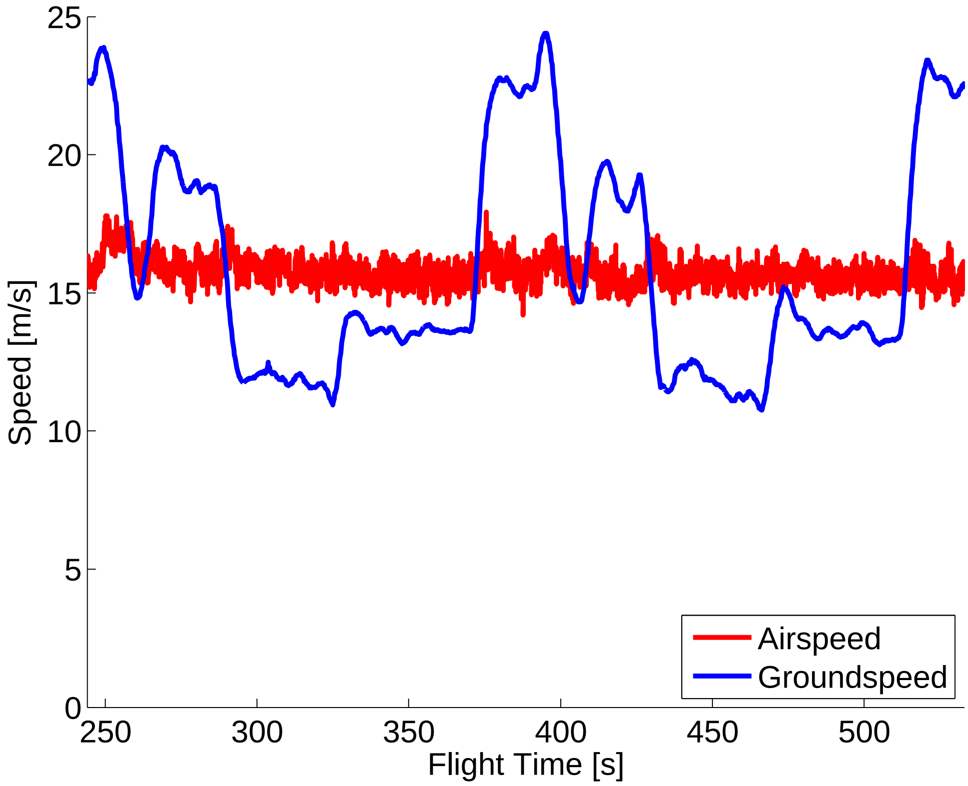

Figure 55: Comparison between the airspeed (Pitot tube) and the ground speed (GPS).

Comparing the different measures of speed and the mission progress, it is possible to determine the direction of the wind: in terms of the rectangle, the wind blows towards the right top corner meaning that it has a component going towards the right and another towards the top of the rectangle.

Consequently, the explanation of the differences in the oscillations is as follows. When the plane is flying along the bottom side of the rectangle, the wind is against the motion (and the ground velocity is smaller than the airspeed). As the plane reaches the bottom left corner, it starts to turn. The turn causes the plane to accelerate from the ground point of view. The aircraft is pushed further by the wind, resulting in a larger oscillation. A similar behaviour is observed when the vehicle reaches the top left waypoint: here, it turns but due to the wind (and that the radius of the waypoint is fixed[10]), it tends to make a larger turn.

When the plane reaches the top right corner, it starts to turn, but now instead of a tailwind, it encounters a headwind. As a result, the turn is smaller and the oscillations are more gentle. A similar conclusion is drawn about the last corner.

Another graph to look at is the one of the altitude as shown in Fig.56. Two types of altitude are actually measured: there is the altitude measurement from the GPS and the altitude from the barometer. The two are more or less equal although there is a nearly constant offset between them. The barometer data are used in order to discuss the behaviour of the plane because it is the one that is commonly used.

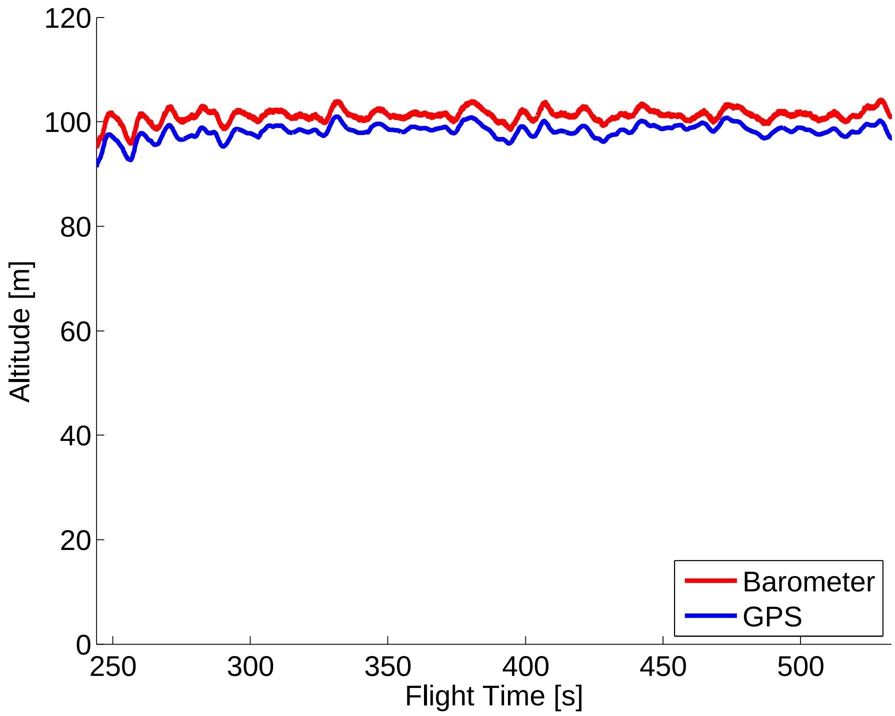

Figure 56: Comparison between the altitude from the GPS and the one from the barometer.

During cruise, the altitude was set to $100\ m$. The error between the prescribed altitude and the real one is plotted in Fig.57.

[10]According to me, an improvement of the code could be to make an adaptation of the waypoint radius based on the difference between the ground speed and the airspeed.

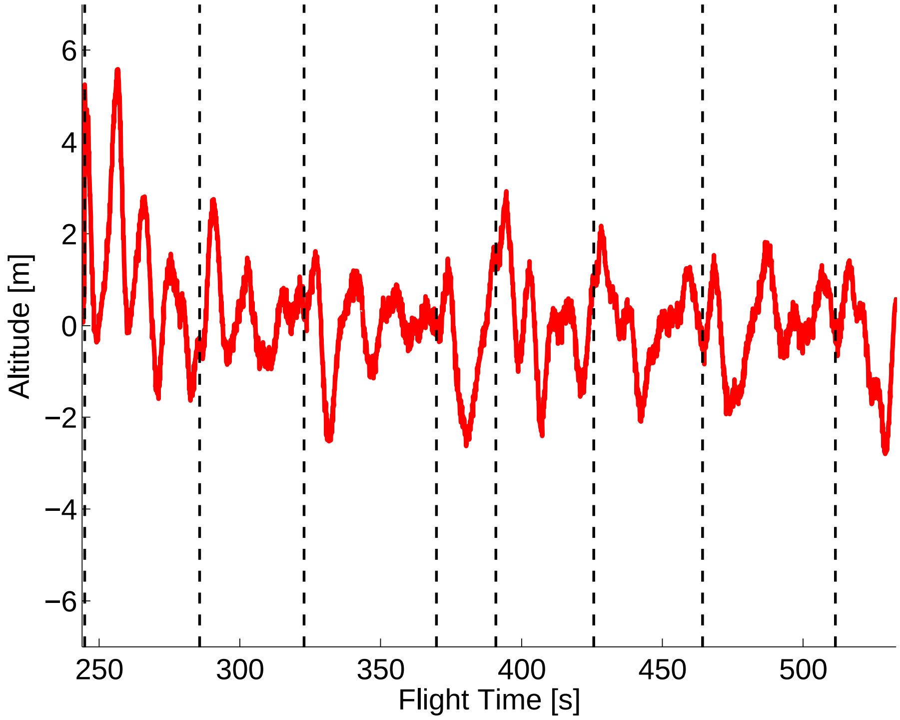

Figure 57: Altitude error between the mission instructions and the plane flight. Dashed lines represent the validation of a waypoint by the aircraft.

Apart from the beginning of the mission where two bigger peaks are present, the rest of the mission is fairly constant with an oscillation in height of about $\pm 2\ m/s$. The beginning of the mission also coincides with the end of the climb from the take-off, which might explain the overshoot in altitude.

During cruise, the mean of the error is $0.17\ m$ with a standard deviation of $1.2\ m$, which is the trend observed in the graph. Moreover, larger deviations from the desired altitude tend to occur just after that the plane has accomplished a turn. Indeed, when the vehicle is turning, its lift distribution is altered and if the turn is too long, the aircraft will loose height. However, in order to avoid this, some pitch is added during the manoeuvre. Although the modification of the altitude is limited, it causes variations to occur. These variations do not seem to be detrimental for the flight.[11]

If filming is an objective in the future, it is necessary to take into account the oscillations in the path of the aircraft after a turn. Indeed, when planning the mission, it is important to ensure that the turns are a bit outside the filming path objective to avoid to have the plane out of the tracked path while taking the pictures.

6.2.2 LOITER mode

This mode has been flown on the same day as the previous mission but with one or two hours in between. However, a similar effect of the wind should be observed. The choice of the radius is based on two facts. Firstly, the plane needs to be able to fly a circle of this radius. Indeed, if the radius is too small, it will not be able to follow it due to the limitation of the bank angle for example. On the other hand, the radius should not be excessively large because it is

[11]However, this could cause a problem in an application where a lot of accuracy is required.

important to keep a clear eye contact with the plane above the home position. After different tests, a radius of $100\ m$ has shown an adequate behaviour.

Fig.58 represents the variations in altitude when the plane is flying in LOITER mode. On average, it flies at a height of $111.1\ m$ with a standard deviation of $0.7\ m$. The target altitude is the one that the plane had when it entered that mode, which was $111\ m$ in this case. This means that the oscillations in altitude are rather small.

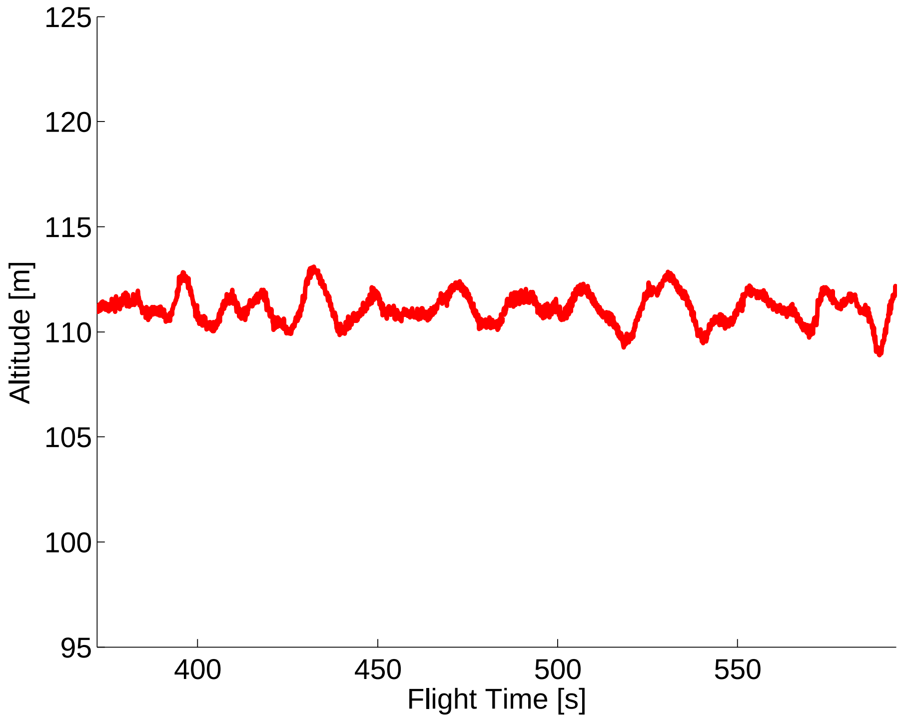

Figure 58: Variation in altitude when the plane is flying in LOITER mode.

Additionally, it is also possible to display the comparison between the ground speed and the airspeed, as shown in Fig.59. This comparison is particularly useful to see if there is a problem with the calibration of the Pitot tube. Indeed the difference between the two velocities is mainly the wind and flying a circle means that the aircraft is affected by the wind in all relative directions.

Using the present information, on average, the plane has an airspeed of $14.6\ m/s$ with a deviation of $2.61\ m/s$. On the other hand, the ground speed is of $15.1\ m/s$ with a standard deviation of $5.51\ m/s$. As a result a difference of $0.5\ m/s$ is observed between the two means, which does not appear to be a problem.

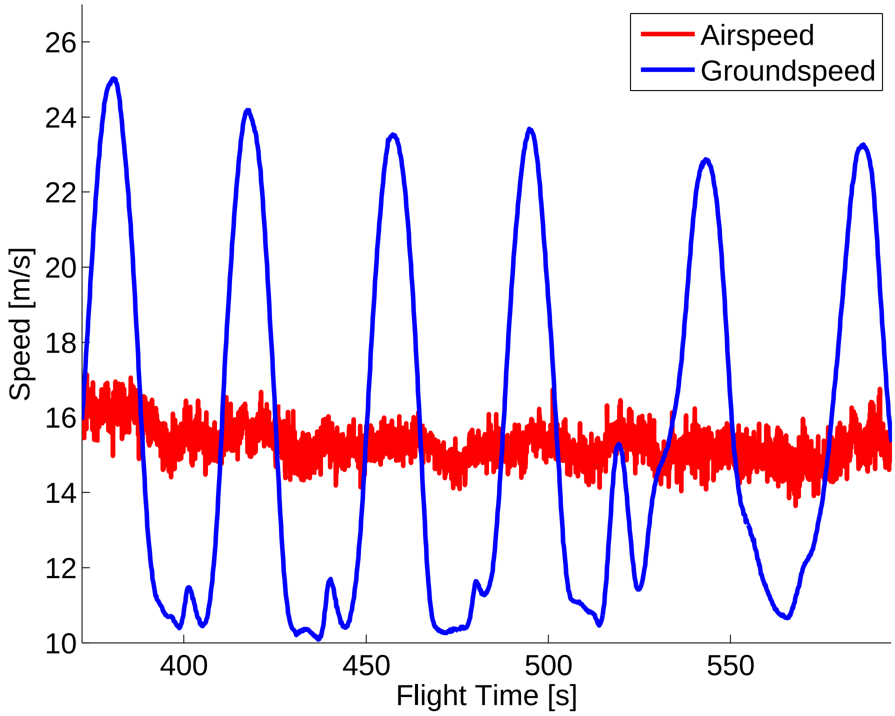

Figure 59: Comparison between the ground speed and the airspeed when the plane is flying in LOITER mode.

6.3 Take-off

In these paragraphs, the beginning of a flight is explained: the take-off is configured and an example is detailed.

6.3.1 Principle

For this manoeuvre, the configuration of the landing gear is important. Indeed, different parameters are used for a hand launch, a catapult, a tricycle, or a tail dragger.

The present aircraft is a tail dragger. This configuration is actually the one that requires the most parameters to be set (due to the acceleration over the runway). The take-off procedure can be divided in different steps as shown in Fig.60.

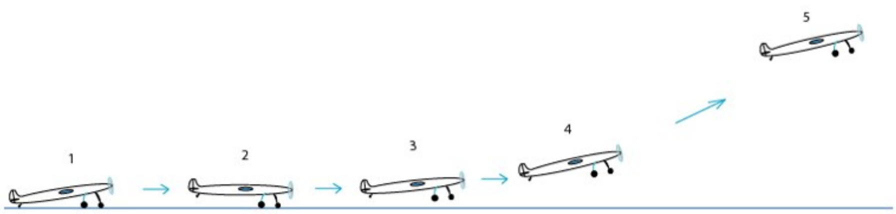

Figure 60: Representation of the different steps for take-off with a tail dragger landing gear [31].

At the beginning of the procedure (step 1), the plane accelerates gradually from rest. The first part is a ground run. During that phase, a little elevator up is also applied to ensure that the rear wheel stays on the ground. This is because, for a classical tail dragger configuration, this wheel allows to control the plane as it moves on the ground. Consequently, it is better to have a good adherence in order to steer correctly. However, the wheel from the *Plane G5* is fixed and there is no way to steer while this wheel is still on the ground. Unless there is an obstacle or an irregularity in the runway, the aircraft moves in a straight line. Nevertheless, the elevator is still deflected upwards to ensure a better stability of the tail during take-off. In other words, the tail does not start to make little bounds for example.

Then, when the aircraft has sufficient velocity (step 2), the tail is lifted up and yaw control is now achieved using the rudder. The velocity at which the tail is lifted up should be below the stall speed.

As the place reaches the rotation velocity (step 3), a brief deflection of the elevator initiates the climb. The rotation velocity should be above the stall speed in order to ensure that the aircraft has a sufficiently high speed to be able to fly.

Finally, the plane continues to climb until it reaches a given height where the autopilot considers that the take-off is finished and initiates the rest of the mission (steps 4-5). For this project, this height has been set to $40\ m$ because it ensures that the plane is above any obstacle (trees) with enough safety margin. The climb is flown just after the ground run because it is important to keep the wing level in order to avoid stall while turning.

In Mission Planner, to set the instruction of take-off, it is necessary to give the height at which the flight controller considers to end the take-off but also the pitch angle at which the plane needs to climb. This pitch angle needs to be chosen sufficiently high to rise above obstacles before meeting them. However, the aircraft should also be able to do this angle (i.e. not excessively large). If it is set too high, the angle will be limited by the maximum pitch angle obtained from the tuning procedure (based on the energy controller). Indeed there is a risk of stall if the plane tries to reach a pitch angle that is higher than what it can achieve when it is at full throttle. Then, to start the take-off, the aircraft is placed at the position from which we want it to accelerate and also with the right heading. Once the mode AUTO is turned on, the aircraft starts to accelerate and to take-off in a straight line.

6.3.2 Analysis

From the information saved in the memory of the flight controller, it is possible to analyse the different steps of take-off. Fig.61 presents the command inputs given by the autopilot for the elevator and the throttle. The take-off starts at the black-dashed line which corresponds to the moment when the flight mode AUTO was activated. The neutral position of the elevator is obtained when the PWM of the corresponding channel is at about $1550\ \mu s$. This value includes the trim. The throttle does not have a neutral position, it has an idle position: the one corresponding to the minimum of the channel (plus the trim if there is any): $991\ \mu s$. The PWM limits for the elevator and throttle channels are given in Table 6.

	Elevator [μs]	Throttle [μs]
Minimum	983	991
Maximum	2025	2016
Trimmed	1550	991

Table 6: PWM limits of the channels of the elevator and of the throttle.

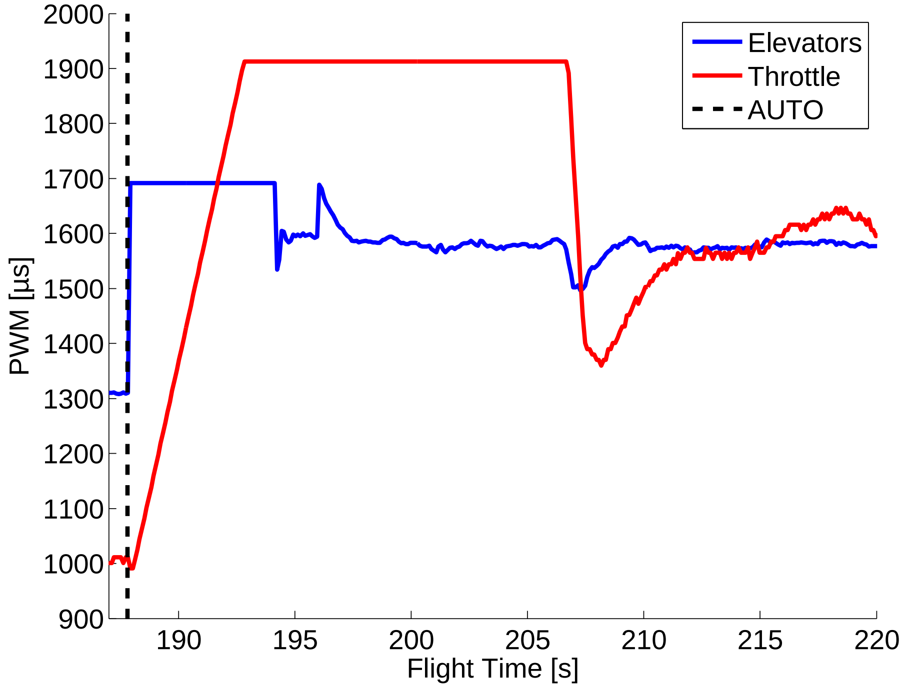

Figure 61: PWM of the channels of the elevator and of the throttle during take-off.

Regarding the throttle curve (in red), at the beginning of the flight, there is a gradual acceleration until the engine reaches its maximum power. It needs $5\ s$ to do so: this is a parameter that was set in the APM. Once it has reached its maximum power, it will continue in that way until the take-off is over because, using the autopilot, all take-offs are performed with maximum power. In fact, the maximum power was set to be 90% of the maximum throttle. This choice is due to the tuning procedure of the energy controller because the maximum throttle should be the one that allows to fly level with the maximum speed.

Concerning the command of the elevator, at the beginning, it is clear that a little deflection of the elevator is imposed; this is to maintain the tail on the ground. It has been decided to deflect the elevator upwards by 30%. This actually means that 30% of the maximum PWM is sent to the channel: $1692\ \mu s$ as indicated by Eq.12.

$$PWM = 1550 + 30\% \times (2025 - 1550) = 1692\ \mu s \tag{12}$$

Two other events are also clearly visible in the blue curve of Fig.61. The first one is the moment when, while being on the ground run, the aircraft raises the tail by releasing the elevator. This happens when the plane has acquired an airspeed of $8\ m/s$. This velocity is under the stall speed but is high enough to raise the tail. The variation of the speed of the vehicle during take-off is given in Fig.62.

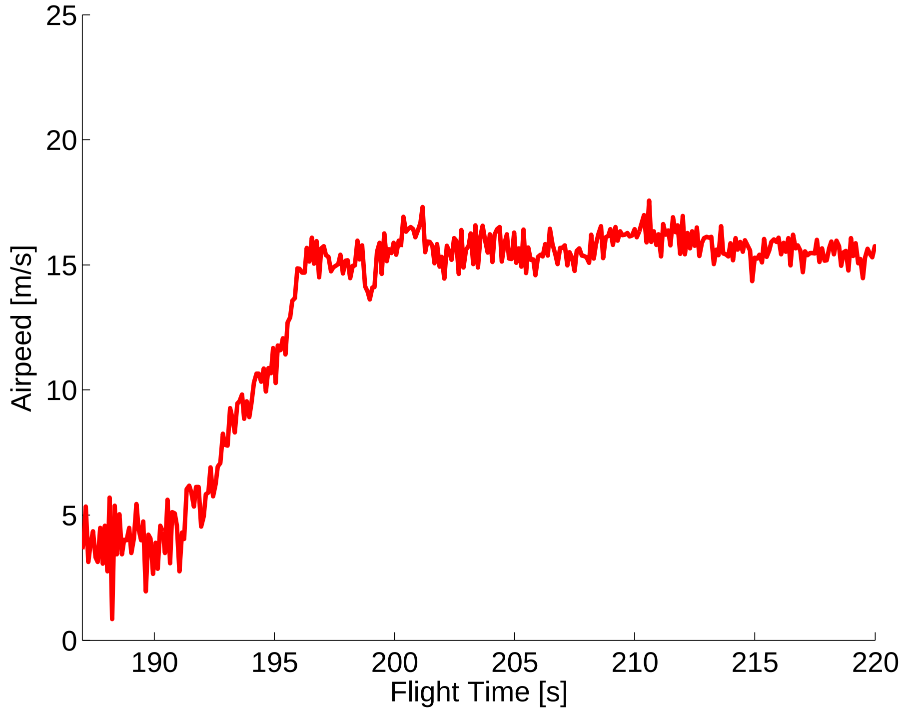

Figure 62: Evolution of the airspeed during take-off.

When the plane has acquired a velocity of $12.5\ m/s$, the rotation occurs and, during a brief time, the elevator is deflected to engage the climb phase. Then, when the plane has the correct pitch angle, it continues climbing without the elevator deflected. Once it reaches the pre-set altitude, the flight controller considers that the take-off is terminated and levels the plane before going to the first waypoint. Fig.62 also shows that the measurements of the Pitot tube at low velocities are not representative of the reality and should not be trusted (below $5\ m/s$).

The variation of the altitude during the take-off is plotted in Fig.63. It should be noted that, during the ground run, the altitude is not exactly zero which is actually an inaccuracy of the sensor. The barometer is subjected to imprecisions, which can cause the indicated altitude to be wrong by a few meters. During take-off, this inaccuracy is not an issue but during landing, it becomes an important consideration, as will be explained in the next section.

The second thing to notice is the end of the take-off. When the plane reaches $40\ m$, the autopilot should initiate directly the mission. Each time the plane passes by a waypoint, it wants to level a little before continuing the mission further. This is shown by the plateau in the figure. However, the plane levels at $46\ m$ instead of the expected $40\ m$. The barometer is not the most accurate sensor but the plane also requires a little time to change its attitude.

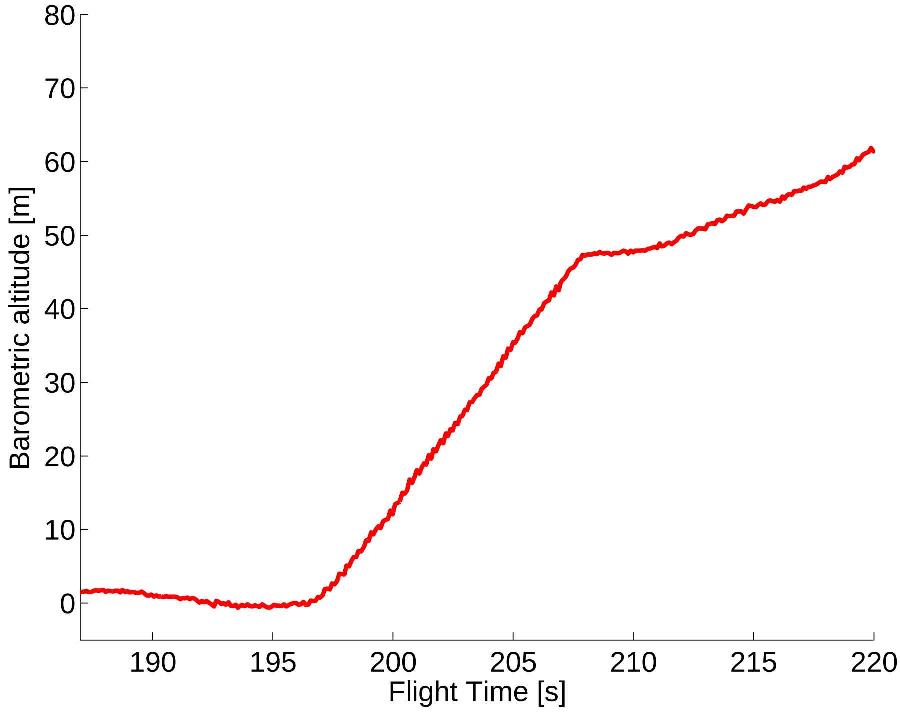

Figure 63: Evolution of the altitude during take-off.

Fig.64 presents a comparison between the pitch demanded by the flight controller and the one realised by the plane during the take-off. The different steps of the take-off are represented but additional comments can be made based on this plot.

First, the real pitch angle is at around $10°$ while the aircraft stays on the ground. Indeed, due to the configuration of the landing gear, when the plane is at rest on the ground, it lies at an angle of about $10°$ to the horizontal.

The demanded pitch angle is not $0°$ but $5°$ during the ground run. This is a security written in the source code of the flight controller in case the rotation speed is badly estimated. Indeed, with an angle of $5°$, most airframes should be able to take-off safely if they have reached a high enough velocity.

Now, during the first step of the take-off, the autopilot actually tries to impose to have a pitch angle of $5°$, but this channel is in reality overwritten by the 30% elevator deflection in order to maintain the rear wheel on the ground. The demand of $5°$ is therefore only applied when the plane has passed a velocity of $8\ m/s$ for the tail to be raised. However, this angle is never well realised; there is probably insufficient time to do this.

When the rotation speed is reached, the aircraft acquires its climb pitch angle. In this flight, this angle was set to $20°$ but as the pitch is limited to $18°$, the autopilot demands a pitch angle of $18°$.

Once the vehicle attains an altitude of $46\ m$, there is a brief instant of levelling before continuing the mission. In this case, the mission was the rectangle described previously, at an altitude of $100\ m$. Therefore, two or three waypoints were used to make the transition smoothly. As a result, it can be seen in Fig.64 that the plane continues to climb.

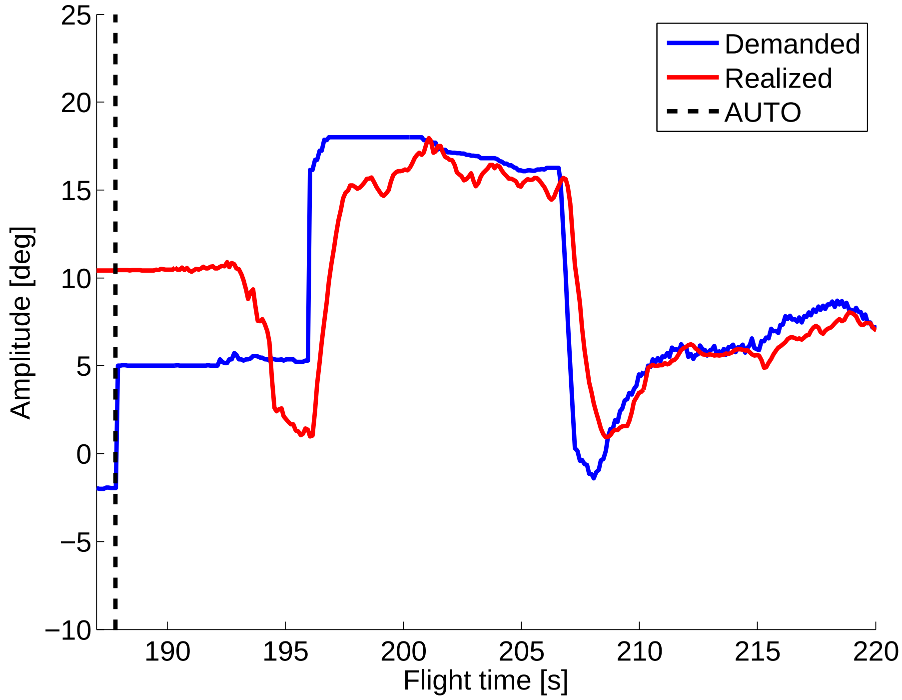

Figure 64: Comparison between the demanded pitch and the realised pitch during take-off.

6.4 Landing

This section is about the end of the flight, which is the landing. This is also realised autonomously.

6.4.1 Principle

A diagram similar to the one for the take-off can be used to explain the different steps of a landing. This is shown in Fig.65.

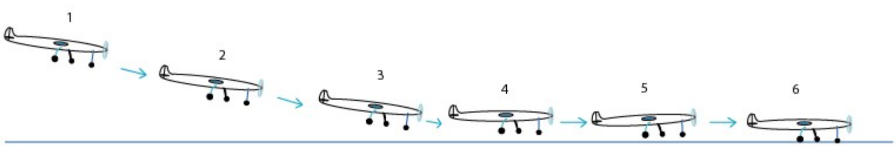

Figure 65: Representation of the different steps for landing [31].

For a smooth landing, the placement of the last waypoints is important. Indeed, the objective of this preparation (also called "approximation") is to lower the altitude of the plane to a correct height to initiate the landing. This height mainly depends on the obstacles nearby. On the other hand, the last waypoint is crucial because, in addition to this height, it also determines the orientation of the plane during (and after) landing. Indeed, the trajectory during and after the landing is a straight line going from the last waypoint and passing by the landing point, which corresponds to the touch-down. In this thesis, a height of about $30\ m$ works well; in particular, if the plane is landing from the right because there is no high obstacle there, which is not the case on the other side. Finally, the altitude and the distance of the last waypoint also determine what will be the angle of the descent. The higher it is (e.g. the closer the waypoint to the runway), the harder the landing. As a result, it is a good idea to have an angle that is not too high. A commercial plane uses an angle of 3° but it is impossible to use a similar value here because it would require to start the landing from too far. Therefore, an angle of about $8 - 9°$ seems appropriate in the present conditions. The choice to land from the left or from the right depends on the wind. It is always better to land into the wind (like the take-off).

Between the last waypoint and the landing position (on the runway), the plane will descend with two objectives: a descent rate and the landing point. On the one hand, it will try to maintain a specific descent rate, which has been chosen to be about $2\ m/s$ (after some tests). On the other hand, the aircraft wants to land at the exact position that was set in the mission plan. However, these two objectives can be impossible to satisfy simultaneously. Therefore, at the beginning of the slope, the speed is considered more important while, as it approaches the end, it is the position that becomes more critical. This is a special parameter of the flight controller which changes the weighting of the two parameters as the vehicle descends.

After that, just before touching the ground, there is the flare: it is a manoeuvre to increase the angle of attack of the plane in order to slow down before touching the ground. There are two parameters that can initiate the flare, the time left before touching the ground if it continues with the same descent rate or a given altitude. It has been decided to set a time of $2\ s$ to flare before touching the runway. The altitude setting is used only if the first parameter does not trigger by the time the vehicle has the fixed altitude. This altitude should be set to a value that accounts for a little barometric drift because this sensor can be slightly inaccurate. For this project, an altitude of $4\ m$ was used. Indeed, it would have been possible to improve this figure if a more accurate altitude sensor was used (which is not the case here).

After the flare, the plane continues to navigate but with a reduced descent rate of $0.5\ m/s$ and with the throttle set at its minimum. Additionally, the roll is also limited to $\pm 5°$ to avoid to touch the ground with the wing. This also means that if there is a strong crosswind, the aircraft can deviate from its planned trajectory. Finally, it decelerates over the runway and stops. The plane is disarmed automatically if no action occurs while it is on the runway after $20\ s$.

6.4.2 Analysis

As for the take-off, a similar analysis can be carried by observing different parameters saved to the memory of the autopilot.

Fig.66 represents an example of an approach path followed by the aircraft during an autonomous landing. The different waypoints used to lower the altitude are displayed as well as their height. It is clearly visible that the last waypoint is very important. Indeed, during its final descent, the plane follows a straight line passing by this waypoint and the landing position. It can be seen that, at the end, there is a sharp little turn on the ground but this will be discussed afterwards, looking to other parameters.

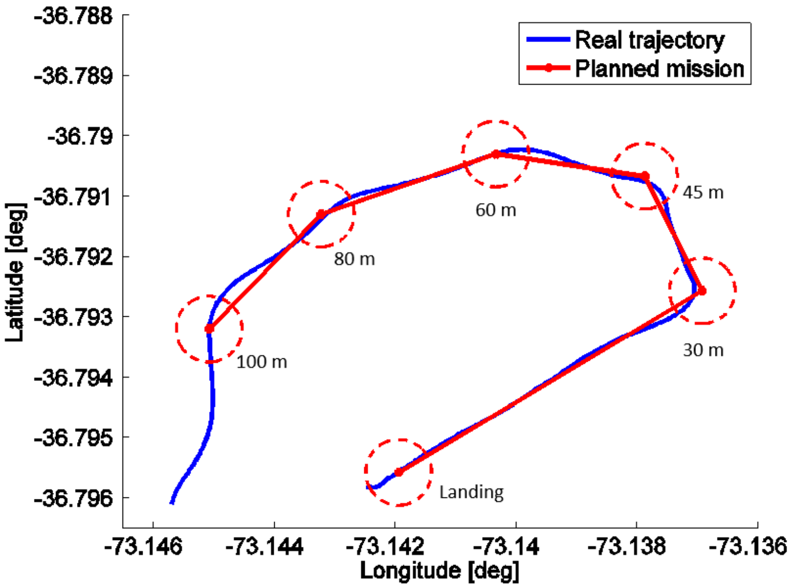

Figure 66: Trajectory followed by the aircraft during the different landing steps. The altitude that the plane should reach for the different waypoints is indicated.

In order to analyse the other parameters, it is interesting to determine the exact time at which the plane touches the ground. This can be done by looking to Fig.67. When the aircraft touches the ground, it produces a shock that is clearly visible in the measurement from the accelerometer, particularly in the vertical direction. As a result, we know that the plane touches the ground at $621\ s$.

It is also possible to notice in this plot that the plane stops moving at about $633\ s$ because, from that moment, the vibrations are reduced and correspond only to those of the engine working at the minimum throttle. Moreover, the acceleration in the x direction is no longer centred around zero. This is caused by the inclination the plane has when it is on the ground due to the landing gear. As a result, a component of gravity is also measured in the x direction.

It is difficult to explain the sharp little turn on the ground. Indeed, my first thoughts were that the plane changed his trajectory due to an obstacle on the runway. However, this would cause a peak in the vibrations. It can be seen that there is one around $626\ s$ but it corresponds to a little jump the plane did over a bump on the runway. As a result, it might be possible that the trajectory was a little off and that the flight controller deflected the rudder to correct it. Moreover, as the rear wheel is fixed compared to a traditional tail-dragger, the aircraft stopped its motion in this turn because at the beginning of the correction the tail was off the ground but once the tail touches the runway, the only thing the plane can do is to continue in a line. However, this is not certain because out of three completely autonomous missions, this is the only one that has shown this behaviour. Amongst other possible reasons, it could have been due to the effect of a sudden lateral wind[12].

[12]No device was used to measure the wind: thus, it is impossible to validate or not this assumption.

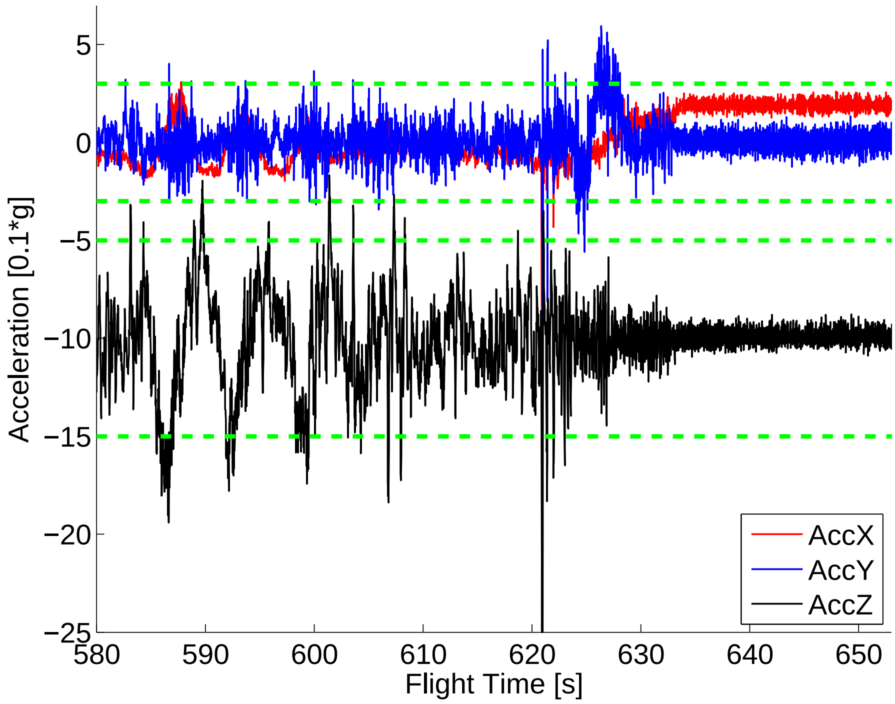

Figure 67: Vibrations of the aircraft at the end of the flight.

Another property that can be analysed is the pitch. The comparison between the demanded pitch and the realised one during the approach and the landing is shown in Fig.68. The flare can be visualised, at $620\ s$. It corresponds to the small flat zone where the demanded pitch is zero (just before landing). The plane does not have a zero pitch angle by the end of the flare but the pitch that remains is small.

After touchdown, the pitch demand signal reaches $7°$ and then quickly reduces to zero. Touchdown probably pushes the nose down because the new friction force creates a nose down moment that is not balanced by any other moments. The autopilot reacts by demanding higher pitch in order to keep the nose level. As the plane touches the ground, the autopilot would like that the aircraft continues to level. Actually, this is what is happening when the plane has enough velocity. However, the plane also decelerates over the runway and there is a moment when the velocity is no longer sufficient in order to keep the tail off the ground. As a result, the inclination of the plane is the one that it has with his tail down.

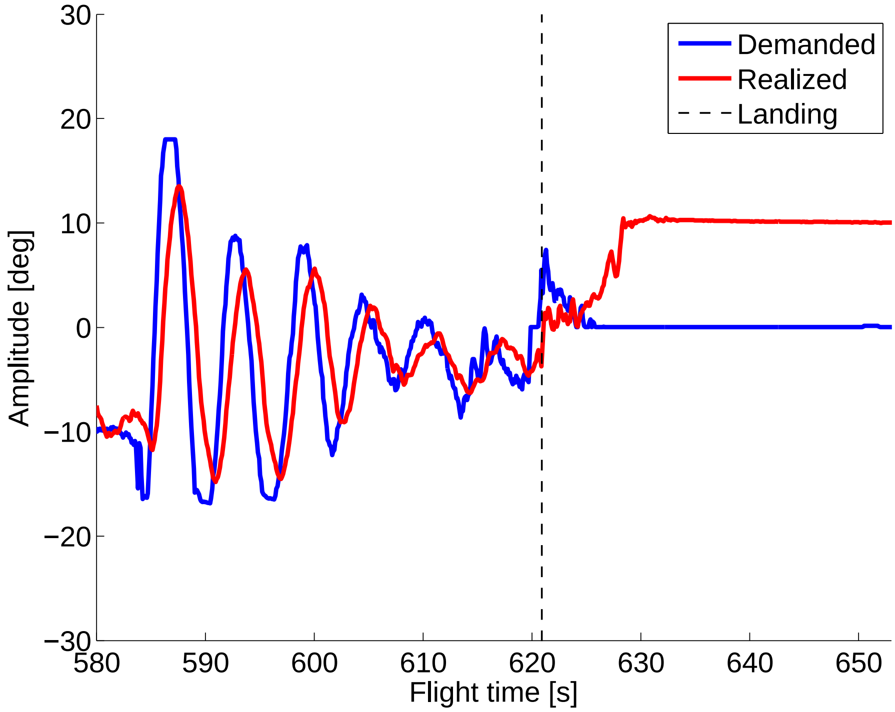

Figure 68: Comparison between the demanded and realised pitch angles during landing.

Fig.69 plots the PWM signals sent to the elevator and throttle channels. After the flare, the throttle is completely cut, meaning that the engine turns on idle. However, the propeller is still rotating because it would have been dangerous to turn off the engine completely as it is a combustion engine. For example, it would be impossible to switch it on again if a problem arises.

Regarding the elevator, it initiates the descent after each waypoint but otherwise it is around its trimmed configuration. When the tail of the plane is on the ground (at the end), it is deflected downward because the flight controller would like to level the aircraft again.

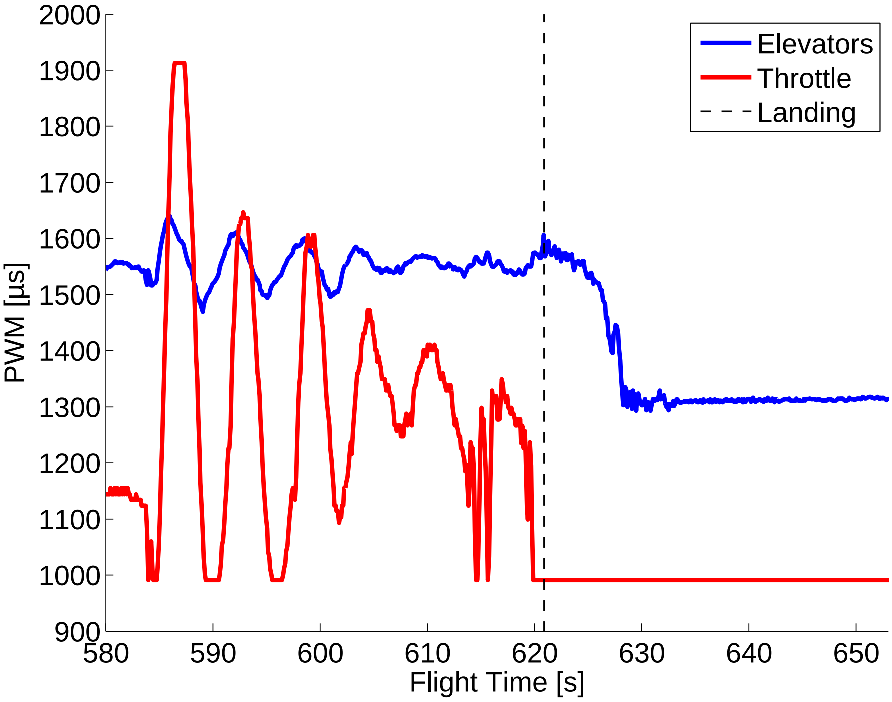

Figure 69: PWM of the channels of the elevator and of the throttle during landing.

7 Conclusion

In this thesis, the understanding of the functioning of an open source autopilot has been discussed. It is based on the *APM 2.6* from the ArduPilot family. It works based on a cascade of PID controllers to monitor the attitude and the navigation of the plane.

The flight controller and the other components required for the navigation were installed in a RC aircraft. This plane has a tail-dragger landing gear; consequently, it lies on the ground with a pitch angle of $10°$. This has led to some difficulties in the installation of some components such as the Pitot tube due to the necessity to align it with the airflow in cruise. Moreover, repairs were made on the plane because of human errors at the beginning.

Additionally, some supports were successively designed and 3-D printed. In particular, the support of the flight controller board has allowed to have a good vibration level, which was a concern in this work due to the combustion engine.

The different parameters have been tuned and discussed. The plane shows good flying qualities and can accomplish a completely autonomous mission, including take-off and landing. However, landing was at the end of this work and not a lot of time was spent on this phase of the flight. In particular, the descent parameters could be optimized. Moreover, conservative values for the flare altitude were considered to account for a possible barometric shift. Using a sensor of distance (e.g. a LIDAR) should improve this phase of the flight. It would also mean to switch to the newer version of the flight controller, the *PixHawk*, in order to have a bigger memory. Indeed, the one of the *APM 2.6* used in this project is full. Therefore, using the new version of the autopilot should improve some flight features and a better optimization of some parameters could be possible, although a significant difference should not be expected. Moreover, it would also be possible to record a longer flight.

Perspectives

As explained in the introduction, this thesis is the first work of a series that will be realised by the University of Concepción. Indeed, after a long tradition of flight controllers installed in copters, it has been decided to try to (re-)investigate the plane features.

The use of the complete system (aircraft and autopilot) could lead to different types of analyses of flight dynamics. Indeed, some studies have been carried out with other planes, but most of them are powered electrically and are often a little heavier. Installing, a sensor of angular of attack and, even if it is more difficult, a load cell to monitor the thrust could lead to possible interesting conclusions to the scientific community. The installation of a flight controller leads to a level flight that is much easier to perform than without it.

In the same order of ideas, a level flight greatly improves the accuracy and the quality of filming. As a result, the (re)installation of a set of cameras around the plane could be an exciting work for future students. It would potentially not have the same quality of resolution that what could be achieved with a copter in stationary flight but an aircraft is capable of travelling a much longer distance. Therefore, it might give a better overview of a region. This would pass by a re-tuning of a part of the parameters, mainly the PID gains in roll and in pitch as a weight variation will be noticeable. Additionally, a particular care should be considered when filming in order to ensure that the plane is well on its planned trajectory. Turns and the oscillations that follow should therefore be outside of the desired objectives.

Furthermore, by using different sensors such as the LIDAR (light detection and ranging), already considered here-above, it would be possible to analyse the topography of different areas. As a result, the relief could be scanned and analysed afterwards.

A last idea is to transform somehow the plane into what is called a quad-plane. This is an aircraft that can accomplish vertical take-off and landing. This would combine the knowledge that the laboratory has acquired during the past years about stationary flights, vertical take-offs with copters, etc. and the one described in the present report.

8 References

Articles

[1] D.H.Nguyen and B.Widrow. “Neural Networks for Self-Learning Control Systems.” In: *IEEE Control Systems Magazine.* (April 1990), pp. 18–23.

[2] J.Deyst S.Park and J.P.How. “A New Nonlinear Guidance Logic for Trajectory Tracking.” In: *Proceedings of the AIAA Guidance, Navigation and Control Conference* (2004).

[3] Y.Cao H.Chao and Y.Chen. “Autopilots for Small Fixed-Wing Unmanned Air Vehicles: A Survey.” In: *International Conference on Mechatronis and Automation* (2007), pp. 3144–3149.

[4] L.Kunqin Y.Shengyi and S.Jiao. “Design and Simulation of the Longitudinal Autopilot of UAV Based on Self-Adaptive Fuzzy PID Control.” In: *International Conference on Computational Intelligence and Security* (2009), pp. 634–638.

[5] A.Alsaraj and G.Stuffle. “Surface-to-air Missile Autopilot Design Using LQG/LTR Gain Scheduling Method.” In: *Chinese Journal of Aeronautics.* (2011), pp. 279–286.

[6] Alan Hitchcox. “Fundamentals of Pressure Transducers.” In: *Hydraulic and Pneumatic* (2013).

[7] A.Alsaraj and G.Stuffle. “Missile Autopilot Design using Artificial Neural Networks.” In: *International Journal of Engineering Trends and Technology (IJETT).* 29.6 (2015), pp. 284–289.

[8] A.Sarhan and S.Qin. “Adaptive PID Control of UAV Altitude Dynamics Based on Parameter Optimization with Fuzzy Interference.” In: *International Journal of Modeling and Optimization* 6.4 (2016), pp. 246–251.

[9] A.Sarhan and S.Qin. “Autonomous Intelligent Flight Control of Fixed-Wing UAV Based on ADaptive Neuro-Fuzzy Inference System.” In: *IJRET:International Journal of Research in Engineering and Technology.* 5 (2016), pp. 92–100.

[10] A.Calise Y.Shin and M.Motter. “Application of Adaptive Autopilot Designs for an Unmanned Aerial Vehicle.” In: *American Institue of Aeronautics and Astronautics.* ().

Books

[11] K.Aström and T.Hägglund. *PID Controllers: Theory, Design and Tuning, 2nd Edition*. 1995. ISBN: 1-55617-516-7.

[12] V.A.Ugrinovskii I.R.Petersen and A.V.Savkin. *Robust Control Design Using H∞ methods*. Springer, 2000. ISBN: 978-1-4471-1144-3.

[13] T.H.Lee S.S. Ge C.C.Hang and T.Zhang. *Stable Adaptive Neural Network Control*. Springer Science, 2002. ISBN: 978-1-4419-4932-5.

[14] Christopher J.Hegarty Elliot D.Kapplan. *Understanding GPS Principles and Applications*. Artech House, 2006. ISBN: 1-58053-894-0.

[15] A.Tewari. *Automatic Control of Atmospheric and Space Flight Vehicles: Design and Analysis with Matlab and Simulink*. Birkhäuser, 2010. ISBN: 978-0-8176-4863-3.

[16] G.J.Vachtsevanos et al. K.Valvanis. *Handbook of Unmanned Aerial Vehicles*. Springer Netherlands, 2015. ISBN: 978-90-481-9708-1.

Thesis

[17] C.Andersson and M.Lindberg. “Autotuning of a PID-controller”. Lund Institute of Technology, 2004.

[18] J.Gadewadikar. “H-Infinity Output-Feedback Control: Application to Unmanned Aerial Vehicle”. University of Texas, May 2007.

[19] Ingrid Hagen Johansen. “Autopilot Design for Unmanned Aerial Vehicles”. Norwegian University of Science and Technology, 2012.

Websites

[20] *ArduPilot*. URL: http://ardupilot.org/.

[21] Tom BENSON. *Aerodynamics*. URL: https://www.grc.nasa.gov/www/k-12/VirtualAero/BottleRocket/airplane/short.html.

[22] B.Jones. *Plane:L1 Control for Straight and Curved Path Following*. URL: https://github.com/ArduPilot/ardupilot/pull/101.

[23] Marshall Brain. *How Two Strokes Engines Work?* URL: http://science.howstuffworks.com/transport/engines-equipment/two-stroke.htm.

[24] C.Anderson. *A little bit of history*. URL: http://diydrones.com/profiles/blogs/a-little-bit-of-history.

[25] Stéphane CHAUSSEDENT. *Statique et dynamique des fluides*. URL: http://res-nlp.univ-lemans.fr/NLP_C_M02_G02/co/NLP_C_M02_C02_web.html.

[26] Peter H.Dana. *Global Positioning System Overview*. URL: http://www.colorado.edu/geography/gcraft/notes/gps/gps_f.html.

[27] *Pressure Transducers Introduction to Pressure Transducers and Transmitters*. URL: http://www.omega.com/prodinfo/pressuretransducers.html.

[28] *PWM*. URL: https://developer.android.com/things/sdk/pio/pwm.html.

[29] Q.Abdullah. *Geospatial Applications of Unmanned Aerial Systems*. URL: https://www.e-education.psu.edu/geog892/node/643.

[30] R.Colon. *Development of Aviation Technology*. URL: http://www.century-of-flight.freeola.com/Aviation%20history/evolution%20of%20technology/uav.htm.

[31] *Takeoff Procedure*. URL: http://www.rc-airplane-advisor.com/takeoff-procedure.html.

[32] Unknown. *RC Model Airplane Engines*. URL: http://www.rc-airplane-world.com/model-airplane-engines.html.

Others

[33] T.Andrianne. *Aircraft Design: Aerodynamics*. University of Liege, 2015-2016.

[34] N.Kuyvenhoven. *PID Tuning Methods: An Automatic PID Tuning with MathCad.* Calvin College, 2002.

[35] P.Williams-Hayes et al. J.Burken. *Adaptive Control Using Neural Network Augmentation for a Modified F-15 Aircraft.* 2006.

[36] G. Dimitriadis. *Flight Dynamics and Aircraft Performance*. University of Liege, 2016.

[37] *APM2.6 APM Flight Controller Board For Multicopter.* URL: http://www.nyplatform.com/index.php?route=product/product&product_id=1365.

[38] *MAX-55AX Instruction Manual*. URL: http://manuals.hobbico.com/osm/55ax-manual.pdf.

[39] *MPXV7002 Integrated Silicon Pressure Sensor On-Chip Signal Conditioned, Temperature Compensated and Calibrated.* URL: http://www.nxp.com/docs/en/data-sheet/MPXV7002.pdf.

[40] *Question about Pitot tube placement.* URL: http://diydrones.com/forum/topics/question-about-pitot-tube.

[41] *Super Frontier Senior - 46S.* URL: https://www.theworldmodels.com/store/?action=productDetail&id=7411.

A Static thrust measurements

In this appendix, the measurements of the static thrust are provided as well as the method followed to take them. The collected data are presented in Table 7.

Throttle [%]	Static thrust [N]	RPM
0	0	2730
20	8.1	6000
30	9.9	6900
35	11.7	7300
40	13.5	7800
50	16.2	8500
60	20.7	9400
70	22.5	9800
80	23.85	10020
90	25.2	10470
100	25.2	10500

Table 7: Table presenting the static thrust for different positions of the throttle. The number of RPM for each of these positions are also measured.

The analog dynamometer is attached to the plane at the rear wheel and the plane is on the ground as shown in Fig.70. Therefore, friction influences a bit the results as, in order to measure a force, this one needs to be sufficient to counter the friction. Static thrust is measured with a dynamometer in kilograms and is then converted to Newtons. On the other hand, a tachiometer is also considered to measure the RPM.

Figure 70: Set-up of the measurements.

It is also possible to visualise the results in a plot such as the one in Fig.71. It is clear that even if the engine is rotating when the throttle is at its minimum, no static thrust is produced: this is caused by the friction of the landing gear with the ground. The engine is still rotating when the throttle is at the minimum value because it would be dangerous in flight to close completely the engine. Indeed, it would be impossible to restart it as a plug igniter is required to do so. As a result, the arm of the servomotor controlling the opening of the throttle is such that a little amount of air still enters the cylinder even when the throttle is at zero. Another consequence of such a practice is that there is no difference between 90 and 100% of the throttle because at 90%, the throttle is already nearly completely opened.

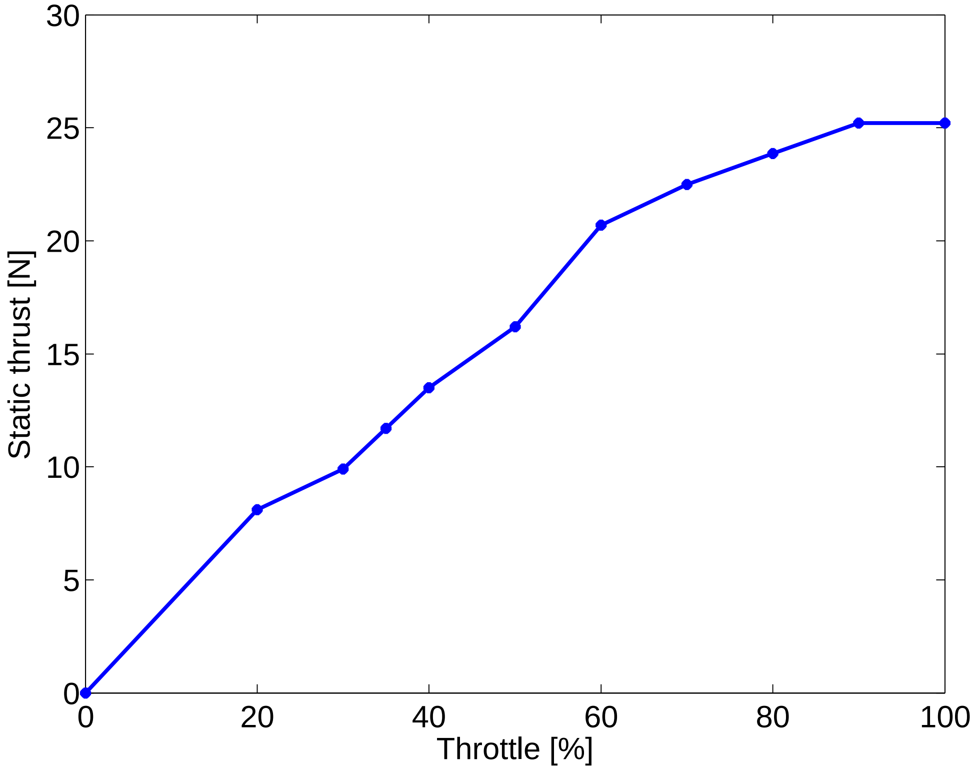

Figure 71: Static thrust measured for different openings of the throttle.

B Different tools

During the realisation of this master thesis, apart from the tools used to work the wood utilised during the modifications and the repairs of the plane, two other techniques were used: the soldering of electric wires and the 3D printing of some supports.

B.1 Soldering

The soldering was used to connect different wires together. The type of soldering that was considered is said to be slow because the solder dries at the ambient temperature (without any process to accelerate it). Wires were soldered for different purposes: to adapt a connector to a battery, to fix the BEC to the rest of the circuit, to build the training cable between the two radios at the beginning, to extend existing cables such as those of the module GPS/compass. However, the most challenging piece was to replace the deficient voltage regulator of the autopilot. The latter one was particularly difficult because it is a surface mounted component and the old soldering was industrially made.

In order to solder correctly, several tools are needed:

- a soldering station (soldering iron),
- a solder wire,
- a lubricant,
- a holding frame,
- a sponge,
- a hair dryer.

The soldering process of two wires in order to make a splice can be described in the following way.

First, the soldering iron is heated up to a temperature above the melting point of the solder wire. This temperature depends on the alliage used and the presence of lead or not (in the EU, it is forbidden to buy a solder with lead nowadays). In addition to that, the temperature should be sufficiently high to have a good heat flux: it depends on the iron tip that is used. Indeed, a tiny tip will tend to require a higher temperature than for a larger tip because the heat transfer is worse when the tip is small. A temperature of $400°$ has shown good results in the realisation of the work.

While the iron is heating up, it is important to prepare the wires by removing the protections where the solder is going to be applied. If possible, it is also better to twist the unprotected wires together. Then, lubricant is placed: this aims to improve the heat flux when solder will be applied.

When the iron is hot enough, the first thing is to ensure that the iron tip is clean. For that purpose a moistened sponge or a copper scouring pad are available. Then, the tip is tinned. After, solder is added until the wire is soaked with the solder. The process is eventually repeated with the second wire.

The two tinned wires are placed side to side with the help of the holding frame. The iron is then hold over them in order to melt the present solder and make the joint.

At the end, a thermoretractable protection is applied around the part that has been soldered in order to protect it from its environment. This heat comes from a hair dryer.

B.2 3D printing

In order to realise the installation of the autopilot and its components in the plane, some parts were printed using a 3D printing machine: the *Ultimaker 2*, which is presented in Fig.72. In this work, successive layers of Polylactic Acid (PLA) to create the designed object. PLA is a thermoplastic derived from resources such as corn starch or sugarcane.

The printing machine has a heating plateau of about $25 \times 25\ cm$. Different parameters need to be configured in order to print a part correctly. The software *Cura* is used to prepare the designed object for the 3D printing machine. It gives also the possibility to control how the layers will be successively printed. More importantly, it is also possible to print supports if the piece has some parts that do not have a base that touches the plate (these supports are removed once the object is printed). The parameters considered for the printings are listed in Table 8. These are based on different tests and discussions with other students from the laboratory. In addition, glue is added to the glass plateau to guarantee the adherence of the printed structure while it is being printed. Otherwise, there could be issues within the first layers.

Figure 72: The 3-D printing machine.

Name	Value
Quality	
Layer height	$0.15\ mm$
Shell thickness	$0.8\ mm$
Enabled retraction	yes
Initial layer thickness	$0.3\ mm$
Initial layer line width	$100\ \%$
Cut off object bottom	$0.0\ mm$
Dual extrusion overlap	$0.15\ mm$
Fill	
Bottom/Top thickness	$1.5\ mm$
Fill density	100%
Speed	
Print speed	$50\ mm/s$
Travel speed	$80\ mm/s$
Bottom layer speed	$30\ mm/s$
Infill speed	$50\ mm/s$
Top/bottom speed	$40\ mm/s$
Outer shell speed	$30\ mm/s$
Inner shell speed	$40\ mm/s$
Support	
Support type	Everywhere
Platform adhesion	none
Machine	
Nozzle size	$0.4\ mm$
Cool	
Minimal layer time	$5\ s$
Enable cooling fan	yes

Table 8: Table presenting the different settings of the 3D printing machine.

An example of piece that was printed is given in Fig.73. It is the support that maintain the module with the GPS and the compass in place. It is a view of the different levels with the supports (in light blue) that are removed afterwards.

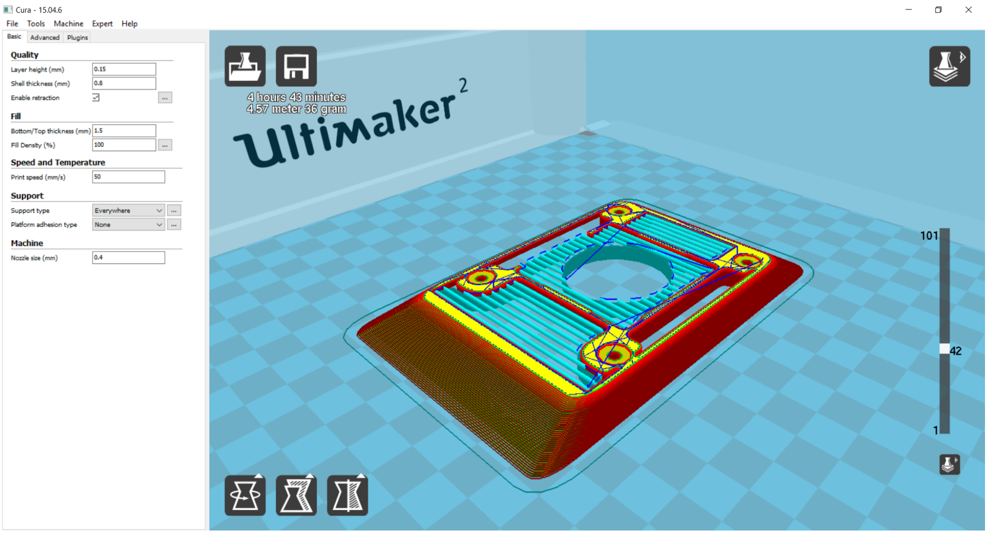

Figure 73: Example of an object being prepared with the software *Cura*. It corresponds to the support of the GPS/compass.

C Checklists

In this appendix, the two check-lists that were used during the thesis are displayed. Although, they were written in Spanish during the work, the translations are also indicated hereunder. The first list concerns the material that is needed when going to the aeromodelism club while the second contains the different steps to ensure that the aircraft is ready to fly.

C.1 Materials needed

Avión/Plane				
Fuselaje/Fuselage Cabina/Cockpit Ala derecha/Right wing Ala izquierda/Left wing Caja del avión/Drawer Tornillos para la ala/Screws for the wing				
Autopiloto/Autopilot				
Autopiloto/Autopilot Batería (Voltaje)/Battery (Voltage) BEC Power module Antena/Antenna GPS, Brújula/GPS, Compass				
Radio				
Taranis (Voltaje)/Taranis (Voltage) Arnés/Harness Antena del computador/Antenna of the computer Cable para la memoria/Wire for the memory				
Flight box				
Combustible/Fuel Instrumentos (Volt-RPM-...)/Instruments (Volt-RPM-...) Calentador de bujía/Plug igniter Starter Batería del starter (Voltaje)/Battery of the starter (Voltage) Gomas/Rubber				
Others				
Computador (Batería)/Computer (Battery) Toalla nova/Cleaning paper Alcohol Instrucciones de vuelo/Flight instructions				

Table 9: Check-list presenting the material needed when leaving the laboratory.

C.2 Before flying

Motor/Engine				
Hélices/Propeller Escape/Exhaust system Spinner/Spinner Nivel de carburante/Fuel level Conexión de las tuberias del tanque al motor/Connections of the fuel tank to the engine Fijaciones del tanque/Fixations of the tank				
Avión/Plane				
Estado fuselaje/State of the fuselage Estado tren de aterrizaje/State of the landing gear				
Ala/Wing				
Estado general/General state				
Superficies de control/Control surfaces				
Estado timón/State of the rudder Conexión servo-timón/Connection servo-rudder Estado elevadores/State of the elevators Conexión servo-elevadores/Connection servo-elevators Estado alerones/State of the ailerons Conexión servo-alerones/Connection servo-ailerons				
Autopiloto/Autopilot				
Estado/State Posición/Position Fijación/Fixation				
Receptor				
Posición/Position Fijación/Fixation Antenas/Antennas				
Conexiones autopiloto-receptor/Connections autopilot-receptor (inputs)				
Ch1-Ch1: Alerones/Ailerons Ch2-Ch2: Elevadores/Elevators Ch3-Ch3: Motor/Engine Ch4-Ch4: Timón/Rudder Ch5-Ch5: Modos de vuelo/Flight modes Ch6-Ch6: Geofence Ch7- / : No utilizado/Not used Ch8-SBUS: Energía entre autopiloto y receptor/Energy between the autopilot and the receptor				
Conexiones autopiloto-servos/Connections autopilot-servos (outputs)				
Ch1: Alerones/Ailerons Ch2: Elevadores/Elevators Ch3: Motor/Engine Ch4: Timón/Rudder Ch5: No utilizado/Not used Ch6: No utilizado/Not used Ch7: No utilizado/Not used				

Ch8-BEC: Energía entre autopiloto y BEC/Energy between the autopilot and the BEC				
GPS(+Brújula)/GPS(+Compass)				
Posición/Position Fijación/Fixation Orientación/Orientation Conexión GPS-GPS/Connexion GPS-GPS Conexión Brújula-IPC/Connexion Compass-IPC				
Tapa/Lid				
Estado/State				
Antena/Antenna				
Posición/Position Fijación/Fixation Conexión antena-telemetry port/Connection antenna-telemetry port				
Power module				
Posición/Position Fijación/Fixation Conexión PM-Autopiloto/Connection PM-Autopilot				
BEC				
Posición/Position Fijación/Fixation Conexión BEC-Autopiloto/Connection BEC-Autopilot				
Batería (sin conexión)/Battery (without connection)				
Posición/Position Fijación/Fixation				
Caja del avión/Drawer of the plane (payload bay)				
Estado/State				
Computador/Computer				
Encender/Switch on Mission Planner Antena del computador/Antenna of the computer				
Fijación del ala/Fixation of the wing				
Conexión tubo de Pitot/Connexion of the Pitot tube => A0 Conexión alerones /Connexion of the ailerons				
Radio Taranis				
Encender/Switch on				
Conexión batería/Connection of the battery **Fijación de la cabina/Fixation of the cockpit**				
Verificaciones/Verifications				
Acelerómetros/Accelerometers Calibración radio/Calibration of the radio Calibración del sensor de velocidad/Calibration of the speed sensor Adquisición del GPS/GPS lock Brújula/Compass				
Misiones/Missions				
Trayectroria/Trajectory				

Puntos de paso/Waypoints Altitudes Posición HOME/Position HOME Geofence				
Modo Manual/Flight mode Manual				
Stick alerones a la derecha/Stick ailerons to the right => Alerón derecha sube - izquierda baja/Right aileron up - left down Stick alerones a la izquierda/Stick ailerons to the left => Alerón derecha baja - izquierda sube/Right aileron down - left up Stick elevadores sube/Stick elevators up => Elevadores baja/Elevators Down Stick elevadores baja/Stick elevators down => Elevadores sube/Elevators up Stick timón a derecha/Stick rudder right => Timón a derecha/Rudder to the right Stick timón a la izquierda/Stick rudder to the left => Timón a la izquierda/Rudder to the left Verficación del motor/Verification of the engine				
Modo FBWA/Flight mode FBWA				
Stick alerones a la derecha/Stick ailerons to the right => Alerón derecha sube - izquierda baja/Right aileron up - left down Stick alerones a la izquierda/Stick ailerons to the left => Alerón derecha baja - izquierda sube/Right aileron down - left up Stick elevadores sube/Stick elevators up => Elevadores baja/Elevators Down Stick elevadores baja/Stick elevators down => Elevadores sube/Elevators up Stick timón a derecha/Stick rudder right => Timón a derecha/Rudder to the right Stick timón a la izquierda/Stick rudder to the left => Timón a la izquierda/Rudder to the left				
Avión a la izquierda/Plane to the left => Alerón derecha sube - izquierda baja/Right aileron up - left down Avión a la derecha/Plane to the right => Alerón derecha baja - izquierda sube/Right aileron down - left up Nariz sube/Nose up => Elevadores baja/Elevators Down Nariz baja/Nose down => Elevadores sube/Elevators up Verficación del motor/Verification of the engine				
Armar el avión/Arm the plane Encender el motor/Start the engine Verificación de la carburación del motor/Verification of the fuel mixture of the engine				
Despegue con el bueno modo de vuelo/Take-off with the correct flight mode				

Table 10: Check-list presenting the preparation of the plane and of the flight controller.

D Autopilot parameters

This is the list of the different parameters configured in the flight controller, in alphabetic order.

```
ACRO_LOCKING 0
ACRO_PITCH_RATE 180
ACRO_ROLL_RATE 180
AHRS_COMP_BETA 0.1
AHRS_GPS_GAIN 1
AHRS_GPS_MINSATS 6
AHRS_GPS_USE 1
AHRS_ORIENTATION 2
AHRS_RP_P 0.2
AHRS_TRIM_X 0.009132295
AHRS_TRIM_Y 0.01556013
AHRS_TRIM_Z 0
AHRS_WIND_MAX 0
AHRS_YAW_P 0.2
ALT_CTRL_ALG 0
ALT_HOLD_FBWCM 0
ALT_HOLD_RTL 15000
ALT_MIX 1
ALT_OFFSET 0
ARMING_CHECK 144
ARMING_REQUIRE 1
ARMING_RUDDER 1
ARSPD_AUTOCAL 0
ARSPD_ENABLE 1
ARSPD_FBW_MAX 20
ARSPD_FBW_MIN 11
ARSPD_OFFSET 2133.261
ARSPD_PIN 0
ARSPD_RATIO 1.9936
ARSPD_SKIP_CAL 0
ARSPD_TUBE_ORDER 2
ARSPD_USE 0
AUTO_FBW_STEER 0
AUTOTUNE_LEVEL 6
BATT_AMP_OFFSET 0
BATT_AMP_PERVOLT 17
BATT_CAPACITY 3300
BATT_CURR_PIN 12
BATT_MONITOR 0
BATT_VOLT_MULT 10.1
BATT_VOLT_PIN 13
BATT2_AMP_OFFSET 0
```

```
BATT2_AMP_PERVOL 17
BATT2_CAPACITY 3300
BATT2_CURR_PIN 12
BATT2_MONITOR 0
BATT2_VOLT_MULT 10.1
BATT2_VOLT_PIN 13
BRD_SERIAL_NUM 0
CAM_DURATION 10
CAM_SERVO_OFF 1100
CAM_SERVO_ON 1300
CAM_TRIGG_DIST 0
CAM_TRIGG_TYPE 0
COMPASS_AUTODEC 1
COMPASS_DEC 0
COMPASS_EXTERNAL 1
COMPASS_LEARN 1
COMPASS_MOT_X 0
COMPASS_MOT_Y 0
COMPASS_MOT_Z 0
COMPASS_MOTCT 0
COMPASS_OFS_X -78.76082
COMPASS_OFS_Y -39.86897
COMPASS_OFS_Z -13.58188
COMPASS_ORIENT 8
COMPASS_USE 1
ELEVON_CH1_REV 0
ELEVON_CH2_REV 0
ELEVON_MIXING 0
ELEVON_OUTPUT 0
ELEVON_REVERSE 0
FBWA_TDRAG_CHAN 0
FBWB_CLIMB_RATE 2
FBWB_ELEV_REV 0
FENCE_ACTION 0
FENCE_AUTOENABLE 0
FENCE_CHANNEL 6
FENCE_MAXALT 200
FENCE_MINALT 100
FENCE_RET_RALLY 0
FENCE_RETALT 150
FENCE_TOTAL 0
FLAP_1_PERCNT 0
FLAP_1_SPEED 0
FLAP_2_PERCNT 0
FLAP_2_SPEED 0
FLAP_IN_CHANNEL 0
```

```
FLAP_SLEWRATE 75
FLAPERON_OUTPUT 0
FLTMODE_CH 5
FLTMODE1 0
FLTMODE2 5
FLTMODE3 8
FLTMODE4 10
FLTMODE5 12
FLTMODE6 0
FORMAT_VERSION 13
FS_BATT_MAH 0
FS_BATT_VOLTAGE 0
FS_GCS_ENABL 0
FS_LONG_ACTN 0
FS_LONG_TIMEOUT 5
FS_SHORT_ACTN 0
FS_SHORT_TIMEOUT 1.5
GCS_PID_MASK 7
GLIDE_SLOPE_MIN 15
GLIDE_SLOPE_THR 5
GND_ABS_PRESS 102389.5
GND_ALT_OFFSET 0
GND_TEMP 17.78364
GPS_GNSS_MODE 0
GPS_MIN_ELEV -100
GPS_NAVFILTER 8
GPS_SBAS_MODE 2
GPS_TYPE 1
GROUND_STEER_ALT 1
GROUND_STEER_DPS 90
HIL_ERR_LIMIT 5
HIL_SERVOS 0
INITIAL_MODE 0
INS_ACCEL_FILTER 20
INS_ACCOFFS_X 0.0279031
INS_ACCOFFS_Y 0.06891095
INS_ACCOFFS_Z -0.5071301
INS_ACCSCAL_X 0.9961575
INS_ACCSCAL_Y 0.9925628
INS_ACCSCAL_Z 0.9971783
INS_GYRO_FILTER 20
INS_GYROFFS_X 0.01823274
INS_GYROFFS_Y -0.05600455
INS_GYROFFS_Z 0.005464767
INS_PRODUCT_ID 88
INS_USE 1
```

INVERTEDFLT_CH 0
KFF_RDDRMIX 0.25
KFF_THR2PTCH 0
LAND_DISARMDELAY 20
LAND_FLAP_PERCNT 0
LAND_FLARE_ALT 3
LAND_FLARE_SEC 2
LAND_PITCH_CD 0
LEVEL_ROLL_LIMIT 5
LIM_PITCH_MAX 1800
LIM_PITCH_MIN -1700
LIM_ROLL_CD 2500
LOG_BITMASK 540670
MAG_ENABLE 1
MIN_GNDSPD_CM 0
MIS_RESTART 0
MIS_TOTAL 15
MIXING_GAIN 0.5
NAV_CONTROLLER 1
NAVL1_DAMPING 0.6
NAVL1_PERIOD 18
PTCH2SRV_D 0.03
PTCH2SRV_FF 0
PTCH2SRV_I 0.03333334
PTCH2SRV_IMAX 3000
PTCH2SRV_P 0.4
PTCH2SRV_RLL 1.15
PTCH2SRV_RMAX_DN 75
PTCH2SRV_RMAX_UP 75
PTCH2SRV_TCONST 0.45
RALLY_INCL_HOME 0
RALLY_LIMIT_KM 5
RALLY_TOTAL 0
RC1_DZ 30
RC1_MAX 2028
RC1_MIN 977
RC1_REV -1
RC1_TRIM 1499
RC10_DZ 0
RC10_FUNCTION 0
RC10_MAX 1900
RC10_MIN 1100
RC10_REV 1
RC10_TRIM 0
RC11_DZ 0
RC11_FUNCTION 0

```
RC11_MAX 1900
RC11_MIN 1100
RC11_REV 1
RC11_TRIM 0
RC2_DZ 30
RC2_MAX 2025
RC2_MIN 983
RC2_REV 1
RC2_TRIM 1550
RC3_DZ 30
RC3_MAX 2016
RC3_MIN 991
RC3_REV 1
RC3_TRIM 991
RC4_DZ 30
RC4_MAX 2017
RC4_MIN 996
RC4_REV 1
RC4_TRIM 1504
RC5_DZ 0
RC5_FUNCTION 0
RC5_MAX 1963
RC5_MIN 991
RC5_REV 1
RC5_TRIM 991
RC6_DZ 0
RC6_FUNCTION 0
RC6_MAX 1505
RC6_MIN 1503
RC6_REV 1
RC6_TRIM 1499
RC7_DZ 0
RC7_FUNCTION 0
RC7_MAX 1900
RC7_MIN 1100
RC7_REV 1
RC7_TRIM 1499
RC8_DZ 0
RC8_FUNCTION 0
RC8_MAX 1900
RC8_MIN 1100
RC8_REV 1
RC8_TRIM 1499
RCMAP_PITCH 2
RCMAP_ROLL 1
RCMAP_THROTTLE 3
```

```
RCMAP_YAW 4
RELAY_DEFAULT 0
RELAY_PIN 13
RELAY_PIN2 -1
RELAY_PIN3 -1
RELAY_PIN4 -1
RLL2SRV_D 0.06876053
RLL2SRV_FF 0
RLL2SRV_I 0.03333334
RLL2SRV_IMAX 3000
RLL2SRV_P 0.916807
RLL2SRV_RMAX 75
RLL2SRV_TCONST 0.45
RNGFND_LANDING 0
RSSI_PIN -1
RSSI_RANGE 5
RST_MISSION_CH 0
RST_SWITCH_CH 0
RTL_AUTOLAND 0
RUDDER_ONLY 0
SCALING_SPEED 15
SCHED_DEBUG 0
SERIAL0_BAUD 115
SERIAL1_BAUD 57
SERIAL1_PROTOCOL 1
SERIAL2_BAUD 57
SERIAL2_PROTOCOL 1
SERIAL3_BAUD 38
SERIAL3_PROTOCOL 5
SERIAL4_BAUD 38
SERIAL4_PROTOCOL 5
SKIP_GYRO_CAL 0
SR0_EXT_STAT 2
SR0_EXTRA1 4
SR0_EXTRA2 4
SR0_EXTRA3 2
SR0_PARAMS 10
SR0_POSITION 2
SR0_RAW_CTRL 1
SR0_RAW_SENS 2
SR0_RC_CHAN 2
SR1_EXT_STAT 1
SR1_EXTRA1 1
SR1_EXTRA2 1
SR1_EXTRA3 1
SR1_PARAMS 10
```

```
SR1_POSITION 1
SR1_RAW_CTRL 1
SR1_RAW_SENS 1
SR1_RC_CHAN 1
STAB_PITCH_DOWN 2
STALL_PREVENTION 1
STEER2SRV_D 0.005
STEER2SRV_FF 0
STEER2SRV_I 0.2
STEER2SRV_IMAX 1500
STEER2SRV_MINSPD 1
STEER2SRV_P 1.8
STEER2SRV_TCONST 5
STICK_MIXING 1
SYS_NUM_RESETS 163
SYSID_MYGCS 255
SYSID_SW_TYPE 0
SYSID_THISMAV 1
TECS_CLMB_MAX 7
TECS_HGT_OMEGA 3
TECS_INTEG_GAIN 0.1
TECS_LAND_ARSPD 2
TECS_LAND_DAMP 0.5
TECS_LAND_PMAX 10
TECS_LAND_SINK 0.25
TECS_LAND_SPDWGT 1
TECS_LAND_TCONST 2
TECS_LAND_THR -1
TECS_PITCH_MAX 0
TECS_PITCH_MIN 0
TECS_PTCH_DAMP 0
TECS_RLL2THR 10
TECS_SINK_MAX 6
TECS_SINK_MIN 3
TECS_SPD_OMEGA 2
TECS_SPDWEIGHT 1
TECS_THR_DAMP 0.5
TECS_TIME_CONST 5
TECS_VERT_ACC 7
TELEM_DELAY 0
THR_FAILSAFE 1
THR_FS_VALUE 950
THR_MAX 90
THR_MIN 0
THR_PASS_STAB 0
THR_SLEWRATE 100
```

```
THR_SUPP_MAN 0
THROTTLE_NUDGE 1
TKOFF_FLAP_PCNT 0
TKOFF_ROTATE_SPD 12.5
TKOFF_TDRAG_ELEV 30
TKOFF_TDRAG_SPD1 8
TKOFF_THR_DELAY 2
TKOFF_THR_MAX 0
TKOFF_THR_MINACC 0
TKOFF_THR_MINSPD 0
TKOFF_THR_SLEW 20
TRIM_ARSPD_CM 1600
TRIM_AUTO 0
TRIM_PITCH_CD 0
TRIM_RC_AT_START 0
TRIM_THROTTLE 40
VTAIL_OUTPUT 0
WP_LOITER_RAD 100
WP_MAX_RADIUS 0
WP_RADIUS 60
YAW2SRV_DAMP 0.4
YAW2SRV_IMAX 1500
YAW2SRV_INT 1
YAW2SRV_RLL 1
YAW2SRV_SLIP 1.5
```